



THE UNIVERSITY *of* EDINBURGH

Edinburgh Research Explorer

Mixed-Mode Oscillations in Three Time-Scale Systems: A Prototypical Example

Citation for published version:

Krupa, M, Popovic, N & Kopell, N 2008, 'Mixed-Mode Oscillations in Three Time-Scale Systems: A Prototypical Example' Siam Journal on Applied Dynamical Systems, vol. 7, no. 2, pp. 361-420. DOI: 10.1137/070688912

Digital Object Identifier (DOI):

[10.1137/070688912](https://doi.org/10.1137/070688912)

Link:

[Link to publication record in Edinburgh Research Explorer](#)

Document Version:

Early version, also known as pre-print

Published In:

Siam Journal on Applied Dynamical Systems

General rights

Copyright for the publications made accessible via the Edinburgh Research Explorer is retained by the author(s) and / or other copyright owners and it is a condition of accessing these publications that users recognise and abide by the legal requirements associated with these rights.

Take down policy

The University of Edinburgh has made every reasonable effort to ensure that Edinburgh Research Explorer content complies with UK legislation. If you believe that the public display of this file breaches copyright please contact openaccess@ed.ac.uk providing details, and we will remove access to the work immediately and investigate your claim.



MIXED-MODE OSCILLATIONS IN THREE TIME-SCALE SYSTEMS: A PROTOTYPICAL EXAMPLE

MARTIN KRUPA, NIKOLA POPOVIĆ, AND NANCY KOPELL

ABSTRACT. Mixed-mode dynamics is a complex type of dynamical behavior that is characterized by a combination of small-amplitude oscillations and large-amplitude excursions. Mixed-mode oscillations (MMOs) have been observed both experimentally and numerically in various prototypical systems in the natural sciences. In the present article, we propose a mathematical model problem which, though analytically simple, exhibits a wide variety of MMO patterns upon variation of a control parameter. One characteristic feature of our model is the presence of three distinct time-scales, provided a singular perturbation parameter is sufficiently small. Using geometric singular perturbation theory and geometric desingularization, we show that the emergence of MMOs in this context is caused by an underlying canard phenomenon. We derive asymptotic formulae for the return map induced by the corresponding flow, which allows us to obtain precise results on the bifurcation (Farey) sequences of the resulting MMO periodic orbits. We prove that the structure of these sequences is determined by the presence of secondary canards. Finally, we perform numerical simulations that show good quantitative agreement with the asymptotics in the relevant parameter regime.

1. INTRODUCTION

Mixed-mode dynamics is a complex type of dynamical behavior that is characterized by a combination of small-amplitude oscillations and large-amplitude excursions of relaxation type. *Mixed-mode oscillations* (MMOs) are frequently encountered in multiscale dynamical systems, i.e., in systems of differential equations in which the relevant variables evolve over several distinct scales. Consequently, typical MMO patterns in such systems consist of oscillatory sequences in which amplitudes of different orders of magnitude alternate. Historically, MMOs were first observed in experiments on the well-known Belousov-Zhabotinsky reaction [38]. They have since been found both experimentally and numerically in numerous other contexts in the natural sciences. Examples include prototypical systems from chemical kinetics, electrocardiac dynamics, neuronal modeling, and laser dynamics, as well as from a number of other disciplines, see, e.g., [10, 16, 23, 27, 29, 30, 31, 32] for details and references.

Among the various mechanisms which have been proposed to explain the occurrence of MMOs are the break-up of an invariant torus [21] and the loss of stability of a Shilnikov homoclinic orbit [16]. MMOs have also been linked to slow passage through a delayed Hopf bifurcation, cf., e.g., [22], as well as to the subcritical Hopf-homoclinic bifurcation [12, 13]. In the present article, we consider another explanation for the emergence of MMOs, namely, the so-called *canard mechanism*. To the best of our knowledge, this idea was first brought forward by Milik *et. al.* [27]. More recently, in [2], it was extended to accommodate more general classes of systems that exhibit canard dynamics.

The classical canard phenomenon [1, 5, 8, 9] was first described in the framework of two-dimensional fast-slow systems, i.e., of systems with one fast and one slow variable; a prototypical example is the system of equations given by

$$(1.1a) \quad v' = -z + f_2 v^2 + f_3 v^3,$$

$$(1.1b) \quad z' = \varepsilon(v - \lambda).$$

Date: March 4, 2011.

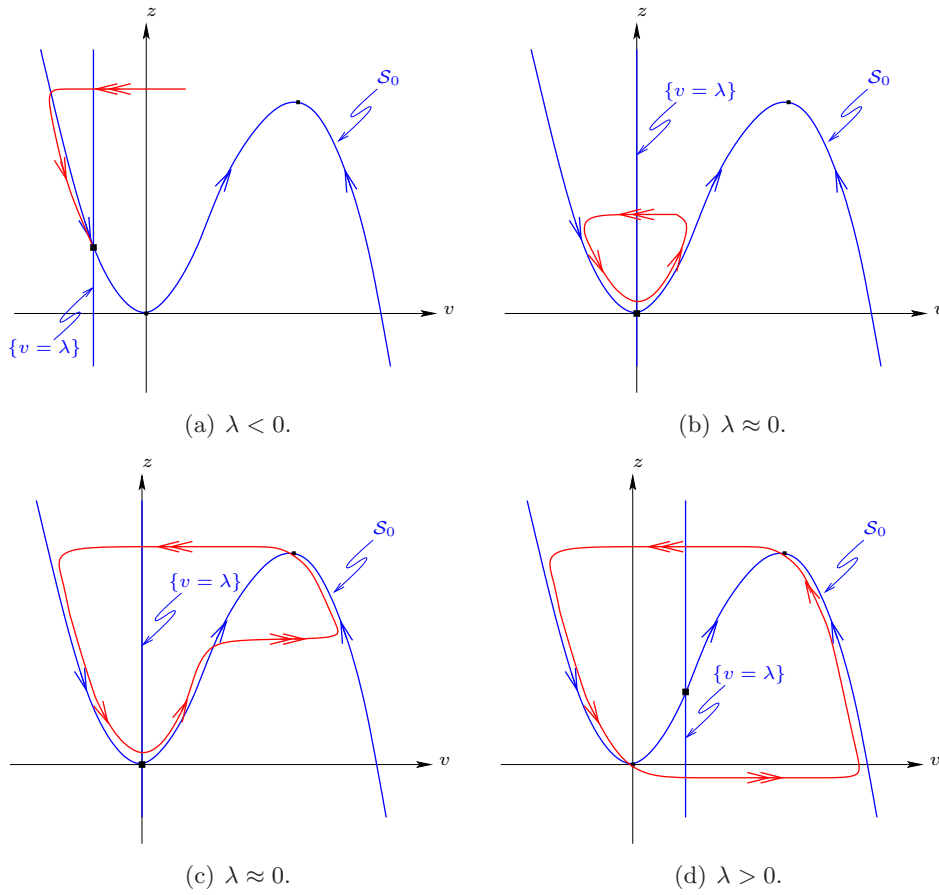


FIGURE 1. Nullcline movement leading to a canard explosion: as the slow nullcline passes through the origin, one observes a transition from (a) a stable equilibrium via a family of canard solutions ((b) “headless canard,” (c) “canard with head”) to (d) a full-scale relaxation oscillation.

(Here, $f_2 > 0$ and $f_3 < 0$ are real constants, $0 < \varepsilon \ll 1$ and λ are small parameters, and the prime denotes differentiation with respect to time t .)

The term *canard explosion* [20] is customarily used to denote a transition in (1.1) from a stable equilibrium through a family of small-amplitude cycles and subsequently to a large-amplitude relaxation oscillation. Notably, this transition occurs within an exponentially small range (in ε) of the relevant control parameter, λ . The basic mechanism of a canard explosion can be described as follows: under the above assumptions, the “fast nullcline” \mathcal{S}_0 for (1.1), which is given by $z = f(v) := f_2 v^2 + f_3 v^3$, is an S-shaped curve. Moreover, \mathcal{S}_0 is a curve of equilibria for the *layer problem* obtained for $\varepsilon = 0$ in (1.1) and is (normally) hyperbolic away from the two *fold points* where $f'(v) = 0$; in particular, the origin is one such point. Rewriting (1.1) in terms of the slow time $\tau = \varepsilon t$, one finds that the corresponding “slow nullcline” is given by $v = \lambda$. As λ passes through 0, this slow nullcline moves through the lower fold point of \mathcal{S}_0 at the origin, which triggers the onset of the canard explosion, see Figure 1. Finally, for $\lambda > 0$ sufficiently “large,” the dynamics of (1.1) enters the relaxation regime.

One important notion that arises in the study of a canard explosion in (1.1) (as well as in other, related systems) is that of a *maximal canard*. In general, a canard is a solution of (1.1) which

originates in the attracting portion of the fast nullcline \mathcal{S}_0 and which then crosses over to the repelling one; cf. again Figure 1. Maximal canards are canard trajectories that remain $\mathcal{O}(\varepsilon)$ -close to the unstable part of \mathcal{S}_0 until they reach the upper fold; they mark the transition from small-amplitude (non-relaxation) oscillations to large-amplitude oscillations of relaxation type during a canard explosion.

One of the main goals in this article is to show how systems that exhibit mixed-mode-type behavior can be constructed from systems that undergo a canard explosion by replacing the parameter moving the slow nullcline with a dynamical variable. In other words, we will argue that the emergence of MMOs in such systems is triggered by a “slow passage through a canard explosion.” More specifically, consider a system of the form

$$(1.2a) \quad v' = -z + f_2 v^2 + f_3 v^3,$$

$$(1.2b) \quad z' = \varepsilon(v - w),$$

$$(1.2c) \quad w' = \varepsilon(\mu + \phi(v, z, w)),$$

where $\mu > 0$ and $\phi = \mathcal{O}(v, z, w)$ is a smooth function that will be specified in the following, and note that the new slow variable w in (1.2) assumes the role of λ in (1.1). Let \mathcal{S}_0 denote the (two-dimensional) *critical manifold* for (1.2), which is defined by the constraint $z = f(v)$. Finally, let $\ell^- = \{(0, 0, w)\}$ and $\ell^+ = \{(-\frac{2f_2}{3f_3}, 0, w)\}$ denote the lower and upper fold lines for (1.2), respectively, and note that ℓ^\pm are determined by imposing $f'(v) = 0$, in addition to $z = f(v)$. Away from these fold lines, \mathcal{S}_0 is normally hyperbolic; it consists of the two attracting sheets

$$(1.3) \quad \mathcal{S}_0^{a-} = \{(v, z, w) \mid v < 0, z < 0\} \quad \text{and} \quad \mathcal{S}_0^{a+} = \{(v, z, w) \mid v > -\frac{2f_2}{3f_3}, z > \frac{4f_2^3}{27f_3^2}\},$$

as well as of a repelling sheet which is given by

$$(1.4) \quad \mathcal{S}_0^r = \{(v, z, w) \mid 0 < v < -\frac{2f_2}{3f_3}, 0 < z < \frac{4f_2^3}{27f_3^2}\};$$

see Figure 2 for an illustration. (Note that, due to $f_2 > 0$ and $f_3 < 0$, there holds $-\frac{2f_2}{3f_3} > 0$ in (1.3) and (1.4).) The *singular limit* of $\varepsilon = 0$ in (1.2) is described by the dynamics of the *reduced problem* on the critical manifold \mathcal{S}_0 .

By standard Fenichel theory [11], for $\varepsilon > 0$ sufficiently small and (v, z, w) in some bounded subset of \mathbb{R}^3 , the critical manifold will perturb to a slow manifold \mathcal{S}_ε away from ℓ^\pm . We will denote the sheets of \mathcal{S}_ε corresponding to \mathcal{S}_0^{a-} , \mathcal{S}_0^{a+} , and \mathcal{S}_0^r by $\mathcal{S}_\varepsilon^{a-}$, $\mathcal{S}_\varepsilon^{a+}$, and $\mathcal{S}_\varepsilon^r$, respectively.

In analogy to the maximal canard encountered in (1.1), we define the so-called *strong canard* Γ_ε^0 for (1.2) as follows: once the two sheets $\mathcal{S}_\varepsilon^{a-}$ and $\mathcal{S}_\varepsilon^r$ are chosen, they are unique up to exponentially small terms in ε [11]. Then, Γ_ε^0 can be defined, for $\varepsilon > 0$ small, as the intersection of the continuation of these two sheets into the fold region. Moreover, as we will show in Section 2, this intersection is transverse, which implies that Γ_ε^0 is well-defined. It was postulated in [27] that the strong canard forms the boundary between two regions of very different dynamical behavior, in that it separates small-amplitude oscillations from large oscillations of relaxation type. We will confirm this postulate in the context of (1.2); in that sense, Γ_ε^0 can be interpreted as the “organizing center” for the emergence of MMOs in (1.2).

The detailed structure of the MMO trajectories that will be observed in (1.2) depends strongly on certain features of the specific equations under consideration. One important aspect concerns the properties of the global return mechanism, defined by the interplay of μ and ϕ in (1.2c), and in particular how far back the value of w is reset by that return.

If, during the return phase, w becomes $\mathcal{O}(1)$ and negative (i.e., if $\mu + \phi$ is not close to zero), the dynamics of (1.2) in the initial phase of the passage near the lower fold is of “node type,” which means that there is strong contraction without any oscillatory behavior. That initial contractive

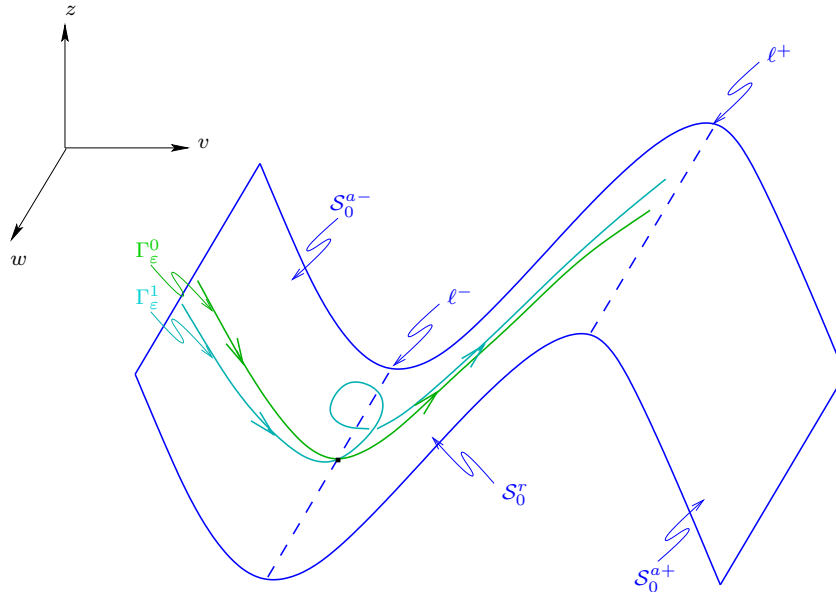


FIGURE 2. The geometry of system (1.2): critical manifold \mathcal{S}_0 with sheets \mathcal{S}_0^{\pm} and \mathcal{S}_0^r , fold lines ℓ^{\pm} , and canard trajectories Γ_{ε}^0 and Γ_{ε}^1 .

phase is followed by oscillatory dynamics which can give rise to MMOs; however, most of the resulting oscillations are of very small amplitude. The class of these so-called *canards of folded-node type* is rather well understood and was analyzed in detail in [36].

By contrast, we will discuss a case where the global return mechanism is relatively weak, in the sense that $\mu + \phi$ is $\mathcal{O}(1)$. Note that this case differs from that of the so-called *folded saddle-node* [31, 6] in that not only is μ assumed to be small, but ϕ is, too, and that the weakness of the return mechanism introduces an additional, “super-slow” time-scale into the problem. In that sense, the folded saddle-node can be regarded as an intermediate case between the folded node and the situation in (1.2). (Note, however, that (1.2) could alternatively be classified as a “folded saddle-node of type II with weak global return” [35].)

The basic dynamics of (1.2) can be characterized as follows: given (v, z, w) small, the system will pass through the small-amplitude phase, where the variable w can grow slightly and become positive. Then, during the subsequent relaxation phase, w is reset to a small (negative or positive) value, and the cycle can start anew. Hence, the fact that w is always close to zero implies that there is no non-oscillatory contraction, contrary to the case of a folded node. Moreover, due to the three time-scale structure of (1.2), no slow passage through a Hopf bifurcation is observed, contrary to the case of a folded saddle-node. This distinction will be made more precise in the following, see also the discussion in Section 4 below.

As we will show in this article, it is the interplay between the two main ingredients of the dynamics, the local flow close to the strong canard and the global return, that underlies the basic canard mechanism for the emergence of MMOs in (1.2). This mechanism can be generalized to other classes of systems, see, e.g., [17, 2] for details. In the following, we will refer to a combination of local, dynamical passage through a canard point and a suitably defined global return as the *generalized canard mechanism*. In other words, (1.2) represents only one specific realization of that very general mechanism. Moreover, as will follow from our analysis, (1.2) is a normal form for this class of three time-scale systems, in the sense that the addition of higher-order terms in (1.2) will not fundamentally influence the resulting dynamics.

Another aspect of the mixed-mode dynamics in (1.2), in addition to the return mechanism, is the family of so-called *secondary canards*. In the context of (1.2), we define the k th secondary canard Γ_ε^k as a trajectory that undergoes k small (non-relaxation) rotations, or “loops,” during its passage “near” the lower fold ℓ^- and that then remains $\mathcal{O}(\varepsilon)$ -close to the critical manifold \mathcal{S}_0 until it reaches the $\mathcal{O}(\varepsilon^{\frac{1}{3}})$ -vicinity of the upper fold ℓ^+ [34]. Note that the strong canard Γ_ε^0 passes through the vicinity of ℓ^- without undergoing any rotation at all, which corresponds to $k = 0$. As we will show, the existence of secondary canards in (1.2) is guaranteed by the fact that they can be defined as trajectories lying in the intersection of $\mathcal{S}_\varepsilon^r$ with subsequent iterates of $\mathcal{S}_\varepsilon^{a-}$ under the return map Π induced by the flow of (1.2), cf. Section 3 below. This will allow us to give a precise asymptotic description of these canards; to the best of our knowledge, comparable results have so far been obtained only in the folded-node case [36], via a combination of asymptotics and numerics. For a qualitative illustration of the canard trajectories Γ_ε^0 and Γ_ε^1 in (1.2), cf. again Figure 2.

The notion of secondary canards leads to another important concept in this context, namely, that of the corresponding *sectors of rotation*, which are defined as (two-dimensional) portions of $\mathcal{S}_\varepsilon^{a-}$ in the fold region that are bounded by the secondary canards. These sectors, which we denote by RS^k , have the following property: trajectories starting in the k th sector undergo k small rotations near ℓ^- . Given that all MMO trajectories pass exponentially close to $\mathcal{S}_\varepsilon^{a-}$ in their relaxation phase, they must enter one of the sectors upon their return to the fold region. This fact can be exploited to reduce the corresponding (two-dimensional) return map Π for (1.2), which is *a priori* defined on an appropriate section for the corresponding flow, to a one-dimensional map Φ . Moreover, as we will show, the width of RS^k is $\mathcal{O}(\varepsilon^{\frac{3}{2}}\sqrt{-\ln\varepsilon})$, independent of k to leading order; see Section 3. Hence, the canard phenomenon occurs rather “robustly” in the context of (1.2), in the sense that the relevant parameter intervals are not exponentially small in ε , as in the classical two-dimensional case [20].

Finally, with each MMO trajectory one can associate a sequence $L_0^{k_0} L_1^{k_1} \dots$, called the *Farey sequence* [4], which describes the succession of large relaxation excursions and small (non-relaxation) oscillations (loops): the segment $L_j^{k_j}$ corresponds to L_j relaxation oscillations followed by k_j small loops. (In the following, we will focus primarily on the case when $L_j = 1$.) As we will show, the Farey sequence of each trajectory is completely determined by the succession of the sectors of rotation visited by the trajectory. A natural question that arises in this context is which Farey sequences are admissible in a system of the form (1.2) and which μ -intervals they correspond to. This question is intimately related to the size of the sectors RS^k themselves, to the distance from the return point on $\mathcal{S}_\varepsilon^{a-}$ to the strong canard Γ_ε^0 after relaxation, and to the contractive (or expansive) properties of the flow induced by Π . These and similar issues will be discussed in detail in Sections 3 and 4.

For the sake of definiteness, we will restrict ourselves to the more specific class of systems of the form

$$\begin{aligned} (1.5a) \quad & v' = -z + f_2 v^2 + f_3 v^3, \\ (1.5b) \quad & z' = \varepsilon(v - w), \\ (1.5c) \quad & w' = \varepsilon^2(\mu - g_1 z) \end{aligned}$$

in the following, with $g_1 > 0$ constant. Note that (1.5) can be understood as a special case of (1.2), with μ rescaled by ε and $\phi(v, z, w) \equiv \phi(z) = \varepsilon g_1 z$. (Other choices of ϕ can be treated in a similar manner, see, e.g., [18].) This specific scaling of μ implies that the dynamics of (1.5) evolves on three distinct time-scales, a fast scale, a slow scale, and a “super-slow” scale. Given that the flow of (1.5c) is governed by that slowest scale, w cannot vary too much, implying that trajectories cannot be reset very far back (in w) during the global return. Consequently, they will return close

to the strong canard Γ_ε^0 of (1.5) after relaxation; equivalently, recalling the analogy between w and the parameter λ in (1.1), one could say that the return is close to the maximal canard of the (v, z) -subsystem in (1.5).

As we will show in Section 3, it is the “lowest” sectors of rotation that will be immediately adjacent to the strong canard. Hence, only few successive small oscillations will be observed in a typical time series of (1.5); moreover, these oscillations are relatively large in amplitude. Since the relevant parameter intervals will turn out to be relatively small, the corresponding dynamics is very sensitive to variations of μ . Also, since the stability intervals of “regular,” L^k -type orbits (i.e., of MMO trajectories with Farey sequence $\{L^k\}$) are smaller still, the time series can be quite irregular; furthermore, there can be many relaxation cycles occurring in succession before the system returns to the small-oscillation phase. (By contrast, in the folded-node case, regular 1^k -type orbits are predicted to be stable for most μ -values; cf. [36].)

Moreover, as μ is varied in (1.5), one observes a passage through neighboring sectors of rotation: for increasing μ , the dynamics of (1.5) will be restricted to lower and lower sectors, admitting fewer and fewer small-amplitude oscillations, until eventually only relaxation cycles are seen. In other words, one observes the unfolding of a family of MMOs, including trajectories that pass through all sectors of rotation, on a fairly small parameter set. (In a folded-node system, on the other hand, such an unfolding can be expected over a μ -interval whose length is bounded below by a constant [36].) Also, numerical evidence suggests that only the Farey sequences predicted in Section 3 will “generically” occur in a three time-scale system of the type of (1.5). Therefore, we conjecture that (1.5) can be interpreted as a “canonical form” for this particular class of three-dimensional systems. However, a rigorous, analytical justification of this claim is beyond the scope of this work.

In the remainder of this article, we analyze the “canonical” system (1.5) in detail, using a wide range of techniques. One of our aims is to derive asymptotic formulae for the return map induced by the flow of (1.5). To that end, we combine various methods from dynamical systems theory and, in particular, from geometric singular perturbation theory. To approximate the flow away from the fold lines ℓ^\pm , we employ standard results due to Fenichel [11]. Upon entry into the neighborhood of ℓ^\pm , normal hyperbolicity breaks down, and Fenichel’s results are no longer applicable, which necessitates a detailed analysis of the dynamics there. We are especially interested in the lower fold ℓ^- , since it is there that the canard phenomenon occurs. To describe the dynamics close to ℓ^- , we make use of the near-integrable structure of the equations in (1.5). To access that structure, we introduce a rescaling that is akin to the blow-up transformation customarily used in this context, see, e.g., [7, 19] for details. While each of the parts of our analysis taken by itself is rather standard, the combination of the different approaches in the present context is new. In particular, by combining the leading-order global dynamics with detailed local asymptotics, we are able to obtain a closed-form description of the return map Π for (1.5) and, hence, to describe the resulting mixed-mode dynamics in detail.

This article is organized as follows. In Section 2, we prove that the return map Π is well-defined under an appropriate choice of sections for the flow of (1.5), and we derive precise asymptotic estimates for Π by desingularizing the dynamics of (1.5) in the fold region and by making use of the near-integrability of the resulting equations. Section 3 contains the centerpiece of our analysis, in that we show how the “full,” two-dimensional map Π can be reduced to a simpler, one-dimensional map Φ . This reduction is accurate with at most an exponentially small error (in ε) and is carried out in two steps: in a first step, Π is restricted from a two-dimensional section to the union of appropriately defined, one-dimensional curves, which allows us to describe the family of secondary canards, as well as the corresponding sectors of rotation, for (1.5). Then, in a second step, the map Π is further reduced and is restricted to a map Φ that is defined on a single curve. The dynamics of this map is analyzed in detail to make quantitative predictions on the relevant parameter regimes and the associated bifurcation (Farey) sequences in (1.5). In Section 4, we summarize our results,

and we relate them to other mechanisms that have been proposed to explain MMOs. Moreover, we illustrate various properties of the “reduced” flow under Φ , and we compare them numerically to the “full” dynamics of (1.5). In sum, we thus obtain a fairly complete picture of the mixed-mode dynamics of (1.5), both qualitatively and quantitatively. Moreover, in doing so, we provide a framework for an even more detailed analysis of systems of the type of (1.5): once the dynamics of such a system is accurately reduced to that of a one-dimensional map, the well-developed theory of unimodal maps [25] can be applied. Our results on Φ are a first step in this direction, in that there is potential for a more rigorous investigation along the lines of Section 3.

Finally, we note that our analysis of (1.5) was inspired by a more specific problem, a model for the dynamics of the dopaminergic neuron that was proposed by Wilson and Callaway [37]. This model, which consists of a system of N strongly electrically coupled oscillators, was analyzed in [24] as well as in [23] (in a slightly different form) via a combination of asymptotic analysis and numerical techniques. One salient feature of the Wilson-Callaway model is precisely the unfolding of a family of MMO periodic orbits upon variation of one control parameter. In an upcoming companion paper [18], we will show how the Wilson-Callaway model can be fitted into the framework of (1.5) and how the results obtained here can be applied to study its dynamics.

2. THE CANONICAL SYSTEM (1.5)

In this section, we discuss the system of equations (1.5) or, equivalently, the system obtained by rewriting (1.5) in terms of the slow time $\tau = \varepsilon t$,

$$(2.1a) \quad \varepsilon \dot{v} = -z + f_2 v^2 + f_3 v^3,$$

$$(2.1b) \quad \dot{z} = v - w,$$

$$(2.1c) \quad \dot{w} = \varepsilon(\mu - g_1 z).$$

Here, the overdot denotes differentiation with respect to τ , $f_2 > 0$, $f_3 < 0$, and $g_1 > 0$ are $\mathcal{O}(1)$ coefficients, $0 < \varepsilon \ll 1$ is small, and μ is the “free” (bifurcation) parameter; note the presence of three time-scales in (2.1).

Let \mathcal{S}_0 denote the critical manifold for (2.1), as before, and recall that \mathcal{S}_0 is given by $z = f(v) = f_2 v^2 + f_3 v^3$, cf. Section 1. Moreover, recall the definition of $\mathcal{S}_0^{a\pm}$ and \mathcal{S}_0^r in (1.3) and (1.4), respectively, and let $\mathcal{S}_\varepsilon^{a\pm}$ and $\mathcal{S}_\varepsilon^r$ denote the corresponding sheets of the slow manifold, for $\varepsilon > 0$ sufficiently small. Finally, the upper and lower fold lines in (2.1) are again denoted by ℓ^\pm .

2.1. Sections for the flow of (1.5). To derive asymptotic formulae for the return of trajectories under the flow of (1.5), we will define the corresponding return map on suitable sections for the flow, which we introduce below. In the course of our analysis, we will show that the small-amplitude oscillations observed in (1.5) are due to the fact that, in the parameter regime under consideration, the system passes slowly through a canard explosion about the origin in (v, z, w) -space. The large-amplitude components of the mixed-mode time series are generated by the global return mechanism, which takes trajectories back to the fold line ℓ^- after the passage past the origin has been completed. Combining these two aspects of the dynamics will allow us to describe in detail how MMOs can arise in (1.5).

The dynamics of (1.5) can be broken down into the following four components:

- (i) the flow in a neighborhood of the fold line ℓ^- (Section **2.2**);
- (ii) the entry into the fold region (Section **2.3**);
- (iii) the exit from the fold region (Section **2.4**); and, finally,
- (iv) the global return mechanism (Section **2.5**).

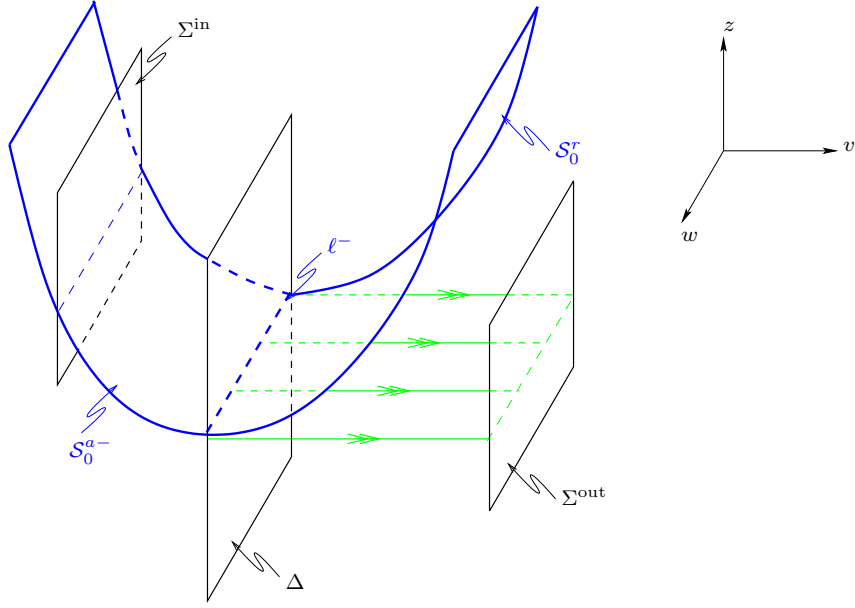


FIGURE 3. The sections Σ^{in} , Δ , and Σ^{out} for the flow of (1.5).

We will construct transition maps for each of the above components of the flow. The desired global return map, which we denote by Π , will then be obtained via the composition of these individual maps.

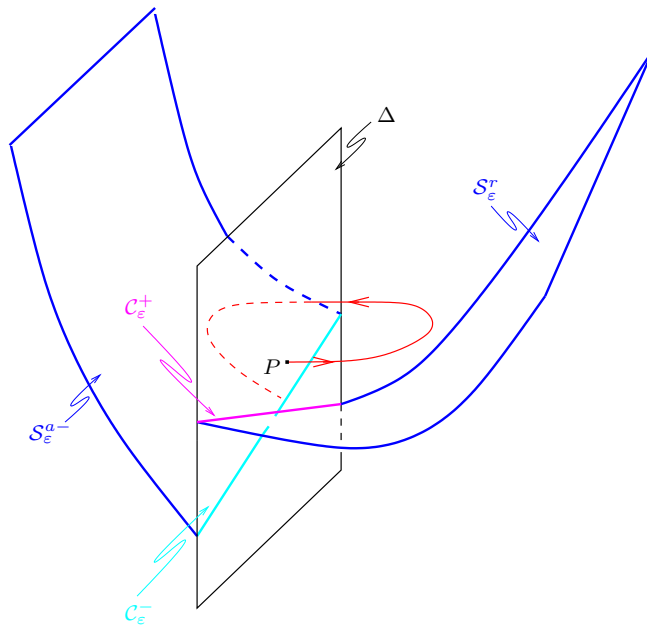
We begin by introducing *sections* for the flow of (1.5): we will require

- (i) a section Σ^{in} across the attracting branch \mathcal{S}_0^{a-} of the critical manifold \mathcal{S}_0 , which is given by $v = -\rho$, with $|z|$ and $|w|$ bounded;
- (ii) a section Δ , which is defined by $v = 0$, with $|z|$ and $|w|$ bounded, implying that Δ lies in the (z, w) -plane and that it bisects the critical manifold \mathcal{S}_0 along ℓ^- (the w -axis); and
- (iii) a section Σ^{out} across the fast foliation of \mathcal{S}_0 , with $v = \delta$ and $|z|$ and $|w|$ bounded.

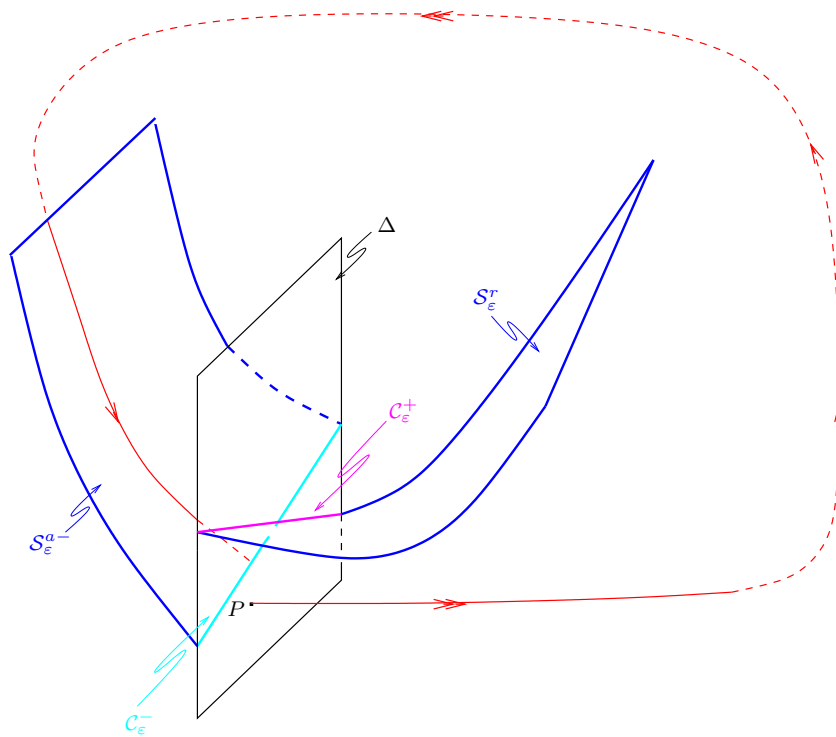
Here, $\rho, \delta > 0$ are small, but fixed (ε -independent) constants; see Figure 3 for an illustration. The section Δ will turn out to be especially important in the following, since the global return map Π will be defined on Δ . (Note that this particular choice of Poincaré section has previously been made by Dumortier and Roussarie in their analysis of canard cycles, see, e.g., [8].)

Next, we introduce two subsets of Δ that will play a crucial role in the description of Π . We first define $\mathcal{C}_\varepsilon^-$ as follows: a point $P \in \Delta$ is an element of $\mathcal{C}_\varepsilon^-$ if P is the endpoint of a segment of trajectory that originates in $\mathcal{S}_\varepsilon^{a-}$. The set $\mathcal{C}_\varepsilon^+$ is defined analogously, with $\mathcal{S}_\varepsilon^{a-}$ replaced by $\mathcal{S}_\varepsilon^r$ and the time reversed, see Figure 4. The sets $\mathcal{C}_\varepsilon^-$ and $\mathcal{C}_\varepsilon^+$ have the following properties:

- (i) If $P \in \Delta$ is above $\mathcal{C}_\varepsilon^+$, the trajectory of P is blocked by $\mathcal{S}_\varepsilon^r$ from entering relaxation. Depending on the position of P , the initial motion may be toward $\mathcal{S}_\varepsilon^r$, but the trajectory must eventually turn toward $\mathcal{S}_\varepsilon^{a-}$ (under the fast flow) and return to Δ , having undergone a small-amplitude oscillation (or loop), see Figure 4(a).
- (ii) If $P \in \Delta$ is below $\mathcal{C}_\varepsilon^+$, the trajectory of P must leave the vicinity of the fold in the direction of the fast flow and may re-enter only through a global return mechanism, since no trajectories can pass through $\mathcal{S}_\varepsilon^r$, see Figure 4(b).
- (iii) Any trajectory that is attracted to $\mathcal{S}_\varepsilon^{a-}$ will be exponentially close to $\mathcal{C}_\varepsilon^-$ when it hits Δ .



(a) Trajectory of $P \in \Delta$ above C_ϵ^+ .



(b) Trajectory of $P \in \Delta$ below C_ϵ^+ .

FIGURE 4. The sets C_ϵ^- and C_ϵ^+ .

Remark 1. Since $\mathcal{S}_\varepsilon^{a-}$ and $\mathcal{S}_\varepsilon^r$ are unique only up to exponentially small terms in ε , the sets $\mathcal{C}_\varepsilon^\pm$ are, strictly speaking, “strips” rather than curves. However, since our construction of Π will rely on leading-order ε -asymptotics throughout, this non-uniqueness will not influence our results. ■

A proof of these claims will be given in Section 3 below. We now proceed with the derivation of the four components of the return map, as outlined above. The description of the dynamics in the fold region is the centerpiece of our analysis and will be discussed first.

2.2. Dynamics in the fold region. Our goal in this subsection is to analyze the flow in the region of the phase space of (1.5) where small-amplitude oscillations (loops) can occur. To describe these loops, we have to study the equations in (1.5) in an $\mathcal{O}(\sqrt{\varepsilon})$ -vicinity of the fold line ℓ^- and, specifically, of the origin in (u, v, w) -space. Recall that under our assumptions on (1.5), ℓ^- is given by the w -axis.

To investigate the dynamics of (1.5) close to ℓ^- , we define the rescaling

$$(2.2) \quad v = \sqrt{\varepsilon}\bar{v}, \quad z = \varepsilon\bar{z}, \quad w = \sqrt{\varepsilon}\bar{w}, \quad \text{and} \quad t = \frac{\bar{t}}{\sqrt{\varepsilon}}.$$

In terms of the new “barred” variables in (2.2), (1.5) becomes

$$(2.3a) \quad \bar{v}' = -\bar{z} + f_2\bar{v}^2 + \sqrt{\varepsilon}f_3\bar{v}^3,$$

$$(2.3b) \quad \bar{z}' = \bar{v} - \bar{w},$$

$$(2.3c) \quad \bar{w}' = \varepsilon(\mu - g_1\varepsilon\bar{z}),$$

where the prime now denotes differentiation with regard to the new rescaled time \bar{t} . Note that (2.3) is a fast-slow system, with two fast variables \bar{v} and \bar{z} and one slow variable \bar{w} . In other words, the scale separation between v and z has vanished after the rescaling, whereas w is still slow and constant to leading order. Hence, we can interpret \bar{w} as a slowly varying parameter.

For $\varepsilon = 0$, the equations in (2.3) reduce to

$$(2.4a) \quad \bar{v}' = -\bar{z} + f_2\bar{v}^2,$$

$$(2.4b) \quad \bar{z}' = \bar{v} - \bar{w},$$

$$(2.4c) \quad \bar{w}' = 0.$$

Note that, up to various rescalings, (2.4) is of the form

$$\begin{aligned} x' &= -y + x^2, \\ y' &= x - \lambda, \end{aligned}$$

which is a prototypical system for the occurrence of a canard explosion (at $\lambda = 0$) [20], see also (1.1). In the following, we will describe how the equations in (2.3) fit into the framework of [20], where the classical two-dimensional scenario is analyzed using geometric singular perturbation theory. The role of the bifurcation parameter λ is taken by \bar{w} in our case. For $\bar{w} = 0$, (2.4) is an integrable system, with constant of motion given by

$$(2.5) \quad H(\bar{v}, \bar{z}) = \frac{1}{2}e^{-2f_2\bar{z}} \left(-\bar{v}^2 + \frac{\bar{z}}{f_2} + \frac{1}{2f_2^2} \right).$$

The equations in (2.4) have a continuous family of periodic orbits which are most conveniently described via the level curves of H ; these are defined by $H(\bar{v}, \bar{z}) = h$, for h constant. The corresponding (time-parametrized) solution curves will be denoted by $\bar{\gamma}_0^h(t) = (\bar{v}_0^h, \bar{z}_0^h)(t)$ in the following.

We first note that $(\bar{v}, \bar{z}) = (0, 0)$ lies on the curve defined by $H(\bar{v}, \bar{z}) = h_0 := (4f_2^2)^{-1}$. For $h > h_0$, there exist no real solutions to $H(\bar{v}, \bar{z}) = h$. Hence, without loss of generality, we consider

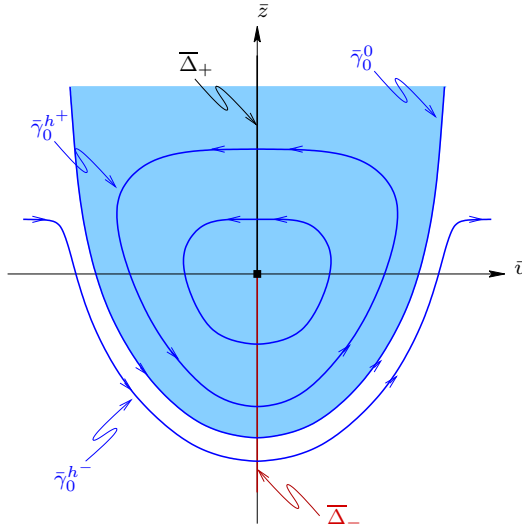


FIGURE 5. Typical integral curves of H , with $h^- < 0 < h^+$. (The region where $h > 0$ is shaded.)

$h \leq h_0$ now, and we note that $h_0 > 0$. For $h = 0$ in (2.5), we obtain the special solution $\bar{\gamma}_0^0$ of (2.4), with

$$(2.6) \quad \bar{\gamma}_0^0(t) = (\bar{v}_0^0, \bar{z}_0^0)(t) = \left(\frac{1}{2f_2}t, \frac{1}{4f_2}t^2 - \frac{1}{2f_2} \right).$$

Note that (2.6) defines an invariant parabola that separates the closed level curves of H , which are obtained for $h > 0$, from the open ones, with $h < 0$; see Figure 5 for an illustration. Since the two branches of this parabola correspond to \mathcal{S}_0^{a-} and \mathcal{S}_0^r for $\bar{w} = 0$, after the rescaling in (2.2), $\bar{\gamma}_0^0$ is a “singular canard solution,” i.e., a solution of (2.3) that connects $\mathcal{S}_\varepsilon^{a-}$ and $\mathcal{S}_\varepsilon^r$ in the singular limit as $\varepsilon \rightarrow 0$. (In fact, as we will see in (2.16) below, the orbit determined by $\bar{\gamma}_0^0$ is precisely the strong canard Γ_ε^0 in this singular limit.)

Let $\bar{\Delta}$ denote the section that corresponds to Δ in the “barred” variables, i.e., let $\bar{\Delta} = \{\bar{v} = 0\}$, with $|\bar{z}|$ and $|\bar{w}|$ bounded. For h fixed, let \bar{z}^h be the corresponding value of \bar{z} in $\bar{\Delta}$, with $H(0, \bar{z}^h) = h$. (In particular, by (2.6), there holds $\bar{z}^0 = -(2f_2)^{-1}$.) Our first result is a direct consequence of the above discussion; see [20] for details.

Proposition 2.1. *To any $h \leq h_0$, with $h_0 = (4f_2^2)^{-1} > 0$, there corresponds precisely one value $\bar{z}^h \leq 0$ of \bar{z} in $\bar{\Delta}$. Moreover, \bar{z}^h is an increasing function of h .*

Since the limiting equations obtained for $\bar{w} = 0 = \varepsilon$ in (2.3) are integrable, we will refer to the original, “perturbed” dynamics as “near-integrable.” (A related treatment of a more general family of near-integrable systems can be found in [15].) The near-integrability of (2.3) will allow us to analyze the dynamics of the equations using a perturbation analysis and to approximate the return map from $\bar{\Delta}$ to itself, which we refer to as $\bar{\Pi}$, to leading order. Naturally, the closed level curves of H will turn out to be the singular “templates” for the small-amplitude component of the mixed-mode dynamics observed in (2.1). Moreover, as we will show, it is the bifurcation structure of $\bar{\Pi}$ that is responsible for the emergence of secondary canards in (2.3); these canards, in turn, determine the qualitative structure of the resulting MMO patterns. In that sense, the rescaling in (2.2) will enable us to access the near-integrable structure of (1.5) close to ℓ^- .

We will define the return map $\bar{\Pi}$ on $\bar{\Delta}_- \subset \bar{\Delta}$, which is the portion of $\bar{\Delta}$ where $\bar{z} < 0$. Although $\bar{\Pi}$ is *a priori* a function of (\bar{z}, \bar{w}) , it is more convenient to parametrize \bar{z} by h , and to describe the

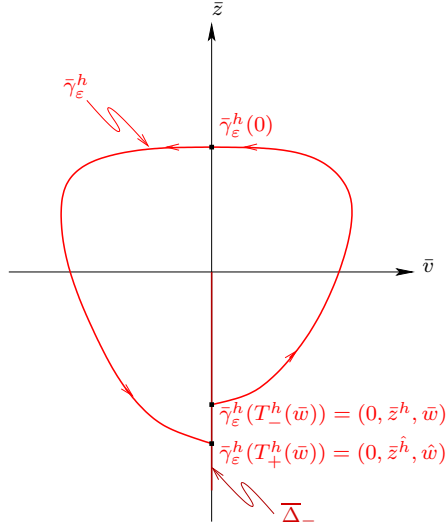


FIGURE 6. The geometry of system (2.3).

asymptotics of $\bar{\Pi}$ in terms of h and \bar{w} in the following. For $h \leq h_0$, with h_0 as above, let \bar{z}^h again denote the corresponding unique value of $\bar{z} \in \bar{\Delta}_-$, and note that we will sometimes identify \bar{z}^h with its associated h -value. Moreover, let $\bar{\gamma}_\varepsilon^h(t)$ be the solution to (2.3) emanating from $(0, \bar{z}^h, \bar{w})$, where the time parametrization is chosen so that $\bar{\gamma}_\varepsilon^h(0)$ is contained in $\bar{\Delta}_+ := \bar{\Delta} \setminus \bar{\Delta}_-$. Then, we define $T_-^h(\bar{w}) < 0$ and $T_+^h(\bar{w}) > 0$ by requiring that $\bar{\gamma}_\varepsilon^h(T_\pm^h(\bar{w})) \in \bar{\Delta}_-$. Moreover, we assume that $T_\pm^h(\bar{w})$ are the times of the first such intersection. Let $T^h : \bar{\Delta}_- \rightarrow \bar{\Delta}_-$ denote the return time of solutions under the flow of (2.3), and note that, by definition, $T^h(\bar{w}) = T_+^h(\bar{w}) - T_-^h(\bar{w})$. Let \hat{h} be defined by the requirement that $\bar{z}^{\hat{h}}$ is the \bar{z} -coordinate of $\bar{\gamma}_\varepsilon^h(T^h(\bar{w})) \in \bar{\Delta}_-$; an illustration of these definitions is given in Figure 6. Finally, for $\bar{w} = 0$, we write $T^h := T_+^h(0)$, which, together with $T_-^h(0) = -T_+^h(0)$, implies

$$(2.7) \quad T^h(0) = T_+^h(0) - T_-^h(0) = 2T^h.$$

We now make the following assumption on \bar{w} , which will be verified *a posteriori* for the parameter regime we are interested in:

Assumption 1. For fixed, real $f_2 > 0$, $f_3 < 0$, $\mu > 0$, and $g_1 > 0$ and $0 < \varepsilon \ll 1$ sufficiently small in (2.3), $\bar{w} = \mathcal{O}(\sqrt{\varepsilon})$ uniformly in \bar{t} .

It will follow from our analysis that Assumption 1 defines an invariant region for the return map Π which roughly corresponds to the regime where $\bar{w} = \mathcal{O}(\sqrt{\varepsilon})$. More precisely, if an initial condition for (2.3) satisfies the assumption, it will be satisfied along the entire corresponding trajectory of (2.3). Finally, since $w = \sqrt{\varepsilon}\bar{w}$, Assumption 1 implies that $w = \mathcal{O}(\varepsilon)$ must hold in (2.1), uniformly in τ .

We state our next result in a slightly more general context than that of (2.3). The reason for this generalization is that we will modify (2.3) later to simplify our estimates of the return time $T^h(\bar{w})$. Thus, instead of (2.3), we now consider the following generalized system of equations,

$$(2.8a) \quad \bar{v}' = -\bar{z} + f_2\bar{v}^2 + \sqrt{\varepsilon}f_3\bar{v}^3 + \sqrt{\varepsilon}F(\bar{w}, \sqrt{\varepsilon}) + \bar{w}G(\bar{w}, \sqrt{\varepsilon}),$$

$$(2.8b) \quad \bar{z}' = \bar{v} - \bar{w} + \mathcal{O}(\varepsilon),$$

$$(2.8c) \quad \bar{w}' = \varepsilon(\mu - g_1\varepsilon\bar{z} + \mathcal{O}(\varepsilon)),$$

where F and G are assumed to be \mathcal{C}^n -smooth, for $n \geq 1$ sufficiently large, in both \bar{w} and $\sqrt{\varepsilon}$. Note that all the definitions and notation introduced in the context of (2.3) extend without modification to (2.8).

Proposition 2.2. *Let $\bar{\Pi} : \bar{\Delta}_- \rightarrow \bar{\Delta}_-$ and $\bar{\gamma}_\varepsilon^h$ be defined as above, and let $(h, \bar{w}) \in \bar{\Delta}_-$. Suppose that $h > 0$, with $h = \mathcal{O}(\varepsilon^M)$ for some $M > 0$ and $\varepsilon > 0$ sufficiently small, and that the trajectory starting at (h, \bar{w}) undergoes a small oscillation (“loop”) before returning to $\bar{\Delta}_-$. Then,*

$$(2.9) \quad (\hat{h}, \hat{w}) := \bar{\Pi}(h, \bar{w}) = (h + \sqrt{\varepsilon} d_{\sqrt{\varepsilon}}^h + \bar{w} d_{\bar{w}}^h + \mathcal{O}((\sqrt{\varepsilon} + \bar{w})^2), \bar{w} + \varepsilon \mu T^h(\bar{w}) + \mathcal{O}(\varepsilon^2)),$$

where the coefficients $d_{\sqrt{\varepsilon}}^h$ and $d_{\bar{w}}^h$ are defined as

$$(2.10) \quad d_{\sqrt{\varepsilon}}^h = \int_{-T^h}^{T^h} \nabla H(\bar{\gamma}_0^h(t)) \cdot (f_3 \bar{v}_0^h(t)^3, 0)^T dt$$

and

$$(2.11) \quad d_{\bar{w}}^h = \int_{-T^h}^{T^h} \nabla H(\bar{\gamma}_0^h(t)) \cdot (0, -1)^T dt,$$

respectively, and $\bar{\gamma}_0^h(t) = (\bar{v}_0^h, \bar{z}_0^h)(t)$ denotes the solution to (2.4) with $H(\bar{v}_0^h, \bar{z}_0^h) = h$.

Remark 2. Given Assumption 1, as well as the fact that $T^h(\bar{w}) \sim \sqrt{-2 \ln h}$ by Lemma A.2, $h = \mathcal{O}(\varepsilon^M)$ implies $\varepsilon T^h(\bar{w}) = \mathcal{O}(\varepsilon \sqrt{-\ln \varepsilon})$ in (2.9) for any $M > 0$. Moreover, the expansion for \hat{h} remains valid even if $M > \frac{1}{2}$, i.e., when the leading-order term in ε is given by $\sqrt{\varepsilon} d_{\sqrt{\varepsilon}}^h$. Hence, it follows that (2.9) describes the map $\bar{\Pi}$ up to an $\mathcal{O}(\varepsilon)$ -error. \blacksquare

Proof. We only sketch the proof here and refer the reader to [19] for details.

To derive the expression for \hat{w} , one makes use of the near-integrability of (2.8) as well as of regular perturbation theory.

To prove the assertion for \hat{h} , we first note that

$$(2.12) \quad \hat{h} - h := H(0, \hat{z}^h) - H(0, \bar{z}^h) = \int_{T_-^h(w)}^{T_+^h(w)} \frac{d}{dt} H(\bar{\gamma}_\varepsilon^h(t)) dt.$$

Since, to lowest order,

$$\frac{d}{dt} H(\bar{\gamma}_\varepsilon^h(t)) = \nabla H(\bar{\gamma}_\varepsilon^h(t)) \cdot (\bar{v}', \bar{z}')^T \Big|_{\bar{\gamma}_\varepsilon^h} = \nabla H(\bar{\gamma}_0^h(t)) \cdot (\bar{v}', \bar{z}')^T \Big|_{\bar{\gamma}_0^h},$$

and since H is a constant of motion, it follows with (2.8a) and (2.8b) that

$$(2.13) \quad \hat{h} - h = \int_{-T^h}^{T^h} \nabla H(\bar{\gamma}_0^h(t)) \cdot (f_3 \bar{v}_0^h(t)^3 + F(0, 0), 0)^T dt \sqrt{\varepsilon} \\ + \int_{-T^h}^{T^h} \nabla H(\bar{\gamma}_0^h(t)) \cdot (G(0, 0), -1)^T dt \bar{w} + \mathcal{O}(2),$$

see also [20]. (Here, $\mathcal{O}(2)$ denotes terms of at least second order in $\sqrt{\varepsilon}$ and \bar{w} .) Since, however, $(\bar{v}_0^h, \bar{z}_0^h)(-t) = (-\bar{v}_0^h, \bar{z}_0^h)(t)$ on $\bar{\gamma}_0^h$ by symmetry, a change of variables via $t \mapsto -t$ in combination with (2.5) shows

$$\int_{-T^h}^{T^h} \frac{\partial H}{\partial \bar{v}}(\bar{\gamma}_0^h(t)) dt = - \int_{-T^h}^{T^h} \bar{v}_0^h(t) e^{-2f_2 \bar{z}_0^h(t)} dt = - \int_{T^h}^{-T^h} \bar{v}_0^h(-t) e^{-2f_2 \bar{z}_0^h(-t)} d(-t) \\ = - \int_{-T^h}^{T^h} \frac{\partial H}{\partial \bar{v}}(\bar{\gamma}_0^h(t)) dt.$$

Therefore, the latter integral must be zero, which implies

$$\int_{-T^h}^{T^h} \frac{\partial H}{\partial \bar{v}}(\bar{\gamma}_0^h(t)) F(0, 0) dt = 0 \quad \text{and} \quad \int_{-T^h}^{T^h} \frac{\partial H}{\partial \bar{v}}(\bar{\gamma}_0^h(t)) G(0, 0) dt = 0.$$

It follows that (2.13) reduces to

$$\hat{h} - h = d_{\sqrt{\varepsilon}}^h \sqrt{\varepsilon} + d_{\bar{w}}^h \bar{w} + \mathcal{O}(2),$$

with the coefficients $d_{\sqrt{\varepsilon}}^h$ and $d_{\bar{w}}^h$ as defined in (2.10) and (2.11). This completes the proof. \blacksquare

Remark 3. Note that the functions $T_{\pm}^h(\bar{w})$ and $T^h(\bar{w})$ depend very sensitively on h , \bar{w} , and $\sqrt{\varepsilon}$; in fact, since $\lim_{(h, \bar{w}, \varepsilon) \rightarrow (0, 0, 0)} T^h(\bar{w}) = \infty$, $T^h(\bar{w})$ has a singularity at the origin. For this reason, it is not immediately obvious that $T_{+}^h(\bar{w})$ and $T_{-}^h(\bar{w})$ can be replaced by T^h and $-T^h$, respectively, in (2.12). However, the arguments in [19] can easily be extended to justify this point. \blacksquare

Given Proposition 2.2, we make the following observations:

- (i) Observe that for $\mu = 0$, the equations in (2.3) have an equilibrium point at the origin. The linearization of (2.3) about this equilibrium has a pair of purely imaginary eigenvalues, as well as a simple eigenvalue 0. The corresponding steady-state Hopf-type interactions mark the onset of small-amplitude oscillations in (2.3), see also [20, Theorem 3.1]. (Note that the presence of the zero eigenvalue, which is due to the absence of a linear \bar{w} -term in (2.3c), introduces a degeneracy at the origin in (2.3).)
- (ii) In order to obtain periodic orbits in (2.3), we have to require $h = \hat{h}$ and $\bar{w} = \hat{w}$, see the definition of $\bar{\Pi}$ in (2.9). Hence, to leading order, we must impose the condition

$$(2.14) \quad d_{\sqrt{\varepsilon}}^h \sqrt{\varepsilon} + d_{\bar{w}}^h \bar{w} = 0$$

on (h, \bar{w}) . To show that (2.14) can be solved for h and \bar{w} , we have to find the next-order correction to \hat{w} in (2.9): integrating (2.3c), we obtain

$$\hat{w} = \bar{w} + 2\varepsilon \mu T^h - g_1 \varepsilon^2 \int_{-T^h}^{T^h} \bar{z}(t) dt,$$

to leading order. Using (2.3a) to express \bar{z} in terms of \bar{v} , we find

$$\hat{w} \sim \bar{w} + \varepsilon \left(2\mu T^h - g_1 \varepsilon \int_{-T^h}^{T^h} (-\bar{v}'(t) + f_2 \bar{v}(t)^2) dt \right).$$

(Here and in the following, the tilde indicates a leading-order asymptotic approximation.) Since, moreover, $\bar{v}(-T^h) = 0 = \bar{v}(T^h)$ by definition, and since (2.3b) implies $\frac{d\bar{z}}{dt} \sim \bar{v}$ by Assumption 1, it follows that

$$\hat{w} \sim \bar{w} + 2\varepsilon \left(\mu T^h - f_2 g_1 \varepsilon \int_{\xi^h}^{\zeta^h} \bar{v}(\bar{z}) d\bar{z} \right).$$

Here, $\xi^h = \bar{z}(-T^h)$ and $\zeta^h = \bar{z}(0)$ denote the \bar{z} -values in $\bar{\Delta}$ corresponding to $\bar{\gamma}_{\varepsilon}^h(-T^h)$ and $\bar{\gamma}_{\varepsilon}^h(0)$, respectively. In sum, the requirement that $\bar{w} = \hat{w}$ gives

$$(2.15) \quad \mu T^h - f_2 g_1 \varepsilon \int_{\xi^h}^{\zeta^h} \bar{v}(\bar{z}) d\bar{z} = 0$$

to lowest order. Since $\frac{1}{T^h} \int_{\xi^h}^{\zeta^h} \bar{v}(\bar{z}) d\bar{z}$ increases monotonically in h as $h \rightarrow 0$, see [19], it follows that for ε and μ small and fixed, one can find h such that (2.15) holds. Given that h -value, one can use (2.14) to determine the associated value of \bar{w} .

- (iii) For μ and ε sufficiently small in (2.1), there exists a canard trajectory lying in the intersection of the manifolds $\mathcal{S}_\varepsilon^{a-}$ and $\mathcal{S}_\varepsilon^r$; this trajectory is the strong canard Γ_ε^0 . Since $\mathcal{S}_\varepsilon^{a-}$ and $\mathcal{S}_\varepsilon^r$ intersect transversely, as we will show in Section 2.3 below, Γ_ε^0 is well-defined; moreover, it is unique once specific sheets of \mathcal{S}_ε have been chosen. The associated *canard critical value* \bar{w}^c , i.e., the value of \bar{w} in the rescaled system (2.3) that corresponds to Γ_ε^0 , is given by

$$(2.16) \quad \bar{w}^c = -\frac{d_{\sqrt{\varepsilon}}^0}{d_{\bar{w}}^0} \sqrt{\varepsilon} + \mathcal{O}(\varepsilon),$$

where $d_{\sqrt{\varepsilon}}^0$ and $d_{\bar{w}}^0$ are obtained from (2.10) and (2.11) in the limit as $h \rightarrow 0$ [19]. In particular, since $\bar{w}^c \rightarrow 0$ for $\varepsilon \rightarrow 0$, (2.16) yields precisely the singular canard solution $\bar{\gamma}_0^0$ in this limit, cf. (2.6). Hence, as $h \rightarrow 0$, (2.3) undergoes a classical (two-dimensional) canard explosion at $\bar{w} = 0 = \varepsilon$ [20].

To evaluate (2.16), note that (2.5) implies

$$(2.17) \quad \frac{\partial H}{\partial \bar{v}} = -\bar{v}e^{-2f_2\bar{z}} \quad \text{and} \quad \frac{\partial H}{\partial \bar{z}} = (f_2\bar{v}^2 - \bar{z})e^{-2f_2\bar{z}}.$$

Using the parametrization of $\bar{\gamma}_0^0$ in (2.6) and taking into account that $T^0 = \infty$, one finds as in [19] that

$$(2.18) \quad d_{\sqrt{\varepsilon}}^0 = -\frac{3f_3}{16f_2^4} \sqrt{2\pi}e \quad \text{and} \quad d_{\bar{w}}^0 = -\frac{1}{2f_2} \sqrt{2\pi}e,$$

see Appendix A for details. Therefore, for given μ , the corresponding value of \bar{w}^c can be obtained from

$$(2.19) \quad \bar{w}^c = -\frac{3f_3}{8f_2^3} \sqrt{\varepsilon} + \mathcal{O}(\varepsilon);$$

note that $\bar{w}^c > 0$ due to $f_2 > 0$ and $f_3 < 0$.

These observations combined suggest the following: for $\varepsilon > 0$ fixed, system (2.3) undergoes a Hopf bifurcation at the origin for $\mu = 0$, by (i); this bifurcation gives rise to small-amplitude limit cycles in (2.3). These cycles will persist as long as both (2.14) and (2.15) can be satisfied, as shown in (ii). In that case, $\mu = \mathcal{O}(\varepsilon)$ must hold, since $T^h = \mathcal{O}(\sqrt{-\ln \varepsilon})$, $\zeta^h = \mathcal{O}(\sqrt{-\ln \varepsilon})$, and $\xi^h = \mathcal{O}(1)$ by Appendix A, while \bar{v} , f_2 , and g_1 are $\mathcal{O}(1)$ by assumption. Hence, for μ sufficiently small, the dynamics of (2.3) will be dominated by 0^k -type orbits, i.e., by MMO trajectories with Farey sequence $\{0^k\}$. As μ is increased, the evolution of \bar{w} in (2.3c) is governed by the positive, μ -dependent drift, with $\bar{w}' \sim \varepsilon\mu$. Since \bar{z} decreases with increasing \bar{w} , see (2.3b), it follows that h must also decrease, by Proposition 2.1. In other words, $h \rightarrow 0$ with increasing μ , and the system moves closer and closer toward a canard explosion, as discussed in (iii). Finally, for $\mu = \mu^c$ large enough, the \bar{w} -drift is sufficiently strong for the dynamics of (2.3) to bypass the fold region and enter the relaxation regime. (The corresponding “critical” μ -value μ^c will be discussed in detail in Section 2.5 below.)

In our analysis, we will focus primarily on the regime where μ is sufficiently large for 0^k -type orbits not to dominate the dynamics of (2.3) anymore. Since these orbits can occur only when (2.3) is close to Hopf bifurcation (i.e., as long as $\mu = \mathcal{O}(\varepsilon)$ and, hence, $\bar{w}' \sim 0$), the degeneracy of the equations at the Hopf point will not be of relevance to us. On the other hand, we will assume that $\mu < \mu^c$, i.e., that μ is not large enough for (2.3) to have entered the relaxation regime, which is characterized by L^0 -type orbits (trajectories with Farey sequence $\{L^0\}$).

As we will show, this “intermediate” regime corresponds precisely to the non-trivial mixed-mode dynamics of (1.5), with orbits of the type $\{L_j^{k_j}\}$, for $L_j, k_j \geq 1$. Correspondingly, h will have to be small, in the sense that $|h| = \mathcal{O}(\varepsilon^M)$ for some $M > 0$ “large;” however, h cannot

be exponentially small in ε , since trajectories must stay away from the strong canard Γ_ε^0 . The statement of Proposition 2.2 pertains exactly to that intermediate case.

Finally, we remark that we will restrict ourselves to a leading-order description of the return map Π in the following, as we did in the proof of Proposition 2.2. The resulting approximation will remain consistent as long as $h = \mathcal{O}(\varepsilon^M)$ is not “too large,” i.e., if $\varepsilon > 0$ is sufficiently small or if $M > 0$ is large enough: due to $T^h(\bar{w}) \sim \sqrt{-2 \ln h} \sim \sqrt{-2M \ln \varepsilon}$, the $\varepsilon T^h(\bar{w})$ -term in (2.9) will dominate the neglected terms of order $\mathcal{O}(\varepsilon)$ in that case. These considerations will be made more explicit in Proposition 3.4 below.

2.3. The transition from Σ^{in} to $\bar{\Delta}_-$. Let Π^{in} denote the transition map from Σ^{in} to $\bar{\Delta}_-$; see Sections 2.1 and 2.2 for the definitions of Σ^{in} and $\bar{\Delta}_-$. Moreover, let us introduce an intermediate section $\bar{\Delta}^{\text{in}}$ for the rescaled equations in (2.3), with $\bar{\Delta}^{\text{in}} = \{(\bar{v}, \bar{z}, \bar{w}) \mid \bar{v} = -\alpha\}$, and let Δ^{in} denote the corresponding section in (v, z, w) -space. (Here, $0 < \alpha \leq \rho$ is some arbitrary constant.) Then, we have the following result on the transition from Σ^{in} to $\bar{\Delta}_-$:

Proposition 2.3. *Let $(z^{\text{in}}, w^{\text{in}}) \in \Sigma^{\text{in}}$. Then, for $\varepsilon > 0$ sufficiently small,*

$$(2.20) \quad (h^-, \bar{w}^-) := \Pi^{\text{in}}(z^{\text{in}}, w^{\text{in}}) \\ = \left(\sqrt{\varepsilon} d_{\sqrt{\varepsilon}}^- + \frac{w^{\text{in}}}{\sqrt{\varepsilon}} d_{\bar{w}}^- + \mathcal{O}((\sqrt{\varepsilon} + w^{\text{in}})^2), \frac{w^{\text{in}}}{\sqrt{\varepsilon}} + w^{\text{in}} f_2 \mu \sqrt{\varepsilon} \ln \varepsilon + \mathcal{O}(\sqrt{\varepsilon}) \right),$$

where $d_{\sqrt{\varepsilon}}^-$ and $d_{\bar{w}}^-$ are defined by

$$(2.21) \quad d_{\sqrt{\varepsilon}}^- = \int_{-\infty}^0 \nabla H(\bar{\gamma}_0^0(t)) \cdot (f_3 \bar{v}_0^0(t)^3, 0)^T dt$$

and

$$(2.22) \quad d_{\bar{w}}^- = \int_{-\infty}^0 \nabla H(\bar{\gamma}_0^0(t)) \cdot (0, -1)^T dt,$$

respectively (see (2.10) and (2.11)), and $\bar{\gamma}_0^0(t) = (\bar{v}_0^0, \bar{z}_0^0)(t)$, as in (2.6).

Remark 4. Since $w^{\text{in}} = \mathcal{O}(\varepsilon)$ by Assumption 1, it follows that $\frac{w^{\text{in}}}{\sqrt{\varepsilon}}$ in (2.20) remains bounded as $\varepsilon \rightarrow 0$. ■

Proof. We first analyze the transition from Σ^{in} to Δ^{in} . To that end, we desingularize the reduced problem associated with (1.5) following the ideas in [2], see also the derivation of (2.44) in Section 2.4. First, we approximate z by $f(v)$, i.e., we restrict ourselves to the critical manifold \mathcal{S}_0^{a-} to leading order. The resulting “reduced” problem for (2.1) has the form

$$(2.23a) \quad f'(v) \dot{v} = v - w,$$

$$(2.23b) \quad \dot{w} = \varepsilon(\mu - g_1 f(v)).$$

(Note that this approximation is reasonable due to the form of (2.23b): since ε multiplies the entire right-hand side in (2.23b), the $\mathcal{O}(\varepsilon)$ -correction to $z = f(v)$ will be $\mathcal{O}(\varepsilon^2)$ for the dynamics.) The desingularized version of (2.23) is obtained by multiplying the right-hand sides by $-f'(v) = -(2f_2 v + 3f_3 v^2)$:

$$(2.24a) \quad \dot{v} = -(v - w),$$

$$(2.24b) \quad \dot{w} = -\varepsilon(\mu - g_1 f(v)) f'(v).$$

We now introduce a new variable

$$W = \frac{w}{v}$$

in (2.24). (The introduction of W corresponds to a projectivization of the vector field in (2.24) that desingularizes the dynamics close to the origin.) After the transformation to the variables (v, W) , system (2.24) becomes

$$(2.25a) \quad \dot{v} = -v(1 - W),$$

$$(2.25b) \quad \dot{W} = W(1 - W) - \varepsilon(\mu - g_1(f_2v^2 + f_3v^3))(2f_2 + 3f_3v).$$

Since we are not interested in the (time-parametrized) solutions of (2.25), but only in the corresponding orbits, we can rescale time by dividing out a factor of $1 - W$ from both right-hand sides in (2.25). Moreover, since we consider $v \in [-\rho, -\alpha\sqrt{\varepsilon}]$ (by the definition of Σ^{in} and Δ^{in}) and $w = \mathcal{O}(\varepsilon)$ (see Assumption 1), W is small. Hence, we can expand $(1 - W)^{-1} = 1 + W + \mathcal{O}(W^2)$ and neglect terms of second order and upward in (v, W) in (2.25b), approximating the resulting equations by

$$(2.26a) \quad \frac{dv}{d\tilde{t}} = -v,$$

$$(2.26b) \quad \frac{dW}{d\tilde{t}} = (1 - 2f_2\mu\varepsilon)W - 2f_2\mu\varepsilon - 3f_3\mu\varepsilon v.$$

(Here, \tilde{t} denotes the new rescaled time.)

Let \tilde{T} be the transition time from Σ^{in} to Δ^{in} under the flow of (2.26), and recall that $v = -\rho$ in Σ^{in} and $v = -\alpha\sqrt{\varepsilon}$ in Δ^{in} , respectively. Then, a simple computation using (2.26a) shows that \tilde{T} satisfies the identity

$$(2.27) \quad e^{\tilde{T}} = \frac{\rho}{\alpha} \frac{1}{\sqrt{\varepsilon}}.$$

(In particular, (2.27) implies that \tilde{T} depends only on α , ρ , and ε , but not on the specific choice of trajectory in (2.26).) By a direct integration of (2.26b), it follows with $\varepsilon v(\tilde{T}) = -\varepsilon\rho e^{-\tilde{T}} = \mathcal{O}(\varepsilon\sqrt{\varepsilon})$ that

$$(2.28) \quad W(\tilde{T}) = (W^{\text{in}} - 2f_2\mu\varepsilon)e^{(1-2f_2\mu\varepsilon)\tilde{T}} + 2f_2\mu\varepsilon + \mathcal{O}(\varepsilon\sqrt{\varepsilon}),$$

where $W^{\text{in}} = -\frac{w^{\text{in}}}{\rho}$ is the value of W in Σ^{in} . The geometry of (2.26) is illustrated in Figure 7.

Now, note that $w = -\alpha\sqrt{\varepsilon}W(\tilde{T})$ holds in Δ^{in} for the w -value corresponding to $W(\tilde{T})$. Hence, expanding the exponential in (2.28), we obtain

$$(2.29) \quad w(T) = w^{\text{in}} + w^{\text{in}}f_2\mu\varepsilon \ln \varepsilon + \mathcal{O}(\varepsilon),$$

where T denotes the transition time from Σ^{in} to Δ^{in} in the original system (2.24).

To complete the proof, we have to describe the second part of the transition, from Δ^{in} to $\bar{\Delta}_-$. To that end, we slightly modify the ideas of Section 2.2. Recall the rescaled equations in (2.3), as well as the singular version obtained for $\varepsilon = 0$, cf. (2.4), and the parametrization of the \bar{z} -coordinate therein by h . (For \bar{z} fixed, the corresponding (unique) value of h is determined from $H(0, \bar{z}) = h$, cf. (2.5).) Also, recall that for $h = 0$, there exists a parabolic level curve for H which corresponds to the special (singular canard) solution $\bar{\gamma}_0^0$ to (2.4) and which acts as a separatrix between the closed level curves (where $h > 0$) and the open ones (with $h < 0$).

Let $\bar{\Pi}^{\text{in}}$ denote the transition map from $\bar{\Delta}^{\text{in}}$ to $\bar{\Delta}_-$, and let $(\bar{z}, \bar{w}) \in \bar{\Delta}^{\text{in}}$. Since we are interested in describing the dynamics close to \mathcal{S}_0^{a-} , we may assume that $(-\alpha, \bar{z}, \bar{w})$ is the endpoint of a trajectory originating in $\mathcal{S}_\varepsilon^{a-}$. We claim that

$$(2.30) \quad (h^-, \bar{w}^-) = \bar{\Pi}^{\text{in}}(\bar{z}, \bar{w}) = (\sqrt{\varepsilon}d_{\sqrt{\varepsilon}}^- + \bar{w}d_{\bar{w}}^- + \mathcal{O}(2), \bar{w} + 2\alpha f_2\mu\varepsilon + \mathcal{O}(\varepsilon^2)),$$

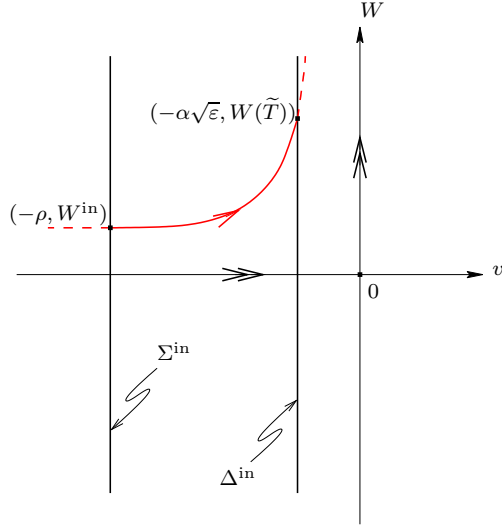


FIGURE 7. The geometry of system (2.26).

where $d_{\sqrt{\varepsilon}}^-$ and $d_{\bar{w}}^-$ are defined as in (2.21) and (2.22), respectively, and $\mathcal{O}(2) = \mathcal{O}((\sqrt{\varepsilon} + \bar{w})^2)$, as before.

To derive the expression for \bar{w}^- in (2.30), we simply integrate the \bar{w} -equation in (2.3) to obtain $\bar{w}^- = \bar{w} + \varepsilon\mu\bar{T}^{\text{in}} + \mathcal{O}(\varepsilon^2)$, where \bar{T}^{in} denotes the transition time from $\bar{\Delta}^{\text{in}}$ to $\bar{\Delta}$ in (2.4). Then, by integrating (2.4) directly from $\bar{v} = -\alpha$ to $\bar{v} = 0$ along $\bar{\gamma}_0^0$, we find $\bar{T}^{\text{in}} = 2\alpha f_2$.

The expression for h^- is obtained from the near-integrability of (2.3) and from the analysis in [20], see also the proof of Proposition 2.2. More specifically, the condition for $(\bar{v}, \bar{z}, \bar{w})$ to be on a trajectory originating in $\mathcal{S}_{\varepsilon}^{a-}$ is

$$(2.31) \quad h^- = \sqrt{\varepsilon}d_{\sqrt{\varepsilon}}^- + \bar{w}d_{\bar{w}}^- + \mathcal{O}(2),$$

which proves (2.30). (Here, the limits of integration in the definition of $d_{\sqrt{\varepsilon}}^-$ and $d_{\bar{w}}^-$ follow from the fact that $T_+^h(0) \rightarrow \infty$ as $h \rightarrow 0$.)

Finally, the assertion of the proposition follows by combining (2.29) and (2.30), taking into account that $\bar{w} = \frac{w}{\sqrt{\varepsilon}}$. \blacksquare

Remark 5. Note that to the order considered here, the definition of the intermediate section $\bar{\Delta}^{\text{in}}$ does not influence the asymptotics of $\bar{\Pi}^{\text{in}}$, as expected. \blacksquare

Proposition 2.3 has the following important implication: recall the set $\mathcal{C}_{\varepsilon}^- \subset \bar{\Delta}_-$ consisting of the endpoints of trajectories starting in $\mathcal{S}_{\varepsilon}^{a-}$. Then, it follows from (2.31) that $\mathcal{C}_{\varepsilon}^-$ can be represented as the graph of a function $h^-(\bar{w}, \sqrt{\varepsilon})$ satisfying

$$(2.32) \quad h^-(\bar{w}, \sqrt{\varepsilon}) = \sqrt{\varepsilon}d_{\sqrt{\varepsilon}}^- + \bar{w}d_{\bar{w}}^- + \mathcal{O}(2).$$

In analogy to (2.21) and (2.22), one can define the coefficients

$$(2.33) \quad d_{\sqrt{\varepsilon}}^+ = - \int_0^{\infty} \nabla H(\bar{\gamma}_0^0(t)) \cdot (f_3 \bar{v}_0^0(t)^3, 0)^T dt$$

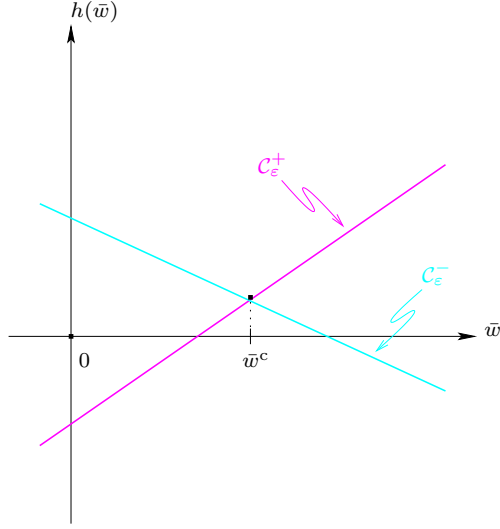


FIGURE 8. The curves $\mathcal{C}_\varepsilon^-$ and $\mathcal{C}_\varepsilon^+$.

and

$$(2.34) \quad d_{\bar{w}}^+ = - \int_0^\infty \nabla H(\bar{\gamma}_0^0(t)) \cdot (0, -1)^T dt$$

to describe the leading-order dynamics on $\mathcal{S}_\varepsilon^r$. Hence, it follows that the set $\mathcal{C}_\varepsilon^+$ can also be represented as the graph of a function $h^+(\bar{w}, \sqrt{\varepsilon})$ satisfying

$$(2.35) \quad h^+(\bar{w}, \sqrt{\varepsilon}) = \sqrt{\varepsilon} d_{\bar{w}}^+ + \bar{w} d_{\bar{w}}^+ + \mathcal{O}(2).$$

Note that $d_{\bar{w}}^\pm = \mp \frac{1}{2} d_{\bar{w}}^0$ and, similarly, $d_{\bar{w}}^\pm = \mp \frac{1}{2} d_{\bar{w}}^0$ by symmetry, where $d_{\bar{w}}^0$ and $d_{\bar{w}}^0$ are defined in (2.18).

Given the above representation of $\mathcal{C}_\varepsilon^\mp$, we make the following observations:

- (i) Due to $d_{\bar{w}}^- < 0$ and $d_{\bar{w}}^+ > 0$, (2.32) and (2.35) imply that $\mathcal{C}_\varepsilon^-$ and $\mathcal{C}_\varepsilon^+$ intersect transversely for $\bar{w} = \bar{w}^c$, with \bar{w}^c as in (2.19). Hence, the strong canard Γ_ε^0 is indeed well-defined; recall the discussion in Section 1. In particular, the resulting geometry justifies the heuristic picture sketched in Figure 4, cf. Figure 8.
- (ii) Similarly, the representations in (2.32) and (2.35) will be used in the definition of secondary canards Γ_ε^j , for $j \geq 1$, as the transverse intersection of subsequent iterates of $\mathcal{C}_\varepsilon^-$ under $\bar{\Pi}$ with $\mathcal{C}_\varepsilon^+$, see Section 3.3 for details.

2.4. The transition from $\bar{\Delta}_-$ to Σ^{out} . We now discuss the behavior of trajectories that exit the fold region in the direction of positive v and that then undergo relaxation. We begin by making a change of coordinates which transforms $\mathcal{C}_\varepsilon^+$ to the plane $\bar{z} = \bar{z}^0$, where \bar{z}^0 denotes the \bar{z} -value corresponding to $h = 0$ in (2.3). To that end, we define

$$(2.36) \quad \Delta \bar{z}(\bar{w}, \sqrt{\varepsilon}) = \bar{z}^0 - \bar{z}^{h^+(\bar{w}, \sqrt{\varepsilon})},$$

where h^+ is as in (2.35), and we let

$$(2.37) \quad \tilde{z} = \bar{z} + \Delta \bar{z}(\bar{w}, \sqrt{\varepsilon}).$$

The transformation in (2.37) is introduced to “flatten” the repelling sheet $\mathcal{S}_\varepsilon^r$ of \mathcal{S}_ε in Δ , for $\varepsilon > 0$ sufficiently small: by (2.36), the \bar{z} -value corresponding to h^+ , \bar{z}^{h^+} is transformed into $\bar{z}^{h^+} + \bar{z}^0 -$

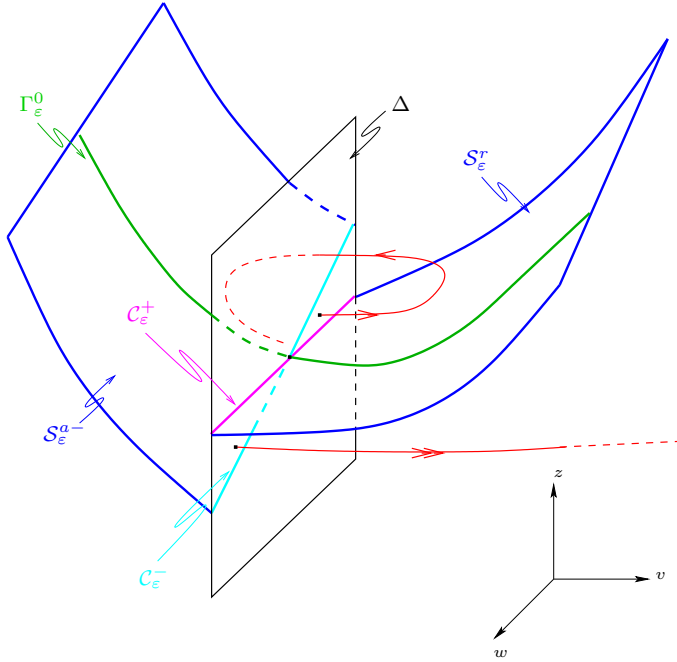


FIGURE 9. The curves $\mathcal{C}_\varepsilon^-$ and $\mathcal{C}_\varepsilon^+$ after the transformation in (2.35).

$\tilde{z}^{h^+} = \tilde{z}^0$; hence, $\mathcal{C}_\varepsilon^+$ is represented as the graph of the zero function after the transformation:

$$(2.38) \quad \mathcal{C}_\varepsilon^+ = \{(0, \bar{w}) \mid \bar{w} = \mathcal{O}(\sqrt{\varepsilon})\}.$$

Recall that in the singular limit of $\varepsilon = 0 = \bar{w}$, $h = 0$ separates the small-oscillation regime in (2.3), where $h > 0$, from the relaxation regime (with $h < 0$), see Proposition 2.1. By introducing \tilde{z} , as defined in (2.37), we extend this characterization to the case where ε (and, hence, also \bar{w}) is positive but small: given (2.38), trajectories with $h < 0$ will end up “below” $\mathcal{S}_\varepsilon^r$ in Δ^- , implying that they will leave the fold region and undergo relaxation; trajectories with $h > 0$, on the other hand, will remain trapped “above” $\mathcal{S}_\varepsilon^r$ and will therefore stay in the small-oscillation regime close to ℓ^- . (This fact will simplify the following analysis and, in particular, the study of secondary canards in Section 3.3, since it will facilitate the evaluation of the conditions that define these canard trajectories.)

In analogy to h^+ , the function h^- in (2.32) is mapped to

$$(2.39) \quad \begin{aligned} h^0(\bar{w}) &\equiv h^0(\bar{w}, \sqrt{\varepsilon}) = h^-(\bar{w}, \sqrt{\varepsilon}) - h^+(\bar{w}, \sqrt{\varepsilon}) \\ &= \sqrt{\varepsilon}(d_{\sqrt{\varepsilon}}^- - d_{\sqrt{\varepsilon}}^+) + \bar{w}(d_{\bar{w}}^- - d_{\bar{w}}^+) + \mathcal{O}(2) \\ &= \sqrt{\varepsilon}d_{\sqrt{\varepsilon}}^0 + \bar{w}d_{\bar{w}}^0 + \mathcal{O}(2) \end{aligned}$$

by (2.37), where we suppress the $\sqrt{\varepsilon}$ -dependence of h^0 for brevity. Hence, after performing the coordinate transformation in (2.37), we find that $\mathcal{C}_\varepsilon^-$ is given by

$$(2.40) \quad \mathcal{C}_\varepsilon^- = \{(h^0(\bar{w}), \bar{w}) \mid \bar{w} = \mathcal{O}(\sqrt{\varepsilon})\}.$$

The situation is illustrated in Figure 9; note the change from Figure 4, in that $\mathcal{C}_\varepsilon^+$ is now parallel to the w -axis, with $\mathcal{C}_\varepsilon^-$ “tilted” accordingly.

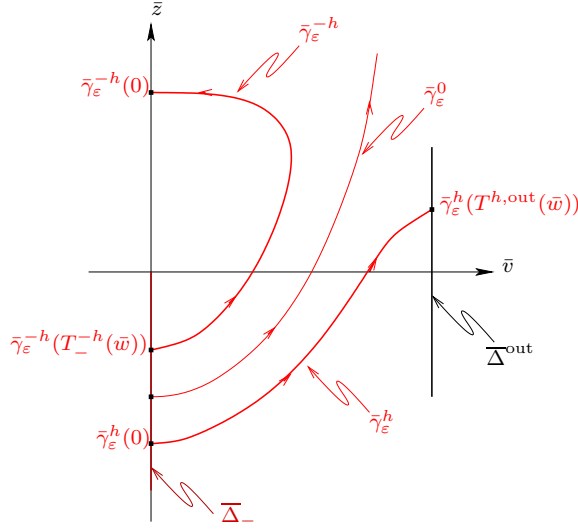


FIGURE 10. The definition of $T^{h,\text{out}}(\bar{w})$ for $h < 0$.

Next, we note that the higher-order terms that are introduced into (2.3) by the transformation in (2.37) are precisely of the form $\mathcal{O}(\bar{w}, \sqrt{\varepsilon})$. Hence, the resulting, transformed system is of the form (2.8), and the results of Proposition 2.2 can be applied directly to it.

Finally, in analogy to the transition times $T^h(\bar{w})$ defined for $h > 0$ above, we now define

$$(2.41) \quad T^{h,\text{out}}(\bar{w}) = -T_-^{-h}(\bar{w})$$

for $h < 0$. We have the following result on the transition from $\bar{\Delta}_-$ to Σ^{out} :

Proposition 2.4. *Let $(h, \bar{w}) \in \bar{\Delta}_-$, with $h < 0$ and $h = \mathcal{O}(\varepsilon^M)$ for some $M > 0$ and $\varepsilon > 0$ sufficiently small. Then,*

$$(2.42) \quad (z^{\text{out}}, w^{\text{out}}) := \Pi^{\text{out}}(h, \bar{w}) = (\varepsilon \tilde{z}^{\text{out}} + \mathcal{O}(\varepsilon \ln \varepsilon), \sqrt{\varepsilon} \bar{w} + \varepsilon \sqrt{\varepsilon} T^{h,\text{out}}(\bar{w}) \mu + \mathcal{O}(\varepsilon \sqrt{\varepsilon})),$$

where \tilde{z}^{out} is the \tilde{z} -value corresponding to $h^{\text{out}} = h + \sqrt{\varepsilon} d_{\sqrt{\varepsilon}}^{\text{out}} + \bar{w} d_{\bar{w}}^{\text{out}}$, with $d_{\sqrt{\varepsilon}}^{\text{out}}$ and $d_{\bar{w}}^{\text{out}}$ defined by

$$d_{\sqrt{\varepsilon}}^{\text{out}} = - \int_0^{T^{h,\text{out}}(\bar{w})} \nabla H(\bar{\gamma}_0^h(t)) \cdot (f_3 \bar{v}_0^h(t)^3, 0)^T dt$$

and

$$d_{\bar{w}}^{\text{out}} = - \int_0^{T^{h,\text{out}}(\bar{w})} \nabla H(\bar{\gamma}_0^h(t)) \cdot (0, -1)^T dt,$$

respectively (see (2.10) and (2.11)).

Proof. For $(h, \bar{w}) \in \bar{\Delta}_-$ with $h < 0$ and $h = \mathcal{O}(\varepsilon^M)$, let $\bar{\Pi}^{\text{out}}$ denote the time- $T^{h,\text{out}}(\bar{w})$ transition map for (2.8), i.e., for the system obtained from (2.3) after the transformation to \tilde{z} . Moreover, let $\bar{\Delta}^{\text{out}} := \bar{\Pi}^{\text{out}}(\bar{\Delta}_-)$, which implies that the definition of the intermediate section $\bar{\Delta}^{\text{out}}$ is now “implicit” (\bar{w} -dependent); cf. Figure 10. Then, it follows as in the proof of Proposition 2.2 that

$$(2.43) \quad (h^{\text{out}}, \bar{w}^{\text{out}}) := \bar{\Pi}^{\text{out}}(h, \bar{w}) = (h + \sqrt{\varepsilon} d_{\sqrt{\varepsilon}}^{\text{out}} + \bar{w} d_{\bar{w}}^{\text{out}} + \mathcal{O}(2), \bar{w} + \varepsilon T^{h,\text{out}}(\bar{w}) \mu + \mathcal{O}(\varepsilon \sqrt{\varepsilon})),$$

where again $\mathcal{O}(2) = \mathcal{O}((\sqrt{\varepsilon} + \bar{w})^2)$, $T^{h,\text{out}}(\bar{w})$ is, by the definition of $\bar{\Delta}^{\text{out}}$, the transition time from $\bar{\Delta}$ to $\bar{\Delta}^{\text{out}}$ in (2.8), and $d_{\sqrt{\varepsilon}}^{\text{out}}$ and $d_{\bar{w}}^{\text{out}}$ are defined as above.

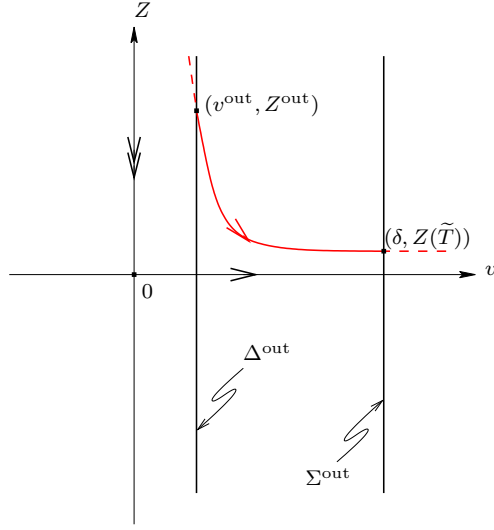


FIGURE 11. The geometry of system (2.46).

To study the second part of the transition, from $\overline{\Delta}^{\text{out}}$ to Σ^{out} , we introduce a new variable Z in the original (unmodified) system (1.5), where Z is defined by $z = v^2 Z$. This transformation serves to desingularize (1.5) close to the origin, for v positive and small: in terms of (v, Z, w) , (1.5) becomes

$$(2.44a) \quad v' = v^2(-Z + f_2 + f_3 v),$$

$$(2.44b) \quad Z' = -2Zv(-Z + f_2 + f_3 v) + \frac{\varepsilon}{v} \left(1 - \frac{w}{v}\right),$$

$$(2.44c) \quad w' = \varepsilon^2(\mu - g_1 v^2 Z).$$

Now, let $\Psi(v, Z) = v^2(-Z + f_2 + f_3 v)$; then, dividing the right-hand sides of (2.44) by $\Psi(v, Z)$, we find

$$(2.45a) \quad \frac{dv}{d\hat{t}} = 1,$$

$$(2.45b) \quad \frac{dZ}{d\hat{t}} = -\frac{2}{v}Z + \frac{\varepsilon}{v\Psi(v, Z)} \left(1 - \frac{w}{v}\right),$$

$$(2.45c) \quad \frac{dw}{d\hat{t}} = \frac{\varepsilon^2}{\Psi(v, Z)}(\mu - g_1 v^2 Z);$$

here, \hat{t} denotes the new, rescaled time.

We first investigate the dynamics of Z in the transition. Let Δ^{out} denote the section in (v, Z, w) -space corresponding to $\overline{\Delta}^{\text{out}}$. Given an initial v -value v^{out} for (1.5) in Δ^{out} , it then follows that $v^{\text{out}} = \mathcal{O}(\sqrt{\varepsilon} T^{h, \text{out}}(\bar{w})) = \mathcal{O}(\sqrt{-\varepsilon \ln \varepsilon})$ must hold, which, together with (2.45a) and $w = \mathcal{O}(\varepsilon)$ (see Assumption 1), implies that $\frac{w}{v}$ is small throughout. Since, moreover, $\frac{dw}{d\hat{t}} = \mathcal{O}(\varepsilon(\ln \varepsilon)^{-1})$ by (2.45c), w remains almost constant, and we can neglect its evolution.

Hence, expanding Ψ in (2.45b) and truncating the resulting equation, we find that to leading order,

$$(2.46) \quad \begin{aligned} \frac{dv}{dt} &= 1, \\ \frac{dZ}{dt} &= -\frac{2}{v}Z + \frac{\varepsilon}{f_2 v^3} (1 + \mathcal{O}(v, Z)). \end{aligned}$$

The transition from Δ^{out} to Σ^{out} under the flow of (2.46) is illustrated in Figure 11. Now, for $(v^{\text{out}}, Z^{\text{out}}) \in \Delta^{\text{out}}$, we can solve (2.46) explicitly to leading order by variation of constants, which gives

$$(2.47) \quad Z(v) = \frac{(v^{\text{out}})^2 Z^{\text{out}}}{v^2} + \frac{\varepsilon}{f_2 v^2} \ln \frac{v}{v^{\text{out}}} + \mathcal{O}(\varepsilon).$$

Here, we have neglected the effect of the inhomogeneous $\mathcal{O}(v, Z)$ -terms in (2.46), since it can be shown that these contribute only terms of order $\mathcal{O}(\varepsilon)$ in (2.47). Now, the corresponding expression in the original variable z is given by

$$z(v) = \varepsilon \tilde{z}^{\text{out}} + \frac{\varepsilon}{f_2} \ln \frac{v}{v^{\text{out}}} + \mathcal{O}(\varepsilon)$$

for \tilde{z}^{out} in $\bar{\Delta}^{\text{out}}$, where we have used $v^2 Z = z = \varepsilon \tilde{z}$. Recalling that $v^{\text{out}} = \mathcal{O}(\sqrt{-\varepsilon \ln \varepsilon})$ as well as that $v = \delta$ in Σ^{out} , we find

$$(2.48) \quad z(T) = \varepsilon \tilde{z}^{\text{out}} + \mathcal{O}(\varepsilon \ln \varepsilon);$$

here, T denotes the transition time from Δ^{out} to Σ^{out} .

We now use the estimate for $z(T)$ in (2.48) to derive an estimate for $w(T)$. Since $dv = \Psi(v, Z) dt$, see (2.44a), and since, moreover, $Z = \mathcal{O}(1)$, there certainly holds $\frac{1}{2}\Psi(v, 0) \leq \Psi(v, Z)$. Hence, it follows that T satisfies the inequality

$$(2.49) \quad T \leq 2 \int_{v^{\text{out}}}^{\delta} \frac{dv}{\Psi(v, 0)},$$

to leading order. The integral on the right-hand side of (2.49) can be evaluated explicitly, giving

$$T \leq \frac{2}{f_2 v^{\text{out}}} - \frac{f_3}{f_2^2} \ln \varepsilon + \mathcal{O}(1).$$

Integrating the w -equation (2.44c) directly and taking into account (2.43) as well as $v^{\text{out}} = \mathcal{O}(\sqrt{-\varepsilon \ln \varepsilon})$ and $w = \sqrt{\varepsilon} \bar{w}$, we obtain

$$(2.50) \quad \begin{aligned} w(T) &= \sqrt{\varepsilon} \bar{w}^{\text{out}} + \varepsilon^2 \left(\mu T - g_1 \int_{v^{\text{out}}}^{\delta} \frac{z(v)}{\Psi(v, 0)} dv \right) + \mathcal{O}(\varepsilon^3) \\ &= \sqrt{\varepsilon} \bar{w} + \varepsilon \sqrt{\varepsilon} T^{h, \text{out}}(\bar{w}) \mu + \mathcal{O}(\varepsilon \sqrt{\varepsilon}). \end{aligned}$$

To complete the proof, it remains to collect the above estimates: with \tilde{z}^{out} the \tilde{z} -value corresponding to h^{out} (see (2.43)), we find the desired expression for z^{out} in (2.42) from (2.48). The estimate for the w^{out} -component of Π^{out} follows directly from (2.50). \blacksquare

2.5. The global return mechanism. In this subsection, we describe the global mechanism that determines the return of trajectories of (1.5) from Σ^{out} back to Σ^{in} . The corresponding return map will be denoted by Π^{ret} . Since the necessary analysis is largely based on standard geometric singular perturbation (Fenichel) theory [11], we do not discuss it in full detail here; moreover, for the sake of exposition, we will make a number of additional, simplifying assumptions throughout this subsection. As it turns out, the resulting leading-order asymptotics of Π^{ret} will still give an

approximation for the composite return map Π that is consistent to the order considered here; cf. Section 4 below.

In a first approximation, we may assume that $z = f(v)$ is satisfied, i.e., for $\varepsilon > 0$ sufficiently small, we may restrict ourselves to the singular dynamics of (1.5) on \mathcal{S}_0 . We recall the definition of the corresponding reduced system from (2.24):

$$(2.51a) \quad \dot{v} = -(v - w),$$

$$(2.51b) \quad \dot{w} = -\varepsilon(\mu - g_1 f(v)) f'(v).$$

Moreover, we can safely neglect the w -term on the right-hand side of (2.51a), since this term is assumed to be small throughout, see Assumption 1. Then, we rewrite (2.51) with v as the independent variable, i.e., we divide (2.51b) by (2.51a), which gives

$$(2.52) \quad \frac{dw}{dv} = \varepsilon(\mu - g_1 f(v)) \frac{f'(v)}{v}.$$

Given an initial v -value v^* on \mathcal{S}_0 , (2.52) can be integrated explicitly as follows:

$$(2.53) \quad w(v) - w(v^*) = \varepsilon \mathcal{G}(v^*, v, \mu) := \varepsilon \int_{v^*}^v (\mu - g_1 f(\sigma)) \frac{f'(\sigma)}{\sigma} d\sigma.$$

To describe the return of trajectories from Σ^{out} to Σ^{in} under the flow of (2.52) on \mathcal{S}_0 , we need to consider two separate parts of the transition, namely, the parts where v evolves along \mathcal{S}_0^{a+} and \mathcal{S}_0^{a-} , respectively. (Note that by restricting ourselves to the slow flow on \mathcal{S}_0 , we are implicitly neglecting the transition from ℓ^- to \mathcal{S}_0^{a+} and from ℓ^+ to \mathcal{S}_0^{a-} , respectively, under the fast flow of (1.5), since, by standard Fenichel theory [11], the corresponding contributions to Π^{ret} are of higher order; cf. Figure 12.) The relevant integrals in (2.53) are given by

$$\mathcal{G}(v_0, v_{\max}, \mu) = \int_{v_0}^{v_{\max}} (\mu - g_1 f(\sigma)) \frac{f'(\sigma)}{\sigma} d\sigma$$

and

$$\mathcal{G}(v_{\max}^*, -\rho, \mu) = \int_{v_{\max}^*}^{-\rho} (\mu - g_1 f(\sigma)) \frac{f'(\sigma)}{\sigma} d\sigma,$$

respectively. Here, v_{\max} is the value of v for which f attains its local maximum, $v_{\max}^* < 0$ is defined by the requirement that $f(v_{\max}^*) = f(v_{\max})$, and $v_0 > 0$ is the second (non-trivial) zero of f , with $f(v_0) = 0$; see again Figure 12. To facilitate further the evaluation of these integrals, we will approximate $\mathcal{G}(v_{\max}^*, -\rho, \mu)$ by $\mathcal{G}(v_{\max}^*, 0, \mu)$, i.e., we will evaluate the integral over \mathcal{S}_0^{a-} down to and including ℓ^- . (In fact, a straightforward though lengthy computation shows that this approximation will offset precisely the part of the $\mathcal{O}(\sqrt{\varepsilon})$ -error term in Π^{in} that is independent of w^{in} , cf. Proposition 2.3.)

Hence, in sum, it follows that the w -component \hat{w} of $\Pi^{\text{ret}} : \Sigma^{\text{out}} \rightarrow \Sigma^{\text{in}}$ is given by

$$(2.54) \quad \hat{w} = w + \varepsilon(\mathcal{G}(v_0, v_{\max}, \mu) + \mathcal{G}(v_{\max}^*, 0, \mu)),$$

to lowest order. In particular, note that (2.54) determines the global ‘‘amount of return’’ of w after one relaxation cycle, expressed as a function of the parameter μ . (This fact will prove especially useful in Section 3 below.) Let

$$D_\mu = \frac{d}{d\mu} (\mathcal{G}(v_0, v_{\max}, \mu) + \mathcal{G}(v_{\max}^*, 0, \mu)),$$

and observe that the rate of change of the return point with respect to μ is given by $D_\mu \varepsilon$. From the above, it follows that D_μ can easily be approximated to lowest order in terms of the function

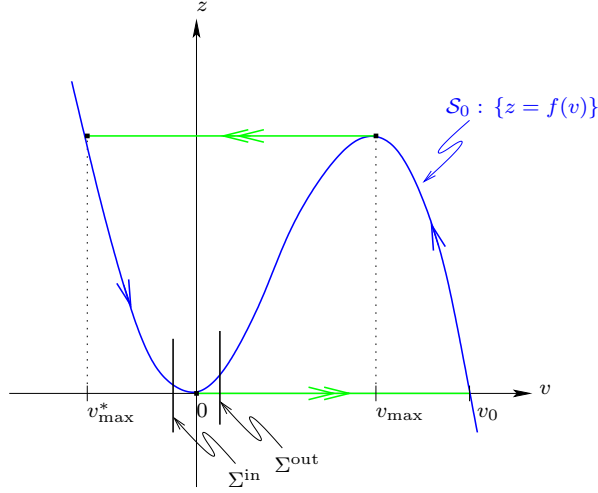


FIGURE 12. The geometry of the global return mechanism.

\mathcal{G} : by the definition of \mathcal{G} and making use of the fact that

$$v_{\max} = -\frac{2f_2}{3f_3}, \quad v_{\max}^* = \frac{f_2}{3f_3}, \quad \text{and} \quad v_0 = -\frac{f_2}{f_3},$$

we obtain

$$(2.55) \quad \mathcal{G}(v_0, v_{\max}, \mu) + \mathcal{G}(v_{\max}^*, 0, \mu) = \frac{g_1}{18} \frac{f_2^5}{f_3^3} - \mu \frac{f_2^2}{f_3}.$$

Differentiating (2.55) with respect to μ , we find $D_\mu = -\frac{f_2^2}{f_3}$.

Similarly, the critical value μ^c of μ for which MMOs cease to exist in (1.5) is to leading order determined by requiring $\hat{w} = w$ in (2.54) or, alternatively, by finding μ such that (2.55) equals zero; again, a simple computation shows

$$(2.56) \quad \mu^c = \frac{g_1}{18} \frac{f_2^3}{f_3^2}.$$

For $\mu > \mu^c$, the dynamics of (1.5) is in the pure relaxation regime, in the sense that the only admissible periodic trajectories are those with Farey sequence $\{L^0\}$.

Remark 6. Note that the fold line ℓ^+ will in general contribute logarithmic terms (in ε) to (2.56); see, e.g., [34]. In our case, however, these terms can be shown to be of higher order and are hence negligible. \blacksquare

2.6. Summary: the return map $\Pi : \bar{\Delta}_- \rightarrow \bar{\Delta}_-$. Given the analysis of the previous subsections, we can now define the composite return map $\Pi : \bar{\Delta}_- \rightarrow \bar{\Delta}_-$. We note that the definition of Π will depend on the sign of h : if $h > 0$, the corresponding trajectory of (1.5) will remain in the fold region, i.e., in the small-oscillation regime, and undergo another “loop.” Hence, the return to $\bar{\Delta}_-$ is described by $\bar{\Pi}$ in that case, cf. Proposition 2.2. If, on the other hand, $h < 0$, the trajectory will exit the fold region and undergo relaxation, i.e., it will leave $\bar{\Delta}_-$ in the direction of the fast flow of (1.5), move “up” the slow manifold $\mathcal{S}_\varepsilon^{a+}$ under the slow flow until it reaches ℓ^+ , “jump” to $\mathcal{S}_\varepsilon^{a-}$, and move “down” that manifold until it re-enters a neighborhood of ℓ^- , cf., e.g., Figure 12. Therefore, the return to $\bar{\Delta}_-$ is described by the composition of Π^{out} , Π^{ret} , and Π^{in} in that case,

see Propositions 2.3 and 2.4 as well as the discussion in Section 2.5. Hence, in sum, the desired expression for Π is given as follows:

$$(2.57) \quad \Pi(h, \bar{w}) = \begin{cases} \bar{\Pi}(h, \bar{w}) & \text{if } h > 0, \\ \Pi^{\text{in}} \circ \Pi^{\text{ret}} \circ \Pi^{\text{out}}(h, \bar{w}) & \text{if } h < 0. \end{cases}$$

3. PARTIAL DIMENSION REDUCTION FOR THE MAP Π

In this section, we show how the two-dimensional return map Π formulated in Section 2.6 can be accurately approximated by an appropriately defined one-dimensional map, which we denote by Φ . More precisely, we will prove that the resulting approximation error will be exponentially small in ε . The reduction itself is carried out in two steps: first, the map Π is restricted from the two-dimensional section $\bar{\Delta}_-$ to a union of one-dimensional curves $\cup \mathcal{C}_\varepsilon^j$, to be specified in Section 3.1. In the second step, this restricted map is reduced further, in Section 3.4, to a map Φ that is defined on the single curve $\mathcal{C}_\varepsilon^-$. For a detailed study of the dynamics of Φ , we require some preparatory analysis: in Section 3.2, we approximate the derivative $\frac{d\Pi}{d\bar{w}}$, which, in turn, allows us to derive estimates for $\frac{d\Phi}{d\bar{w}}$ in Section 3.5. The latter are needed for analyzing the contractive (or expansive) properties of the reduced flow under Φ . In Section 3.3, we characterize the secondary canards introduced in Section 1 above: we derive the defining conditions for these trajectories, and we use those conditions to describe the family of the associated sectors of rotation. Finally, in Section 3.6, we study the dynamics of Φ on these sectors by combining the results of Sections 3.3 and 3.5, and we derive precise asymptotic estimates for the bifurcation structure of the resulting mixed-mode dynamics in (1.5).

3.1. The curves $\mathcal{C}_\varepsilon^j$. In this subsection, we perform the first step in our exponentially accurate reduction of Π to a one-dimensional map Φ . More precisely, we show how Π can be restricted from $\bar{\Delta}_-$ to a union of one-dimensional curves $\cup \mathcal{C}_\varepsilon^j$ that will be defined below.

Recall the definition of the curves $\mathcal{C}_\varepsilon^-$ and $\mathcal{C}_\varepsilon^+$ from Section 2.1, as well as the fact that $\mathcal{C}_\varepsilon^-$ can be represented as the graph of the function $h^0(\bar{w})$ defined in (2.39), see (2.40). For $j \geq 1$, we now make the inductive definition

$$\mathcal{C}_\varepsilon^j = \bar{\Pi}(\{(h, \bar{w}) \in \mathcal{C}_\varepsilon^{j-1} \mid h > 0\}),$$

where we define $\mathcal{C}_\varepsilon^0 \equiv \mathcal{C}_\varepsilon^-$ for the zeroth iterate of $\mathcal{C}_\varepsilon^-$ under $\bar{\Pi}$. Next, we show that for $j \geq 1$, each set $\mathcal{C}_\varepsilon^j$ can be written as the graph of a function $h^j(\bar{w})$, in analogy to the representation of $\mathcal{C}_\varepsilon^-$ given in (2.40). We first consider the case when $j = 1$. Note that by Proposition 2.2,

$$(h^1, \bar{w}^1) = \bar{\Pi}(h^0(\bar{w}), \bar{w}) = (h^0(\bar{w}) + \sqrt{\varepsilon} d_{\sqrt{\varepsilon}}^{h^0(\bar{w})} + \bar{w} d_{\bar{w}}^{h^0(\bar{w})} + \mathcal{O}(2), \bar{w} + \varepsilon \mu T^{h^0(\bar{w})} + \mathcal{O}(\varepsilon^2)),$$

where $\mathcal{O}(2) = \mathcal{O}((\sqrt{\varepsilon} + \bar{w})^2)$, as before. Since $h^0 = \sqrt{\varepsilon} d_{\sqrt{\varepsilon}}^0 + \bar{w} d_{\bar{w}}^0 + \mathcal{O}(2)$ by (2.39) and since $d_{\sqrt{\varepsilon}}^{h^0} \sim d_{\sqrt{\varepsilon}}^0$ and $d_{\bar{w}}^{h^0} \sim d_{\bar{w}}^0$, respectively, it follows that

$$(3.1) \quad h^1(\bar{w}) = 2\sqrt{\varepsilon} d_{\sqrt{\varepsilon}}^0 + 2\bar{w} d_{\bar{w}}^0 + \mathcal{O}(2).$$

Similarly, for higher iterates of $\bar{\Pi}$, there holds

$$(3.2) \quad (h^j, \bar{w}^j) = \bar{\Pi}^j(h^0(\bar{w}), \bar{w}) \\ = \left(h^0(\bar{w}) + \sqrt{\varepsilon} \sum_{i=0}^{j-1} d_{\sqrt{\varepsilon}}^{h^i(\bar{w})} + \bar{w} \sum_{i=0}^{j-1} d_{\bar{w}}^{h^i(\bar{w})} + \mathcal{O}(\varepsilon), \bar{w} + 2\varepsilon \mu \sum_{i=0}^{j-1} T^{h^i(\bar{w})} + \mathcal{O}(\varepsilon^2) \right)$$

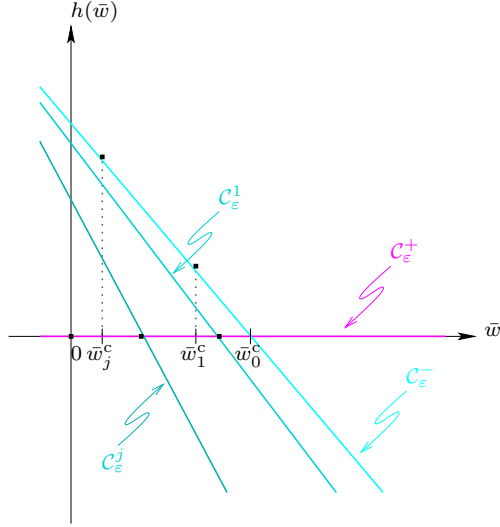


FIGURE 13. The curves $\mathcal{C}_\varepsilon^j$ for $j \geq 0$, where $\mathcal{C}_\varepsilon^- \equiv \mathcal{C}_\varepsilon^0$.

and, therefore,

$$(3.3) \quad h^j(\bar{w}) = (j+1)\sqrt{\varepsilon}d_{\sqrt{\varepsilon}}^0 + (j+1)\bar{w}d_{\bar{w}}^0 + \mathcal{O}(2).$$

This gives the desired representation of $\mathcal{C}_\varepsilon^j$ as the graph of the function $h^j(\bar{w})$ in (3.3), with

$$(3.4) \quad \mathcal{C}_\varepsilon^j = \{(h^j(\bar{w}), \bar{w}) \mid \bar{w} = \mathcal{O}(\sqrt{\varepsilon})\}$$

for $j \geq 1$; cf. Figure 13.

Finally, we prove that the map Π can be restricted from $\bar{\Delta}_-$ to the union of the set of curves $\mathcal{C}_\varepsilon^j$ with an only exponentially small error; here, Π^j denotes the j th iterate of the map Π defined in (2.57).

Proposition 3.1. *Let $(h, \bar{w}) \in \bar{\Delta}_-$, and fix $\varepsilon > 0$ sufficiently small. Then, there exists $k > 0$ such that for $1 \leq j \leq k$, $\Pi^j(h, \bar{w})$ is exponentially close (in ε) to $\cup_{j=1}^k \mathcal{C}_\varepsilon^j$.*

Proof. First, observe that all trajectories must become exponentially close to $\mathcal{S}_\varepsilon^{a-}$ after relaxation; consequently, they must return to $\bar{\Delta}_-$ exponentially close to $\mathcal{C}_\varepsilon^-$. This is equivalent to saying that for any (h, \bar{w}) with $h < 0$, $\Pi(h, \bar{w})$ is exponentially close to $\mathcal{C}_\varepsilon^-$.

We now prove that $\Pi^2(h, \bar{w})$ must be exponentially close to $\mathcal{C}_\varepsilon^- \cup \mathcal{C}_\varepsilon^1$. Let $(h^1, \bar{w}^1) = \Pi(h, \bar{w})$, and note that if $h^1 < 0$, the forward trajectory of (h^1, \bar{w}^1) must undergo relaxation. Hence, by the above argument, $\Pi(h^1, \bar{w}^1) = \Pi^2(h, \bar{w})$ is exponentially close to $\mathcal{C}_\varepsilon^-$ in that case. Let us suppose that $h^1 \geq 0$ now and consider $h^1 = \mathcal{O}(\varepsilon)$ first, which is in the domain of $\bar{\Pi}$. Since the map $\bar{\Pi}$ is induced by the flow of (2.8) and since $T^{h^1}(\bar{w}^1) = \mathcal{O}(\sqrt{-\ln \varepsilon})$ for the return time to $\bar{\Delta}$ (cf. Appendix A), the expansion that can be incurred during that return is of at most algebraic order in ε . Consequently, $\Pi(h^1, \bar{w}^1)$ must be exponentially close to $\mathcal{C}_\varepsilon^1$. If, on the other hand, h^1 is exponentially small, i.e., if $\mathcal{O}(e^{-\frac{\kappa}{\varepsilon}})$ for some $\kappa > 0$, the argument from the first part of the proof can be applied to show that $\Pi(h^1, \bar{w}^1)$ is again exponentially close to $\mathcal{C}_\varepsilon^-$.

The transitional regime between $h^1 = \mathcal{O}(\varepsilon)$ and exponentially small h^1 is more difficult to describe. This issue is addressed in detail in [20], where it is shown, roughly speaking, that the contraction and expansion in the z -direction cancel each other out to leading order near the fold. An analogous property can be proven to hold in our case, which allows us to conclude that $\Pi(h^1, \bar{w}^1)$

is exponentially close to $\mathcal{C}_\varepsilon^1$ even in that transitional regime. Finally, by an iteration of the above argument, it follows that $\Pi^3(h, \bar{w})$ must be exponentially close to $\mathcal{C}_\varepsilon^- \cup \mathcal{C}_\varepsilon^1 \cup \mathcal{C}_\varepsilon^2$, and so on.

To conclude the proof, we note that there exists a finite number k such that for any point (h, \bar{w}) with $h > 0$, there is $1 \leq j \leq k$ such that the h -coordinate of $\Pi^j(h, \bar{w})$ is negative, so that $\Pi^{j+1}(h, \bar{w})$ must again be close to $\mathcal{C}_\varepsilon^-$. (Note that k gives the maximum possible number of small oscillations a trajectory can undergo.) It follows that for any $(h, \bar{w}) \in \bar{\Delta}_-$, the trajectory of (h, \bar{w}) under Π must be exponentially close to the union of the sets $\mathcal{C}_\varepsilon^j$, $j = 1, \dots, k$. \blacksquare

In the following, we will assume that the points on a trajectory of Π are on $\mathcal{C}_\varepsilon^-$ or on one of the curves $\mathcal{C}_\varepsilon^j$. By Proposition 3.1, this assumption incurs at most an exponentially small error. To find the restriction of Π to $\mathcal{C}_\varepsilon^j$, we recall that $\mathcal{C}_\varepsilon^j$ can be represented as the graph of a function $h^j(\bar{w})$, see (3.4). In analogy to the definition of Π in (2.42), we again have to distinguish between $h^j > 0$ and $h^j < 0$ here. In the former case, Π reduces to $\bar{\Pi}$, whereas in the latter case, we have to take the composition of Π^{out} , Π^{ret} , and Π^{in} to describe the return to $\cup \mathcal{C}_\varepsilon^j$; see the discussion in Section 2.6 for details. Moreover, since $\mathcal{C}_\varepsilon^j$ is parametrized by \bar{w} , cf. (3.4), it is natural to consider Π as a function of \bar{w} . Hence, combining the definition of Π in (2.42) with (2.9) for $h^j > 0$ and with the estimates in (2.20), (2.42), and (2.54) for $h^j < 0$, respectively, we finally obtain

$$(3.5) \quad \Pi(\bar{w}) \equiv \Pi(h^j(\bar{w}), \bar{w}) = \begin{cases} \bar{w} + \varepsilon \mu T^{h^j(\bar{w})}(\bar{w}) + \mathcal{O}(\varepsilon^2) & \text{if } h^j(\bar{w}) > 0, \\ \bar{w} + \varepsilon \mu T^{h^j(\bar{w}), \text{out}}(\bar{w}) + \bar{w} f_2 \mu \varepsilon \ln \varepsilon \\ \quad + \sqrt{\varepsilon} (\mathcal{G}(0, v_{\max}, \mu) + \mathcal{G}(v_{\max}^*, v_0, \mu)) + \mathcal{O}(\varepsilon) & \text{if } h^j(\bar{w}) < 0. \end{cases}$$

3.2. The derivative of Π . To estimate the contractive (or expansive) properties of the flow induced by Π on $\cup \mathcal{C}_\varepsilon^j$, we need to estimate the derivative $\frac{d\Pi}{d\bar{w}}$ of Π . Given (3.5), it follows that the following approximation holds to leading order, i.e., up to an $\mathcal{O}(\varepsilon)$ -error:

$$(3.6) \quad \frac{d\Pi}{d\bar{w}} \sim \begin{cases} 1 + \varepsilon \mu \frac{dT^{h^j(\bar{w})}(\bar{w})}{d\bar{w}} & \text{if } h^j(\bar{w}) > 0, \\ 1 + \varepsilon \mu \frac{dT^{h^j(\bar{w}), \text{out}}(\bar{w})}{d\bar{w}} + f_2 \mu \varepsilon \ln \varepsilon & \text{if } h^j(\bar{w}) < 0. \end{cases}$$

(Here, we have used the fact that the function \mathcal{G} is independent of \bar{w} , see (2.53).) Now, recall that $T^h(0) = 2T^h$ by (2.7), and note that for (h, \bar{w}) small, $T^h(\bar{w})$ depends much more sensitively on h than on \bar{w} . Therefore, to evaluate (3.6), we can in a first approximation neglect the \bar{w} -dependence of $T^h(\bar{w})$ and write

$$\frac{dT^{h^j(\bar{w})}(\bar{w})}{d\bar{w}} \sim 2 \frac{dT^{h^j(\bar{w})}}{dh^j}.$$

Due to $T^h \sim (-2 \ln h)^{\frac{1}{2}}$ (see Appendix A), it follows that

$$(3.7) \quad \frac{dT^{h^j(\bar{w})}(\bar{w})}{d\bar{w}} \sim -\frac{2}{h^j(\bar{w})} \frac{1}{\sqrt{-2 \ln h^j(\bar{w})}} (h^j)'(\bar{w});$$

similarly, we can use the definition of $T^{h, \text{out}}(\bar{w})$ in (2.41) to conclude

$$(3.8) \quad \frac{dT^{h^j(\bar{w}), \text{out}}(\bar{w})}{d\bar{w}} \sim -\frac{1}{h^j(\bar{w})} \frac{1}{\sqrt{-2 \ln h^j(\bar{w})}} (h^j)'(\bar{w}).$$

To complete the computation of the derivative of Π , we require approximate formulae for the derivatives of h^j with respect to \bar{w} : by (3.3), it follows that

$$(3.9) \quad (h^j)'(\bar{w}) = (j+1) d_{\bar{w}}^0 + \mathcal{O}(\sqrt{\varepsilon}, \bar{w}).$$

Combining (3.7) and (3.9), we finally obtain

$$(3.10) \quad \frac{dT^{h^j(\bar{w})}(\bar{w})}{d\bar{w}} \sim -\frac{2}{h^j(\bar{w})} \frac{1}{\sqrt{-2 \ln h^j(\bar{w})}} (j+1) d_{\bar{w}}^0$$

as well as

$$(3.11) \quad \frac{dT^{h^j(\bar{w}), \text{out}}(\bar{w})}{d\bar{w}} \sim -\frac{1}{h^j(\bar{w})} \frac{1}{\sqrt{-2 \ln h^j(\bar{w})}} (j+1) d_{\bar{w}}^0,$$

which can be substituted into (3.6) to obtain a more explicit expression for $\frac{d\Pi}{d\bar{w}}$.

3.3. Secondary canards and sectors of rotation. Recall the definition of the j th secondary canard Γ_ε^j as a trajectory of (1.2) that undergoes j small oscillations (loops) during its passage through the fold region. In this subsection, we derive the conditions on the rescaled equations (2.8) by which these trajectories are defined. The corresponding analysis will require us to refine the results of Proposition 2.2, see Proposition 3.2 below. Given the family of secondary canards $\{\Gamma_\varepsilon^j\}$, for $j = 0, \dots, k$, we will define the corresponding family of sectors of rotation, $\{RS^j\}$. We will then analyze the geometry of these sectors; in particular, we will estimate the sector width (Proposition 3.3), and we will show that it is independent of j to lowest order. Here, we note that the family $\{RS^j\}$ will be crucial for the reduction of the (two-dimensional) map Π to the (one-dimensional) map Φ in Section 3.4 below. Finally, in Proposition 3.4, we discuss the uniform validity of our asymptotic estimates.

Let $(h^0(\bar{w}), \bar{w}) \in \mathcal{C}_\varepsilon^-$, as before, and recall the definition of the transition map $\bar{\Pi}$ for (2.8), see Proposition 2.2. Moreover, let P_h and $P_{\bar{w}}$ denote the projections onto the h -coordinate and the \bar{w} -coordinate, respectively. Then, the defining condition for the j th secondary canard is given by

$$(3.12) \quad P_h \bar{\Pi}^j(h^0(\bar{w}), \bar{w}) = 0,$$

i.e., the h -coordinate of the j th iterate of $(h^0(\bar{w}), \bar{w})$ under $\bar{\Pi}$ has to be zero. In other words, we are interested in finding the points of intersection of subsequent iterates of $\mathcal{C}_\varepsilon^-$ under $\bar{\Pi}$ (i.e., of $\mathcal{C}_\varepsilon^j$) with $\mathcal{C}_\varepsilon^+$. For $j \geq 1$ fixed, let \bar{w}_j^c denote the corresponding solution of (3.12). Then, \bar{w}_j^c fixes a point in $\mathcal{C}_\varepsilon^-$ that will determine the location of the j th secondary canard Γ_ε^j ; see Figure 13 for an illustration. In particular, for the first secondary canard, we have the requirement that

$$P_h \bar{\Pi}(h^0(\bar{w}_1^c), \bar{w}_1^c) = 0.$$

Remark 7. Recall that $\mathcal{C}_\varepsilon^-$ corresponds to the intersection of the locally invariant slow manifold $\mathcal{S}_\varepsilon^{a-}$ in (1.5) with Δ , before the rescaling. Since the critical manifold \mathcal{S}_0 for (1.5) is normally hyperbolic away from ℓ^\pm , it follows that the slow manifold \mathcal{S}_ε is unique up to exponentially small terms [11, 14]. Once the corresponding sheets of $\mathcal{S}_\varepsilon^{a-}$ and $\mathcal{S}_\varepsilon^r$ are chosen, the strong canard Γ_ε^0 is uniquely determined. Similarly, since the j th secondary canard Γ_ε^j , with $j \geq 1$, is defined as the trajectory lying in the intersection of the j th iterate of $\mathcal{S}_\varepsilon^{a-}$ under $\bar{\Pi}$ with $\mathcal{S}_\varepsilon^r$, all secondary canards will originate in the same sheet of $\mathcal{S}_\varepsilon^{a-}$. Thus, we can restrict ourselves to $\mathcal{C}_\varepsilon^-$ when studying secondary canards. \blacksquare

Given the asymptotics of the return map $\bar{\Pi} : \bar{\Delta}_- \rightarrow \bar{\Delta}_-$, as derived in Proposition 2.2 (cf. (2.9)), we can write

$$(3.13) \quad \bar{\Pi}(h, \bar{w}) = \bar{\Pi}_0(h, \bar{w}) + \mathcal{O}(\varepsilon),$$

where $\bar{\Pi}_0(h, \bar{w})$ denotes the return map for the system

$$(3.14) \quad \begin{aligned} \bar{v}' &= -\bar{z} + f_2 \bar{v}^2 + \sqrt{\varepsilon} f_3 \bar{v}^3 + \sqrt{\varepsilon} F(0, 0) + \bar{w} G(0, 0), \\ \bar{z}' &= \bar{v} - \bar{w}, \\ \bar{w}' &= 0. \end{aligned}$$

We begin by showing that the leading-order approximation $\bar{\Pi}_0$, which is obtained by omitting the $\mathcal{O}(\varepsilon)$ -terms in (3.13), is not sufficiently accurate to give non-trivial solutions of (3.12), i.e., solutions that are not exponentially close (in ε) to the canard critical value \bar{w}^c for (3.14). (Recall that \bar{w}^c is the \bar{w} -value corresponding to the strong canard Γ_ε^0 , after the rescaling in (2.2), with

$$\bar{w}^c = \frac{d^0}{d\bar{w}^0} \sqrt{\varepsilon} + \mathcal{O}(\varepsilon)$$

by (2.16).) Since Γ_ε^0 itself is only unique up to exponentially small terms, we conclude that the map $\bar{\Pi}_0$ will admit no secondary canards.

The argument goes as follows: to determine the \bar{w} -value corresponding to the first secondary canard Γ_ε^1 from $\bar{\Pi}_0$, one would have to solve $P_h \bar{\Pi}_0(h^0(\bar{w}), \bar{w}) = 0$. Solutions of this equation are obtained by applying the Implicit Function Theorem about $(0, \bar{w}^c)$. (Here, we have taken into account that $h^0(\bar{w}^c) = 0$, by the definition of \bar{w}^c , cf. again (2.16).) However, since \bar{w}^c corresponds precisely to the critical value of the canard parameter \bar{w} in the classical (two-dimensional) scenario, it can be shown [20] that $P_h \bar{\Pi}_0(0, \bar{w}_0^c)$ is exponentially small. By the Implicit Function Theorem, it follows that any solution \bar{w}^* of the equation $P_h \bar{\Pi}_0(h^0(\bar{w}), \bar{w}) = 0$ close to \bar{w}^c must be such that $|\bar{w}^* - \bar{w}^c|$ is exponentially small. (Note that this is exactly the situation encountered in a two-dimensional canard explosion, see again [20].)

Hence, in order to find secondary canards, we must refine our analysis and include additional terms in the description of the “local” return map $\bar{\Pi}$. In the following, we will use the partially decoupled truncated system

$$(3.15a) \quad \bar{v}' = -\bar{z} + f_2 \bar{v}^2 + \sqrt{\varepsilon} f_3 \bar{v}^3 + \sqrt{\varepsilon} F(0, 0) + \bar{w} G(0, 0),$$

$$(3.15b) \quad \bar{z}' = \bar{v} - \bar{w},$$

$$(3.15c) \quad \bar{w}' = \varepsilon \mu$$

as the basis for our computation. As it turns out, this refinement will suffice to solve (3.12) for \bar{w} , in a non-trivial fashion, to leading order. Note that the only difference between (3.14) and (3.15) lies in the \bar{w} -equation: instead of keeping \bar{w} constant to lowest order, we let it evolve in (3.15c), according to the leading-order approximation obtained for \bar{w}' from (2.8c), $\bar{w}' = \varepsilon(\mu - g_1 \varepsilon \bar{z} + \mathcal{O}(\varepsilon)) \sim \varepsilon \mu$.

The relevant result on the refined asymptotics of $\bar{\Pi}$ is obtained as follows:

Proposition 3.2. *Let $\bar{\Pi} : \bar{\Delta}^- \rightarrow \bar{\Delta}_-$ denote the return map for (3.15), and fix $\varepsilon > 0$ sufficiently small. Then,*

$$(3.16) \quad \bar{\Pi}(h, \bar{w}) = \begin{pmatrix} P_h \bar{\Pi}_0(h, \bar{w}) + \varepsilon \mu \mathcal{K}(h) + \mathcal{O}(\varepsilon^2) \\ \bar{w} + 2\varepsilon \mu T^h + \mathcal{O}(\varepsilon^2) \end{pmatrix},$$

where $\bar{\Pi}_0$ denotes the return map for (3.14) and \mathcal{K} is defined via

$$\mathcal{K}(h) = \int_{-T^h}^{T^h} \nabla H(\bar{\gamma}_0^h(t)) \cdot (G(0, 0), -1)^T(t + T^h) dt.$$

Proof. Let \bar{w}_0^c denote the critical \bar{w} -value for the “refined” system (3.15). We begin by showing that, to leading order, \bar{w}_0^c equals \bar{w}^c , which is again the corresponding \bar{w} -value determined from

$\bar{\Pi}_0$, cf. (2.16). Suppose that \bar{w} is given and that we wish to find h^- such that $(h^-, \bar{w}) \in \mathcal{C}_\varepsilon^-$ holds. Solving (3.15c), we obtain $\bar{w}(t) = \bar{w} + \varepsilon\mu t$, which we then substitute into (3.15a) and (3.15b):

$$(3.17) \quad \begin{aligned} \bar{v}' &= -\bar{z} + f_2\bar{v}^2 + \sqrt{\varepsilon}f_3\bar{v}^3 + \sqrt{\varepsilon}F(0, 0) + (\bar{w} + \varepsilon\mu t)G(0, 0), \\ \bar{z}' &= \bar{v} - \bar{w} - \varepsilon\mu t. \end{aligned}$$

Fix \bar{w} , and suppose that h_0^- is the h -value obtained from (3.14) such that $(h_0^-, \bar{w}) \in \mathcal{C}_\varepsilon^-$, see the proof of Proposition 2.2. Then, it follows that

$$(3.18) \quad h^- = h_0^- - \varepsilon\mu \int_{-\infty}^0 \frac{\partial H}{\partial \bar{z}}(\bar{\gamma}_0^0(t))G(0, 0)t dt,$$

again by the proof of Proposition 2.2. A similar computation shows that

$$(3.19) \quad h^+ = h_0^+ + \varepsilon\mu \int_0^{\infty} \frac{\partial H}{\partial \bar{z}}(\bar{\gamma}_0^0(t))G(0, 0)t dt,$$

where h^+ and h_0^+ are defined by the requirement that $(h^+, \bar{w}) \in \mathcal{C}_\varepsilon^+$ and $(h_0^+, \bar{w}) \in \mathcal{C}_\varepsilon^+$ in (3.15) and (3.14), respectively. By symmetry, we find that

$$(3.20) \quad \int_{-\infty}^0 -\frac{\partial H}{\partial \bar{z}}(\bar{\gamma}_0^0(t))t dt = \int_0^{\infty} \frac{\partial H}{\partial \bar{z}}(\bar{\gamma}_0^0(t))t dt.$$

It follows that the defining condition for the strong canard in (3.15), which, for (2.8), is given by $h^- = h^+$, reduces to $h_0^- = h_0^+ + \mathcal{O}(\varepsilon^2)$ and, hence, that the corresponding critical values of \bar{w} are indeed the same to leading order.

Finally, the approximation for $\bar{\Pi}$ in (3.16) is derived as in the proof of Proposition 2.2, where we note that the additional \mathcal{K} -term is due to the fact that $h \mapsto h^+ - h^- = h^0 + \varepsilon\mu\mathcal{K}(h)$, by (3.18), (3.19), and (3.20). \blacksquare

Remark 8. It can be shown that the inclusion of additional (higher-order) terms in (3.15) will not alter the result of Proposition 3.2, since these terms will either drop out by symmetry, as in the proof of Proposition 2.2, or contribute only terms of higher order in (3.16). \blacksquare

The asymptotics of \mathcal{K} are studied in Appendix A, where we show that $\mathcal{K}(h) = 2d_{\bar{w}}^0 T^h + \mathcal{O}(1)$; see Lemma A.5. Therefore, the defining condition for the first secondary canard, $P_h \bar{\Pi}(h^0(\bar{w}), \bar{w}) = 0$, can be written as

$$(3.21) \quad P_h \bar{\Pi}_0(h^0(\bar{w}), \bar{w}) = -\varepsilon\mu\mathcal{K}(h^0(\bar{w})) + \mathcal{O}(\varepsilon^2),$$

to leading order. Moreover, recalling that \bar{w}_1^c denotes the value of \bar{w} that solves (3.21), we write $\bar{w}_1^c = \bar{w}_0^c + \Delta\bar{w}$. Then, we have the following estimate for the width $\Delta\bar{w}$ of the first sector of rotation:

Proposition 3.3. *With $\Delta\bar{w}$ defined as above, there holds*

$$(3.22) \quad \Delta\bar{w} = -2\varepsilon\mu\sqrt{-2\ln\varepsilon} + \mathcal{O}(\varepsilon)$$

for $\varepsilon > 0$ sufficiently small.

Proof. Making use of the definition of $\bar{\Pi}_0$, see Proposition 2.2, we first rewrite $P_h \bar{\Pi}_0(h^0(\bar{w}), \bar{w})$ as

$$\begin{aligned} P_h \bar{\Pi}_0(h^0(\bar{w}), \bar{w}) &= P_h \bar{\Pi}_0(0, \bar{w}_0^c) + P_h \bar{\Pi}_0(h^0(\bar{w}), \bar{w}) - P_h \bar{\Pi}_0(0, \bar{w}_0^c) \\ &= P_h \bar{\Pi}_0(0, \bar{w}_0^c) + d_{\bar{w}}^{h^0(\bar{w})}\bar{w} - d_{\bar{w}}^0\bar{w}_0^c + \sqrt{\varepsilon}(d_{\sqrt{\varepsilon}}^{h^0(\bar{w})} - d_{\sqrt{\varepsilon}}^0) + \mathcal{O}(\varepsilon, \sqrt{\varepsilon}\Delta\bar{w}, \Delta\bar{w}^2) \\ &= P_h \bar{\Pi}_0(0, \bar{w}_0^c) + (d_{\bar{w}}^{h^0(\bar{w})} - d_{\bar{w}}^0)\bar{w} + d_{\bar{w}}^0\Delta\bar{w} + \sqrt{\varepsilon}(d_{\sqrt{\varepsilon}}^{h^0(\bar{w})} - d_{\sqrt{\varepsilon}}^0) \\ &\quad + \mathcal{O}(\varepsilon, \sqrt{\varepsilon}\Delta\bar{w}, \Delta\bar{w}^2), \end{aligned}$$

see the discussion in Section **3.1** as well as (2.39). Now, recall that $\bar{w} = \mathcal{O}(\sqrt{\varepsilon})$ by Assumption 1, and note that one can estimate $d_{\bar{w}}^{h^0(\bar{w})} - d_{\bar{w}}^0 = \mathcal{O}(h^0(\bar{w}) \ln(-h^0(\bar{w}))^{\frac{3}{2}})$, cf. (A.9). Also, since $h^0(\bar{w}_0^c) = 0$ by (2.16) and (2.39), a Taylor expansion shows

$$(3.23) \quad h^0(\bar{w}) = d_{\bar{w}}^0 \Delta \bar{w} + \mathcal{O}(\Delta \bar{w}),$$

which implies in sum

$$P_h \bar{\Pi}_0(h^0(\bar{w}), \bar{w}) = P_h \bar{\Pi}_0(0, \bar{w}_0^c) + d_{\bar{w}}^0 \Delta \bar{w} + \sqrt{\varepsilon} (d_{\sqrt{\varepsilon}}^{h^0(\bar{w})} - d_{\sqrt{\varepsilon}}^0) + \mathcal{O}(\varepsilon, \sqrt{\varepsilon}(-\ln \varepsilon)^{\frac{3}{2}} \Delta \bar{w}, \Delta \bar{w}^2).$$

Using the fact that $P_h \bar{\Pi}_0(0, \bar{w}_0^c) = \mathcal{O}(e^{-\frac{\kappa}{\varepsilon}})$ for some $\kappa > 0$ as well as the estimates from (A.9) and Lemma A.5, we conclude that the \bar{w} -value corresponding to the first secondary canard, \bar{w}_1^c , is determined from $d_{\bar{w}}^0 \Delta \bar{w} = -2\varepsilon \mu d_{\bar{w}}^0 T^{h^0(\bar{w})} + \mathcal{O}((\sqrt{\varepsilon} + \Delta \bar{w})^2)$. Hence, we obtain

$$(3.24) \quad \bar{w}_1^c = \bar{w}_0^c - 2\varepsilon \mu T^{h^0(\bar{w}_1^c)} + \mathcal{O}(\varepsilon),$$

which implies in particular $|\bar{w}_1^c - \bar{w}_0^c| \gtrsim \varepsilon$, i.e., $|\bar{w}_1^c - \bar{w}_0^c| > \varepsilon$ as well as $|\bar{w}_1^c - \bar{w}_0^c| \sim \varepsilon$. Due to $h^0(\bar{w}_0^c) = 0$ and $\frac{dh^0}{d\bar{w}} \sim d_{\bar{w}}^0$, it follows from the Intermediate Value Theorem that $h^0(\bar{w}_1^c) \gtrsim \varepsilon$, which, together with Lemma A.2, shows that the desired estimate for the size of the first sector of rotation is given by

$$(3.25) \quad \bar{w}_1^c - \bar{w}_0^c = \Delta \bar{w} = -2\varepsilon \mu \sqrt{-2 \ln \varepsilon} + \mathcal{O}(\varepsilon).$$

This completes the proof. ■

Let $k > 1$, and consider $j = 0, \dots, k$. We now set out to find an analogue of condition (3.21) for the k th secondary canard Γ_ε^k . Let \bar{w}_k^c again denote the corresponding \bar{w} -value, consider an initial condition $(h^0(\bar{w}), \bar{w}) \in \mathcal{C}_\varepsilon^-$, and let

$$\bar{w}^j = P_{\bar{w}} \bar{\Pi}^j(h^0(\bar{w}), \bar{w}),$$

as before. Note that \bar{w}_k^c must be a solution of the equation

$$P_h \bar{\Pi}(h^{k-1}(\bar{w}^{k-1}), \bar{w}^{k-1}) = 0$$

or, equivalently, of

$$(3.26) \quad P_h \bar{\Pi}_0(h^{k-1}(\bar{w}^{k-1}), \bar{w}^{k-1}) = -\varepsilon \mu \mathcal{K}(h^{k-1}(\bar{w}^{k-1})) + \mathcal{O}(\varepsilon^2).$$

Observe that the condition in (3.26) is analogous to (3.21), with h^0 replaced by h^{k-1} ; hence, the structure of (3.21) is replicated at higher orders. Note also that it follows from (3.24) that $\bar{w}_1^{c,1} = \bar{w}_0^c + \mathcal{O}(\varepsilon)$, where $\bar{w}_1^{c,1}$ is the first iterate of \bar{w}_1^c under $\bar{\Pi}$. This estimate, in turn, implies that $h^1(\bar{w}_0^c) = \mathcal{O}(\varepsilon)$, see (3.1). An argument analogous to the derivation of (3.24) now leads to the estimate

$$\bar{w}_2^{c,1} = \bar{w}_0^c - 2\varepsilon \mu T^{h(\bar{w}_2^{c,1})} + \mathcal{O}(\varepsilon)$$

or, equivalently, to

$$(3.27) \quad \bar{w}_2^c = \bar{w}_0^c - 2\varepsilon \mu (T^{h(\bar{w}_2^c)} + T^{h(\bar{w}_2^{c,1})}) + \mathcal{O}(\varepsilon).$$

Proceeding inductively, we obtain $h^{k-1}(\bar{w}_0^c) = \mathcal{O}(\varepsilon)$ and

$$(3.28) \quad \bar{w}_k^c = \bar{w}_0^c - 2\varepsilon \mu \left(\sum_{j=0}^{k-1} T^{h(\bar{w}_k^{c,j})} \right) + \mathcal{O}(\varepsilon),$$

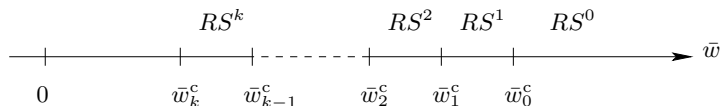


FIGURE 14. The sectors of rotation, RS^j .

where we define $\bar{w}_k^{c,0} \equiv \bar{w}_k^c$. Finally, using Lemma A.2 to again approximate $T^{h(\bar{w}_k^{c,j})}$ by $\sqrt{-2 \ln \varepsilon} + \mathcal{O}(1)$ (non-uniformly in k), we obtain in analogy to (3.25) that

$$(3.29) \quad \bar{w}_k^c = \bar{w}_{k-1}^c - 2\varepsilon\mu\sqrt{-2 \ln \varepsilon} + \mathcal{O}(\varepsilon),$$

which, in conjunction with (2.19), verifies Assumption 1 above.

One question that naturally arises in this context is whether $k > 1$ can be chosen arbitrarily large. Here, we show that our analysis, and, in particular, the estimate in (3.28), does not hold uniformly in k with respect to ε ; rather, (3.28) is valid for k fixed and ε sufficiently small. This is due to the fact that the contributions coming from $T^{h(\bar{w}_k^{c,j})}$ become increasingly smaller with k : since \bar{w}_k^c decreases with k and since $h(\bar{w}) \sim \sqrt{\varepsilon}d_{\sqrt{\varepsilon}}^0 + \bar{w}d_{\bar{w}}^0$ with $d_{\bar{w}}^0 < 0$, see (2.18), it follows that h increases with k . Therefore, $T^h \sim \sqrt{-2 \ln h}$ decreases, and the $\mathcal{O}(\varepsilon)$ -terms can come to dominate the $2\varepsilon\mu(\dots)$ -terms in (3.28) if k is sufficiently large. However, in our analysis, we had to assume that these terms are uniformly of lower order than ε , starting with the leading-order approximation for $\bar{\Pi}$ in Proposition 2.2. In summary, for k “large,” ε thus has to be chosen small enough to ensure that the estimate in (3.28) remains consistent:

Proposition 3.4. *Fix any integer $K > 0$. Then, there exists an $\varepsilon > 0$ sufficiently small such that the estimate in (3.28) holds for $k \leq K$.*

For $j = 1, \dots, k$, we now define the j th sector of rotation RS^j as follows:

$$RS^j = \{(h^0(\bar{w}), \bar{w}) \in \mathcal{C}_\varepsilon^- \mid \bar{w}_j^c \leq \bar{w} < \bar{w}_{j-1}^c\}.$$

This definition provides a connection between the family of secondary canards $\{\Gamma_\varepsilon^j\}$ and the corresponding sectors of rotation: the j th sector, RS^j , is bounded by the secondary canards Γ_ε^{j-1} and Γ_ε^j , in that the corresponding points \bar{w}_{j-1}^c and \bar{w}_j^c on $\mathcal{C}_\varepsilon^-$ define the boundaries of RS^j .

For notational purposes, we also introduce the zeroth sector RS^0 via

$$RS^0 = \{(h, \bar{w}) \in \mathcal{C}_\varepsilon^- \mid \bar{w}_0^c \leq \bar{w}\},$$

and we note that this definition is equivalent to requiring that $h < 0$, see (2.37). An illustration of these sectors of rotation is given in Figure 14. In particular, since $\bar{w}_j^c < \bar{w}_{j-1}^c$ for any $j \geq 1$, the sector RS^j lies further “to the left” of RS^0 with increasing j .

It follows from the preceding analysis that all of the sectors RS^j are of equal size to leading order, cf. (3.29). (However, we conjecture that due to higher-order corrections, the sector size actually decreases as j increases.) Moreover, for ε and μ fixed, the number of sectors of rotation RS^j and, hence, also the number of corresponding secondary canards Γ_ε^j , has to be finite: note that the frequency of the small-oscillation component in any mixed-mode time series in (1.5) is globally bounded, with the bound given approximately by the frequency determined by the Hopf bifurcation around the origin in (1.5). Additionally, the speed of the drift in \bar{w} in (2.3c) is always positive for non-zero ε and μ , which implies that $\bar{w} > \bar{w}_0^c$ in finite time. Hence, trajectories of (1.5) can undergo only a finite number of small-amplitude oscillations before entering the relaxation regime, which implies that there can be only a finite number of sectors of rotation lying in $(0, \bar{w}_0^c)$; see again Figure 14.

Remark 9. It follows from Proposition 3.4 that both the number of secondary canards and that of the corresponding sectors of rotation must go to infinity as $\varepsilon \rightarrow 0$. However, it is important to note that Proposition 3.4 gives no bound on the total number of secondary canards for $\varepsilon > 0$. Rather, the integer K can be chosen arbitrarily large provided ε is small enough, implying that our analysis is then valid for all $k \leq K$. \blacksquare

Finally, we observe that the definition of RS^j can be extended to a small neighborhood of $\mathcal{C}_\varepsilon^-$ by the flow of (2.8) and, hence, that the sectors of rotation can be interpreted as two-dimensional subsets of $\mathcal{S}_\varepsilon^{a-}$.

3.4. The return map Φ to $\mathcal{C}_\varepsilon^-$. To show how the “full” map Π (which *a priori* has to be interpreted as a map that is defined on $\bigcup \mathcal{C}_\varepsilon^j$) can be approximated accurately by a “simplified” map, we introduce $\Phi : \mathcal{C}_\varepsilon^- \rightarrow \mathcal{C}_\varepsilon^-$ as follows. Let $k \geq 0$, and recall the definition of the k th sector of rotation, RS^k , from the previous subsection. Then, we define Φ via

$$(3.30) \quad \Phi(\bar{w}) = P_{\bar{w}}(\Pi^{\text{in}} \circ \Pi^{\text{ret}} \circ \Pi^{\text{out}} \circ \bar{\Pi}^k(h^0(\bar{w}), \bar{w})) \quad \text{if } (h^0(\bar{w}), \bar{w}) \in RS^k.$$

Note that Φ is a reinterpretation of Π , in that it is a composition of the same components that were used in the definition of Π in (3.5). However, it is defined on a different domain: the definition in (3.30) reduces the analysis of the flow induced by (1.5) to that of a one-dimensional map that is defined on the single curve $\mathcal{C}_\varepsilon^-$, which will allow us to study the recurrent dynamics on RS^k in considerable detail. Moreover, we note that Φ is still an exponentially accurate approximation for the full, two-dimensional return map Π , which is again due to the fact that all trajectories must return exponentially close to $\mathcal{C}_\varepsilon^-$ after relaxation, i.e., after application of Π^{ret} ; cf. the proof of Proposition 3.1. One drawback of this simplification, however, lies in the fact that the defining formula (3.30) for Φ is k -dependent; in other words, the definition of Φ changes with the sector of rotation under consideration. This k -dependence will have to be taken into account throughout the subsequent analysis.

Finally, we remark that the map Φ is smooth on each of the sectors RS^k , but that it has discontinuities at the points \bar{w}_k^c and \bar{w}_{k-1}^c . We will not study the nature of these discontinuities in detail, since we are not attempting to analyze the dynamics of Φ “very close” to the secondary canards. Rather, we will restrict ourselves to describing Φ on the interior of the individual sectors RS^k .

3.5. The derivative of Φ . In this subsection, we derive estimates for the derivative $\Phi'(\bar{w}) := \frac{d\Phi}{d\bar{w}}$ of Φ on the k th sector of rotation, RS^k . We then investigate some of the properties of Φ' . The resulting estimates are needed for the analysis of the dynamics of Φ in Section 3.6 below and will allow us to characterize the admissible Farey sequences in (1.5), as well as to describe the corresponding parameter intervals.

Let \bar{w} be such that $(h^0(\bar{w}), \bar{w}) \in RS^k$, and let $\bar{w}^j = P_{\bar{w}}\bar{\Pi}^j(h^0(\bar{w}^0), \bar{w}^0)$, where we set $\bar{w}^0 \equiv \bar{w}$. Given the definition of Φ in (3.30), we have the following result:

Lemma 3.5. *To leading order, there holds*

$$(3.31) \quad \frac{d\Phi(\bar{w})}{d\bar{w}} = 1 - \varepsilon\mu d_{\bar{w}}^0 \left(\sum_{j=0}^{k-1} 2(j+1) \frac{1}{h^j(\bar{w}^j)} \frac{1}{\sqrt{-2 \ln h^j(\bar{w}^j)}} + (k+1) \frac{1}{h^k(\bar{w}^k)} \frac{1}{\sqrt{-2 \ln h^k(\bar{w}^k)}} \right) + \mathcal{O}(\varepsilon \ln \varepsilon)$$

for the derivative of Φ on RS^k .

Proof. By the Chain Rule and taking into account the definitions of $\bar{\Pi}$, Π^{in} , and Π^{out} , as well as of Π^{ret} in Propositions 2.2, 2.3, and 2.4 as well as in (2.54), respectively, we have

$$\begin{aligned}
\frac{d\Phi(\bar{w})}{d\bar{w}} &= \prod_{j=0}^{k-1} \left(1 + 2\varepsilon\mu \frac{dT^{h^j(\bar{w})}}{d\bar{w}} \right) \left(1 + \varepsilon\mu \frac{dT^{h^k(\bar{w}),\text{out}}}{d\bar{w}} \right) + \mathcal{O}(\varepsilon \ln \varepsilon) \\
&= 1 + \varepsilon\mu \sum_{j=0}^{k-1} 2 \frac{dT^{h^j(\bar{w})}}{d\bar{w}} + \varepsilon\mu \frac{dT^{h^k(\bar{w}),\text{out}}}{d\bar{w}} + \mathcal{O}(\varepsilon \ln \varepsilon) \\
&= 1 - \varepsilon\mu d_{\bar{w}}^0 \left(\sum_{j=0}^{k-1} 2(j+1) \frac{1}{h^j(\bar{w}^j)} \frac{1}{\sqrt{-2 \ln h^j(\bar{w}^j)}} + (k+1) \frac{1}{h^k(\bar{w}^k)} \frac{1}{\sqrt{-2 \ln h^k(\bar{w}^k)}} \right) \\
&\quad + \mathcal{O}(\varepsilon \ln \varepsilon),
\end{aligned}$$

where the last step follows from (3.10) and (3.11). \blacksquare

Since we assume that $h^j(\bar{w}^j) = \mathcal{O}(\varepsilon\sqrt{-\ln \varepsilon})$ (see the proof of Proposition 3.3 above), we can write

$$\frac{1}{\sqrt{-2 \ln h^j(\bar{w}^j)}} = \frac{1}{\sqrt{-2 \ln \varepsilon}} (1 + \mathcal{O}(1)).$$

This gives a somewhat less accurate but more concise estimate for the derivative of Φ :

$$(3.32) \quad \frac{d\Phi(\bar{w})}{d\bar{w}} \sim 1 - \varepsilon\mu d_{\bar{w}}^0 \frac{1}{\sqrt{-2 \ln \varepsilon}} \left(\sum_{j=0}^{k-1} \frac{2(j+1)}{h^j(\bar{w}^j)} + \frac{k+1}{h^k(\bar{w}^k)} \right).$$

(Note that again due to $h^j(\bar{w}^j) = \mathcal{O}(\varepsilon\sqrt{-\ln \varepsilon})$, the $\mathcal{O}(\varepsilon)$ -correction in (3.32) will actually be of the order $(\ln \varepsilon)^{-1}$, and that we can therefore neglect the $\mathcal{O}(\varepsilon \ln \varepsilon)$ -terms in (3.31).)

To simplify this estimate further, we have to distinguish between different k -values in (3.32). We first focus on the case where $k > 0$; the case when $k = 0$ will be discussed separately.

Given $k > 0$, fix an initial condition $\bar{w}^0 \in RS^k$, and let $\bar{w}^1, \bar{w}^2, \dots, \bar{w}^k$ be defined as in Section 3.4 above, i.e., let \bar{w}^j be the j th iterate of \bar{w}^0 under $\bar{\Pi}$. Then, it follows directly from (3.32) that $\Phi' < 1$ if $\bar{w}^0 \approx \bar{w}_k^c$, respectively, that $\Phi' > 1$ if $\bar{w}^0 \approx \bar{w}_{k-1}^c$. We are interested in approximating more precisely the size of the \bar{w} -intervals where Φ' is less than 1 and greater than 1, respectively.

To that end, let $\Delta\bar{w}^j = \bar{w}_{j-1}^c - \bar{w}_j^c$ be the width of the j th sector of rotation RS^j , and recall that we have the estimate

$$\Delta\bar{w}^j \sim 2\varepsilon\mu\sqrt{-2 \ln \varepsilon},$$

independent of j to leading order. Given any $\bar{w}^0 \in RS^k$, we can write $\bar{w}^0 = \bar{w}_k^c + \nu\Delta\bar{w}^k$ for some $\nu \in [0, 1]$, i.e., the sector RS^k will be parametrized by the variable ν in the following. Moreover, for any $j \geq 0$, we have the following estimates:

$$\begin{aligned}
\bar{w}_j^c &\sim \bar{w}_0^c - 2j\varepsilon\mu\sqrt{-2 \ln \varepsilon}, \\
\bar{w}^j &\sim \bar{w}_0^c - 2((k-j) - \nu)\varepsilon\mu\sqrt{-2 \ln \varepsilon}, \\
h^j(\bar{w}^j) &\sim -2d_{\bar{w}}^0(j+1)((k-j) - \nu)\varepsilon\mu\sqrt{-2 \ln \varepsilon},
\end{aligned}$$

where the last expression is a consequence of (3.3). Using (3.32), we obtain

$$(3.33) \quad \frac{d\Phi(\bar{w})}{d\bar{w}} \sim 1 - \frac{\omega_k(\nu)}{4 \ln \varepsilon},$$

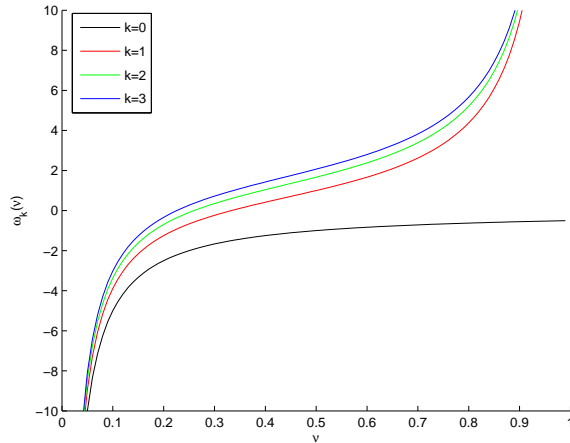


FIGURE 15. The function ω_k on $[0, 1]$ for $k = 0, \dots, 3$.

where the function ω_k is defined via

$$(3.34) \quad \omega_k(\nu) = \sum_{j=0}^{k-1} \frac{1}{(k-j) - \nu} - \frac{1}{2\nu}.$$

Finally, we consider the case where $k = 0$. For any initial condition $\bar{w}^0 \in RS^0$, we can write $\bar{w}^0 = \bar{w}_c^0 + 2\nu\varepsilon\mu\sqrt{-2\ln\varepsilon}$, where ν is now some positive number. Then,

$$(3.35) \quad \frac{d\Phi(\bar{w})}{d\bar{w}} \sim 1 - \frac{\omega_0(\nu)}{4\ln\varepsilon},$$

with $\omega_0(\nu) = -\frac{1}{2\nu}$. Observe that, clearly, $\Phi'(\bar{w}) < 1$ for any $\bar{w} \in RS^0$.

Remark 10. Note that for $k \geq 0$, the function $\omega_k(\nu)$ defined in (3.34) is increasing on $[0, 1]$ and that ω_k changes sign exactly once if $k > 0$, see Figure 15. ■

The zeros of $\omega_k(\nu)$, $k > 0$, give the approximate sizes of the subintervals of RS^k where Φ' is greater than 1 and less than 1, respectively. More precisely, we have proven the following result.

Proposition 3.6. *For $k > 0$ and $\varepsilon > 0$ sufficiently small, the subinterval of RS^k on which $\Phi'(\bar{w}) < 1$ is approximately given by $(\bar{w}_k^c, \bar{w}_k^c + 2\nu_0^k\mu\varepsilon\sqrt{-2\ln\varepsilon})$, where ν_0^k denotes the unique zero of ω_k on RS^k .*

3.6. The dynamics of Φ . In this subsection, we analyze the dynamics of the reduced map Φ in more detail, combining the results obtained so far in Section 3. The aim of our analysis is to relate the properties of Φ to the resulting mixed-mode dynamics in (1.5) and to estimate the relevant parameter (μ -)range corresponding to this dynamics. Our first result (Theorem 3.7) concerns the existence and stability of 1^k -type orbits, i.e., of periodic orbits with symbolic (Farey) sequence $\{1^k\}$; these orbits correspond to the recurrent dynamics of (1.5) on the k th sector of rotation, RS^k . Then, in Theorem 3.9, we derive conditions for when a given orbit will pass through RS^k . In Theorem 3.10, Proposition 3.11, and Corollary 3.12, we apply these conditions to classify the periodic orbits of the more general type $\{L_j^{k_j}\}$, with $L_j, k_j \geq 1$, that can “typically” occur in (1.5).

We start by summarizing some of the features of Φ which follow directly from the results of Sections 3.3 and 3.5; see Figure 16 for a qualitative illustration.

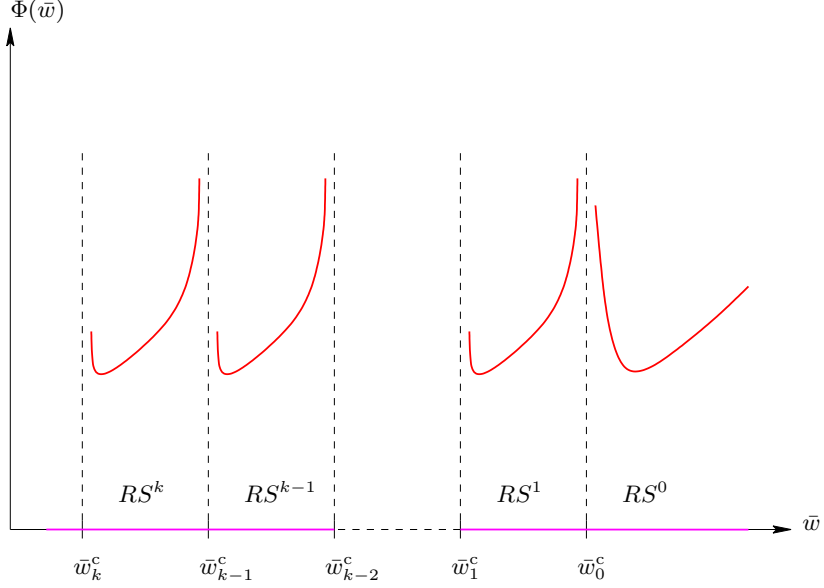


FIGURE 16. A qualitative illustration of the map Φ .

- (i) Φ must be decreasing close to the left boundary of RS^k and increasing on most of RS^k , with $\bar{w}_k^c + \nu_0^k \Delta \bar{w}^k$ giving an estimate of the point where Φ' becomes greater than 1, cf. Proposition 3.6.
- (ii) The derivative Φ' must change sign near $\bar{w}_{\min}^k := \bar{w}_k^c + \nu_{\min}^k \Delta \bar{w}^k$, with ν_{\min}^k determined by the condition that $\omega_k(\nu_{\min}^k) = 4 \ln \varepsilon$. This implies in particular that $\nu_{\min}^k = \mathcal{O}((\ln \varepsilon)^{-1})$ and, hence, that $\bar{w}_{\min}^k \approx \bar{w}_k^c$. (Note that our analysis does not prove the uniqueness of this minimum, though.)
- (iii) A simple computation along the lines of Section 3.5 shows that $\Phi(\bar{w}_{\min}^k) = \Phi_{\min} + \mathcal{O}(\varepsilon)$ is independent of k to lowest order, where

$$(3.36) \quad \Phi_{\min} := \bar{w}_0^c + \sqrt{\varepsilon} (\mathcal{G}(v_0, v_{\max}, \mu) + \mathcal{G}(v_{\max}^*, 0, \mu)) + \varepsilon \mu \sqrt{-2 \ln \varepsilon},$$

cf. (2.54). Indeed, given the formula for Π in (3.5), as well as $P_{\bar{w}} \Pi^k(\bar{w}_{\min}^k) \sim \bar{w}_{\min}^0$, it follows with (3.30) that

$$\begin{aligned} \Phi(\bar{w}_{\min}^k) &\sim \Phi \circ P_{\bar{w}} \Pi^k(\bar{w}_{\min}^k) \\ &\sim \bar{w}_{\min}^0 + \varepsilon \mu T^{h(\bar{w}_{\min}^0), \text{out}} + \bar{w}_{\min}^0 f_2 \mu \varepsilon \ln \varepsilon + \sqrt{\varepsilon} (\mathcal{G}(v_0, v_{\max}, \mu) + \mathcal{G}(v_{\max}^*, 0, \mu)). \end{aligned}$$

Since $\nu_{\min}^0 \gtrsim (\ln \varepsilon)^{-1}$ implies $\bar{w}_{\min}^k \sim \bar{w}_0^c$ and since $T^{h(\bar{w}_{\min}^0), \text{out}} \sim \sqrt{-2 \ln \varepsilon}$, one obtains (3.36).

By definition, fixed points of Φ on RS^k correspond to periodic 1^k -type orbits in (2.1). We are interested in estimating the parameter range (i.e., the μ -interval) in which such orbits can be observed.

Theorem 3.7. *For $\varepsilon > 0$ sufficiently small, the periodic orbit of type 1^k , $k \geq 1$, exists and is stable on a μ -interval of the form $(\underline{\mu}^k, \bar{\mu}^k)$, with*

$$(3.37) \quad \Delta \mu^k := \bar{\mu}^k - \underline{\mu}^k = -\frac{\mu^k}{\sqrt{2D_\mu}} \frac{\sqrt{\varepsilon}}{\sqrt{-\ln \varepsilon}} \int_{\nu_{-2}^k}^{\nu_0^k} \omega_k(\nu) d\nu + \mathcal{O}(\sqrt{\varepsilon}(-\ln \varepsilon)^{-1});$$

here, ν_{-2}^k denotes the ν -value that solves $\omega_k(\nu) = 8 \ln \varepsilon$.

Proof. Note that MMO orbits with Farey sequence $\{1^k\}$ correspond to solutions of the equation

$$(3.38) \quad \Phi(\bar{w}, \bar{\mu}) = \bar{w}$$

with $\bar{w} \in RS^k$, where we have now included explicitly the μ -dependence of Φ . We are interested in determining μ in (3.38) so that the corresponding fixed point of Φ will be stable. To that end, let ν_{-2}^k be defined as in the statement of the theorem, and note that for $\bar{w} \in RS^k$, the leading term of $\Phi'(\bar{w}, \mu)$ satisfies $|\Phi'(\bar{w}, \mu)| < 1$ if and only if $\bar{w} = \bar{w}_k^c + \nu \Delta \bar{w}^k$ with $\nu \in (\nu_{-2}^k, \nu_0^k)$, cf. (3.33).

Now, if (3.38) is interpreted as defining implicitly a function $\mu = \mu(\bar{w})$, we can set $\underline{\mu}^k = \mu(\bar{w}_k^c + \nu_{-2}^k \Delta \bar{w}^k)$ and $\bar{\mu}^k = \mu(\bar{w}_k^c + \nu_0^k \Delta \bar{w}^k)$. We will use the Fundamental Theorem of Calculus to estimate $\Delta \mu^k = \bar{\mu}^k - \underline{\mu}^k$. Applying implicit differentiation to (3.38), we obtain

$$\frac{d\mu}{d\bar{w}} = - \frac{\frac{\partial}{\partial \bar{w}} \Phi(\bar{w}, \mu) - 1}{\frac{\partial}{\partial \mu} \Phi(\bar{w}, \mu)}.$$

Since

$$\frac{\partial}{\partial \mu} \Phi(\bar{w}, \mu) \sim D_\mu \sqrt{\varepsilon}$$

(recall the discussion in Section 2.5), it follows that

$$\frac{d\mu}{d\bar{w}} \sim \frac{1}{4D_\mu \sqrt{\varepsilon} \ln \varepsilon} \omega_k(\nu)$$

for $\bar{w} = \bar{w}_k^c + \nu \Delta \bar{w}^k$ with $\nu \in (\nu_{-2}^k, \nu_0^k)$, see (3.33). Therefore, using $\frac{d\bar{w}}{d\nu} \sim \Delta \bar{w}^k$, we find

$$(3.39) \quad \Delta \mu^k = \bar{\mu}^k - \underline{\mu}^k = \int_{\bar{w}(\underline{\mu}^k)}^{\bar{w}(\bar{\mu}^k)} \frac{d\mu}{d\bar{w}} d\bar{w} \sim \frac{1}{4D_\mu \sqrt{\varepsilon} \ln \varepsilon} \Delta \bar{w}^k \int_{\nu_{-2}^k}^{\nu_0^k} \omega_k(\nu) d\nu.$$

Given that $\Delta \bar{w}^k = 2\varepsilon \mu \sqrt{-2 \ln \varepsilon} + \mathcal{O}(\varepsilon)$, the result follows. \blacksquare

Observe that by the definition of ν_0^k , $\bar{\mu}^k$ marks the value of μ for which the orbit of type 1^k disappears in a saddle-node bifurcation of Φ , since $\Phi' = 1$ there. In the following, we summarize a few additional observations which follow from Theorem 3.7:

(i) Note that

$$\int \omega_k(\nu) d\nu = \ln |\Gamma(-k + \nu)| - \ln |\Gamma(1 + \nu)| - \frac{1}{2} \ln \nu = -\frac{1}{2} \ln \nu + \mathcal{O}(1),$$

where Γ denotes the standard Gamma function. Since the leading-order contribution to the corresponding definite integral in (3.39) comes from $\nu_{-2}^k = \mathcal{O}((\ln \varepsilon)^{-1})$, one can show that, for ε sufficiently small,

$$\Delta \mu^k = \frac{\mu^k}{\sqrt{2} D_\mu} \frac{\sqrt{\varepsilon} \ln(\sqrt{-\ln \varepsilon})}{\sqrt{-\ln \varepsilon}} + \mathcal{O}(\sqrt{\varepsilon} (-\ln \varepsilon)^{-\frac{1}{2}}).$$

Given that the double logarithmic term is “almost constant” (at least if ε does not vary over too many orders of magnitude), it follows that $\Delta \mu^k$ is roughly of the order $\sqrt{\varepsilon} (-\ln \varepsilon)^{-\frac{1}{2}}$ as $\varepsilon \rightarrow 0$.

(ii) The estimate in (3.37) implies that, for ε fixed, the ratio of the widths of the stability intervals of “adjacent” periodic orbits (i.e., of orbits of the types 1^{k+1} and 1^k) is approximately given by the ratio of the corresponding integrals of ω_{k+1} and ω_k . Since $\{\nu_0^k\}$ decays faster with k than $\{\nu_{-2}^k\}$ (see Figure 15), it follows that $\int_{\nu_{-2}^k}^{\nu_0^k} \omega_k(\nu) d\nu$ decreases. Hence, the sequence $\{\Delta \mu^k\}$ is decreasing with k .

- (iii) The well-developed theory of unimodal maps [25] implies that the μ -interval for which there is an attractor for Φ in RS^k is also of size $(\underline{\mu}^k, \bar{\mu}^k)$, to lowest order. Hence, for μ in any interval given approximately by $(\underline{\mu}^k, \underline{\mu}^{k+1})$, the dynamics of Φ must involve at least two different sectors.

Next, we derive a set of conditions under which a given periodic orbit will have to pass through the k th sector of rotation RS^k . For the remainder of this subsection, we will consider only points $\bar{w} \in RS^k$, $k \geq 1$, for which $\bar{w} = \bar{w}_k^c + \nu \Delta \bar{w}^k$, with

$$(3.40) \quad \nu \in \left(\frac{1}{(-\ln \varepsilon)^p}, 1 - \frac{1}{(-\ln \varepsilon)^p} \right)$$

for some fixed integer $p > 1$. Note that the condition in (3.40) is “generic” in that it covers “most of” RS^k ; to put it differently, only \bar{w} -values that are “very close” to the boundary points \bar{w}_k^c and \bar{w}_{k-1}^c are excluded by (3.40).

We begin by proving a simple preparatory result:

Lemma 3.8. *Consider $\bar{w} = \bar{w}_j^c + \nu \Delta \bar{w}^j \in RS^j$ for some $j \geq 1$, and assume that (3.40) holds. Then, if $\bar{w} \leq \bar{w}_{\min}^j$,*

$$(3.41) \quad |\Phi(\bar{w}) - \Phi_{\min}| = \mathcal{O}\left(\frac{\ln(-\ln \varepsilon)}{-\ln \varepsilon}\right) \Delta \bar{w}^j,$$

whereas if $\bar{w} > \bar{w}_{\min}^j$,

$$(3.42) \quad |\Phi(\bar{w}) - \Phi_{\min}| \lesssim \left(1 + \mathcal{O}\left(\frac{\ln(-\ln \varepsilon)}{-\ln \varepsilon}\right)\right) \Delta \bar{w}^j.$$

Proof. Let ν_{\min}^j be the ν -value corresponding to \bar{w}_{\min}^j . By the Fundamental Theorem of Calculus, we have

$$\Phi(\bar{w}) - \Phi_{\min} = \Delta \bar{w}^j \int_{\nu_{\min}^j}^{\nu} \left(1 - \frac{\omega_j(\eta)}{4 \ln \varepsilon}\right) d\eta = \Delta \bar{w}^j \left(\nu - \nu_{\min}^j - \frac{1}{4 \ln \varepsilon} \int_{\nu_{\min}^j}^{\nu} \omega_j(\eta) d\eta\right).$$

Since ν is constrained by condition (3.40), we find

$$\int_{\nu_{\min}^j}^{\nu} \omega_k(\eta) d\eta = \mathcal{O}(\ln \nu) + \mathcal{O}(\ln \nu_{\min}^j) = \mathcal{O}(\ln(-\ln \varepsilon)),$$

see also the proof of Theorem 3.7. Now, if $\nu \leq \nu_{\min}^j$, then $\nu_{\min}^j - \nu = \mathcal{O}((-\ln \varepsilon)^{-1})$, and the estimate in (3.41) follows. If, on the other hand, $\nu > \nu_{\min}^j$, then $\nu - \nu_{\min}^j < 1$, which implies (3.42). \blacksquare

Next, we show that orbits satisfying the generic condition in (3.40) will typically pass through the k th sector of rotation if, additionally, $\Phi_{\min} \in RS^k$ holds.

Theorem 3.9. *Assume that $\Phi_{\min} \in RS^k$ and that, for some q satisfying $0 < q < \frac{1}{2}$,*

$$(3.43) \quad \bar{w}_{k-1}^c - \Phi_{\min} \lesssim \frac{1}{(-\ln \varepsilon)^q} \Delta \bar{w}^k \quad \text{and} \quad \Phi_{\min} - \bar{w}_k^c \lesssim \frac{1}{(-\ln \varepsilon)^q} \Delta \bar{w}^k.$$

Consider a periodic orbit $\{\bar{w}^0, \dots, \bar{w}^j\}$, with $\Phi(\bar{w}^\ell) = \bar{w}^{\ell+1}$ for $\ell = 0, \dots, j-1$, and let $\{\nu^0, \dots, \nu^j\}$ be the corresponding values of ν . Assume that (3.40) holds. Then, the orbit in question must pass through RS^k provided $\varepsilon > 0$ is sufficiently small.

Proof. We will assume that $k \geq 2$ in the following and will omit the remaining cases for the sake of brevity.

First, note that Lemma 3.8 and the assumption in (3.43) imply that, for any $\bar{w} \in \mathcal{C}_\varepsilon^-$, $\Phi(\bar{w}) \in RS^k \cup RS^{k-1} \cup RS^{k-2}$. This follows from the estimates below, which are a straightforward consequence of (3.41), (3.42), and (3.43): we begin by assuming that $\bar{w} \in RS^k$; then,

$$\begin{aligned}\Phi(\bar{w}) - \bar{w}_{k-1}^c &= \Phi(\bar{w}) - \Phi_{\min} + \Phi_{\min} - \bar{w}_{k-1}^c \\ &\lesssim \Phi_{\min} - \bar{w}_{k-1}^c + \Delta \bar{w}^k \left(1 + \mathcal{O}\left(\frac{\ln(-\ln \varepsilon)}{-\ln \varepsilon}\right) \right) \\ &\lesssim \Delta \bar{w}^k (1 + \mathcal{O}((-\ln \varepsilon)^{-q})),\end{aligned}$$

which implies that $\Phi(\bar{w})$ can be no higher than RS^{k-2} in that case.

Similarly, for $\bar{w} \in RS^{k-1} \cup RS^{k-2}$, we have the estimate

$$\begin{aligned}\Phi(\bar{w}) - \bar{w}_{k-2}^c &= \Phi(\bar{w}) - \Phi_{\min} + \Phi_{\min} - \bar{w}_{k-2}^c \\ &\lesssim \Phi_{\min} - \bar{w}_{k-2}^c + \Delta \bar{w}^{k-1} \left(1 + \mathcal{O}\left(\frac{\ln(-\ln \varepsilon)}{-\ln \varepsilon}\right) \right) \\ &\lesssim \mathcal{O}((-\ln \varepsilon)^{-q}) \Delta \bar{w}^{k-1},\end{aligned}$$

see (3.41) as well as (3.43). It follows that for $\bar{w} \in RS^{k-1} \cup RS^{k-2}$, $\Phi(\bar{w})$ can be no higher than RS^{k-2} .

Finally, for any point $\bar{w} \in RS^{k-2}$ which is contained in the image of Φ , there holds

$$\bar{w} - \bar{w}_{k-2}^c \lesssim \mathcal{O}((-\ln \varepsilon)^{-q}) \Delta \bar{w}^{k-1}$$

and, consequently,

$$(3.44) \quad \Phi(\bar{w}) \lesssim \bar{w}_{k-1}^c + \mathcal{O}((-\ln \varepsilon)^{-q}) \Delta \bar{w}^{k-2},$$

by (3.41). It follows that any recurrent set, including the periodic orbit $\{\bar{w}^0, \dots, \bar{w}^j\}$, is contained in $RS^k \cup RS^{k-1} \cup RS^{k-2}$.

Now, suppose that such a periodic orbit is given, and note that there is an unstable fixed point \bar{w}^* of Φ in RS^{k-1} close to \bar{w}_{k-2}^c . Assume that $\bar{w}^0 > \bar{w}^*$. Then, the trajectory of \bar{w}^0 under Φ must eventually enter RS^{k-2} ; moreover, by (3.44), it must terminate at a point \bar{w}^j with $\bar{w}^j < \bar{w}^*$.

Looking at the forward trajectory of \bar{w}^j , we see that it is decreasing until it falls below \bar{w}_{\min}^{k-1} . In other words, there exists $\ell \geq 0$ such that $\bar{w}^j, \bar{w}^{j+1}, \dots, \bar{w}^{j+\ell-1}$ are greater than or equal to \bar{w}_{\min}^{k-1} and $\bar{w}^{j+\ell}$ is less than or equal to \bar{w}_{\min}^{k-1} . Hence, we conclude that either $\bar{w}^{j+\ell} \in RS^k$ or, by combining (3.41) and (3.43), $\bar{w}^{j+\ell+1} \in RS^k$. \blacksquare

It remains to comment briefly on the assumption put forward in (3.43): given that $\Phi(\bar{w}_{\min}^k) \sim \Phi_{\min}$, cf. (3.36), as well as that necessarily $\bar{w}_k^c \lesssim \Phi_{\min} \lesssim \bar{w}_{k-1}^c$ by (3.43), one can show that, to lowest order,

$$(2k-1) \frac{\mu^c}{D_\mu} \sqrt{\varepsilon} \sqrt{-2 \ln \varepsilon} \leq \mu^c - \mu \leq (2k+1) \frac{\mu^c}{D_\mu} \sqrt{\varepsilon} \sqrt{-2 \ln \varepsilon}$$

must hold for (3.43) to be true, with μ^c defined as in (2.56). This condition is consistent with the estimate for $\Delta \mu^k$, e.g., given after the proof of Theorem 3.7, and will typically be satisfied if q is not “too large.”

Remark 11. The restriction to $q < \frac{1}{2}$ in (3.43) is made to ensure that $\Phi_{\min} \in RS^k$ will imply $\Phi(\bar{w}_{\min}^j) \in RS^k$ for $0 \leq j \leq k-1$, since we can *a priori* conclude only $\Phi_{\min} - \Phi(\bar{w}_{\min}^j) = \mathcal{O}(\varepsilon)$ from (3.36). \blacksquare

One important consequence of Theorem 3.9 is that it allows us to give a precise qualitative description of the segments that the symbolic sequence of a given periodic orbit can contain. For any such orbit, let $k \geq 1$ be the largest integer such that the segment 1^k is contained in the corresponding Farey sequence. With this convention, $k = 1$ implies that the sequence can contain only the segments 1^1 and 1^0 ; restrictions on the sequences that can occur when $k \geq 2$ are given in the following theorem:

Theorem 3.10. *Assume that $k \geq 2$. Then, a periodic orbit can occur if its sequence consists of segments of the form 1^k (some number of times in succession), 1^{k-1} (some number of times in succession), and 1^{k-2} (preceded by 1^k and followed by 1^{k-1} or 1^k).*

Proof. First, let us assume that (3.43) is satisfied. Then, the result already follows from the proof of Theorem 3.9.

Now, suppose that (3.43) does not hold, as well as that $\Phi_{\min} \sim \bar{w}_{k-1}^c$. Then, the steps given in the proof of Theorem 3.9 can be retraced until almost the very end, namely, up to the statement that $\bar{w}^{j+\ell}$ will be less than or equal to \bar{w}_{\min}^{k-1} for some $\ell \geq 0$. Instead, if $\bar{w}^{j+\ell} \in RS^{k-1}$, we can now conclude only that $\bar{w}^{j+\ell+1} \in RS^k \cup RS^{k-1}$. The orbit can then either remain in RS^{k-1} or enter RS^k and subsequently jump back to either RS^{k-1} or RS^{k-2} . If, on the other hand, $\Phi_{\min} \sim \bar{w}_k^c$, the same kind of sequences can occur, with k shifted upward by 1. This completes the proof. ■

Given the result of Theorem 3.10, a natural question that arises is how many times in succession a given segment can occur:

Proposition 3.11. *Let $k \geq 2$. If a periodic orbit involves all of the segments 1^{k-2} , 1^{k-1} , and 1^k , then both 1^{k-2} and 1^k can occur at most once in succession.*

Proof. First, note that an orbit can contain all of the segments 1^{k-2} , 1^{k-1} , and 1^k only if $\Phi_{\min} \sim \bar{w}_{k-1}^c$, see the proofs of Theorems 3.9 and 3.10. It follows that any point on the orbit that lies in RS^{k-2} must lie close to \bar{w}_{\min}^{k-1} and, hence, that it must be mapped to $RS^{k-1} \cup RS^k$ under Φ . Similarly, any point on the orbit in RS^k must be close to \bar{w}_{k-1}^c and therefore must be mapped to $RS^{k-2} \cup RS^{k-1}$. ■

Finally, Theorem 3.10 allows us to make a precise statement on the periodic orbits of the type $\{L_j^{k_j}\}$ that can be observed for $L_j \geq 2$:

Corollary 3.12. *For $k \geq 2$, $L \geq 2$, and $L + k \geq 5$, there are no periodic orbits which contain the segment L^k and which pass through the part of RS^k defined by (3.40).*

Proof. Since the segment L^k corresponds to k small loops followed by L large relaxation excursions, this segment can also be written in the form $1^k(1^0)^{L-1}$. If $k = 0$ or $k = 1$, Theorem 3.10 places no restrictions on the existence of such segments. Furthermore, Theorem 3.10 implies that the only remaining admissible k -value is 2 and that $L - 1 = 1$ must hold in that case, implying $L = 2$. ■

To put it differently, one will not “generically” observe Farey sequences of the form $\{L_j^{k_j}\}$ if $L_j \geq 3$; if $L_j = 2$, only segments of the form 2^1 or 2^2 will occur. The segment L_j^1 , however, is admissible for any $L_j \geq 1$; this is due to “leakage” from RS^0 , in the sense that $\Phi(\bar{w}) \lesssim \bar{w}$ for $\bar{w} \approx \bar{w}_0^c$, implying that trajectories can “drift” back into RS^1 .

Finally, we note that we make no assumptions about the stability of the periodic orbits under consideration, neither in Theorem 3.10 nor in Corollary 3.12; indeed, our results apply to any orbit for which the condition in (3.40) is satisfied.

4. CONCLUSIONS AND DISCUSSION

In the present article, we have studied mixed-mode oscillations (MMOs) in a three-dimensional model system of ordinary differential equations with three distinct time-scales, see (1.5). Here, the “super-slow” variable w has been playing the role of a “dynamical parameter” which makes the (v, z) -subsystem of (1.5) move slowly through a canard explosion. One major advantage of our modeling Ansatz is the fact that the resulting system dynamics is “almost” two-dimensional, in the sense that the integrable structure close to a canard explosion can be exploited to derive the return map Π for the induced flow.

We are aware of two specific examples of three time-scale systems which exhibit mixed-mode dynamics akin to that studied here. One is a compartmental model for the dopaminergic neuron, first derived by Wilson and Callaway [37] and subsequently analyzed in [23] and [24], which in fact served as our motivation for formulating the simplified model system considered in this article. The other example is a model for a chemical reaction, discussed by Moehlis [28]. Although these two systems are not exactly analogous to the one studied here, they do share many of the underlying features and can be analyzed in a similar manner; see also the upcoming article [18].

The three time-scale model studied in this article is one realization of a more general canard mechanism that has been put forward to explain the mixed-mode dynamics often observed in multiscale dynamical systems [36, 2]. This generalized canard mechanism is defined as a combination of dynamical (local) passage through a canard point and a (global) return that resets the system dynamics after the passage has been completed, cf. also Section 1. Other mechanisms that do not explicitly involve canards have been proposed to explain MMOs; examples include break-up of an invariant torus [21], loss of stability of a Shilnikov orbit [16], slow passage through Hopf bifurcation [22], and subcritical Hopf-homoclinic bifurcation [12, 13]. While these other mechanisms are consistent with some of the characteristic features of MMOs, they cannot typically explain all of them, see [2]. On the other hand, the generalized canard mechanism is consistent with most examples known to us of systems exhibiting mixed-mode-type behavior [2, 17]. In particular, we note that both the Shilnikov and the delayed Hopf mechanisms can be realized as an aspect of it. These and similar questions are the topic of ongoing research, see, e.g., the forthcoming article [3].

An explanation of mixed-mode dynamics based on the Shilnikov mechanism has been suggested by a number of authors (cf. [16] and the references therein) and is based on the similarities between the respective bifurcation sequences, as well as on the presence of Shilnikov-type equilibria in systems that exhibit mixed-mode-type behavior. Roughly speaking, the Shilnikov phenomenon is the unfolding of a homoclinic orbit to an equilibrium of saddle type with a one-dimensional stable manifold and a two-dimensional unstable manifold of spiral focus type. Since Shilnikov-type equilibria are present in canard-based systems that involve a so-called *folded saddle-node (of type II)*, we propose that the latter systems do realize a “suitably modified” Shilnikov mechanism; cf. [3]. Similarly, a case of slow passage through Hopf bifurcation is seen in the dynamics near a folded saddle-node (of type II) and plays an important role there. This observation was made already in [26] and will also be fully elucidated in [3].

Finally, it is important to note that the equations in (1.2) are neither of Shilnikov type nor of slow-passage-through-Hopf-bifurcation type, though they clearly realize the generalized canard mechanism. Moreover, due to our assumption that $\mu + \phi = \mathcal{O}(1)$ in (1.2), the mixed-mode dynamics analyzed in this article is neither of folded-node type nor of folded saddle-node type, cf. Section 1. More precisely, in a folded-node system, i.e., for $\mu + \phi = \mathcal{O}(1)$ and negative in (1.2), the dynamics in the fold region would be strongly contractive and not oscillatory. Furthermore, this dynamics would be transient, since μ would cause w to increase until the relaxation regime in (1.1) is reached. The MMO patterns observed in this case would be regular and robust; irregular time series with two or more successive relaxation cycles would rarely occur upon variation of μ only. In a folded

saddle-node system with μ small but ϕ large, on the other hand, one would typically observe slow passage through a Hopf bifurcation; moreover, the resulting mixed-mode dynamics would again be fairly regular, in the sense that trajectories would generically consist of one relaxation excursion followed by a large number of “loops;” the amplitudes of these loops would be relatively small. This distinction is clearly reflected in the dynamics of (1.5), as predicted analytically in Section 3 and verified numerically below.

Some of our findings on the mixed-mode dynamics of (1.5) are summarized and discussed in detail in the subsequent paragraphs.

A principal result of our analysis is the accurate reduction of the global return map Π (which is defined as a two-dimensional map on the Poincaré section $\bar{\Delta}_-$) to a one-dimensional map Φ which can be studied in a standard, straightforward way.

The first step of this reduction entails the restriction of Π from $\bar{\Delta}_-$ to the union of a set of (one-dimensional) intersecting curves. (These curves, which we have denoted by $\mathcal{C}_\varepsilon^j$, are defined recursively, with $\mathcal{C}_\varepsilon^0 \equiv \mathcal{C}_\varepsilon^-$ the flow image of the attracting slow manifold $\mathcal{S}_\varepsilon^{a-}$ in $\bar{\Delta}$ and $\mathcal{C}_\varepsilon^j = \Pi(\mathcal{C}_\varepsilon^{j-1})$, $j \geq 1$.) Most importantly, by Proposition 3.1, this reduction incurs an only exponentially small error, i.e., the sequence $\{\mathcal{C}_\varepsilon^j\}$ very accurately approximates the attractor of Π .

Then, in a second step, another reduction is performed, which yields a one-dimensional map Φ that is defined on the curve $\mathcal{C}_\varepsilon^-$. This map again gives an exponentially accurate approximation, this time for the $(k+1)$ th iterate of Π on the k th sector of rotation, RS^k . (In other words, Φ restricted to RS^k describes the recurrent dynamics on RS^k with an exponentially small error.) Even though the map Φ is multimodal and possibly discontinuous at the boundaries of RS^k , it is one-dimensional and thus can be analyzed using techniques from one-dimensional discrete dynamics. It is interesting to note that, conceptually, the reduction to Φ is valid for any finite k , since the return of trajectories under Π will always eventually be to $\mathcal{C}_\varepsilon^-$. However, given the non-uniformity of our results in k (Proposition 3.4), one might have to consider higher-order terms (in ε) or, alternatively, take ε “very small” to describe the asymptotics accurately for “very large” k .

Some authors [23, 27] postulate a reduction to the dynamics of an *interval* map that would capture the properties of MMOs in systems of the type of (1.2). The fact that all MMO trajectories must pass extremely close to $\mathcal{S}_\varepsilon^{a-}$ is a strong indication that the system dynamics of (1.2) is almost two-dimensional in nature. Similarly, one might expect that the corresponding return map Π is almost one-dimensional. However, our results imply that a straightforward reduction of Π to a one-dimensional map defined on a single interval is not possible, whereas the one-dimensional map Φ , which is defined on a *set of intervals* corresponding to the sectors of rotation, approximates Π with an only exponentially small error. By contrast, in [23], the return is approximated by a piecewise linear map, with a jump discontinuity corresponding to the strong canard, that admits a large variety of potential Farey sequences. Our analysis, on the other hand, resolves precisely the rich bifurcation structure of Φ close to the strong canard of (1.2), allowing us to characterize exactly which Farey sequences will actually be observed in (1.2), as well as to give accurate estimates of the relevant parameter intervals. (It is important to note, though, that the analysis in [23] does not focus primarily on resolving the canard structure in detail; rather, it is concerned with the system dynamics close to Hopf bifurcation which we do not analyze in detail here.)

The properties of Φ on RS^k directly determine those of the corresponding MMO trajectories of type 1^k , i.e., of periodic orbits for (1.5) which pass through the k th sector of rotation. Hence, a large part of our analysis is devoted to establishing the qualitative and quantitative asymptotics of the reduced return map Φ . More specifically, our results on the bifurcation structure of Φ as well as on the Farey sequences $L_0^{k_0} L_1^{k_1} \dots$ of the corresponding MMO trajectories include a proof of the existence and stability of 1^k -type orbits (Theorem 3.7), a precise description of the ordering of the Farey sequences that will “generically” occur for $L_j \equiv 1$ (Theorem 3.10 and Proposition 3.11), as

well as a statement on the “improbability” of observing orbits with symbolic sequence $\{L_j^{k_j}\}$ when $L_j \geq 3$ (Corollary 3.12). It is important to note that these restrictions on the dynamics of Φ are by no means exhaustive; rather, they provide a sample of the types of results that can be proved using the techniques of Section 3. A more comprehensive analysis, however, is beyond the scope of this work.

Another important aspect of the generalized canard mechanism is the asymptotic structure of secondary canards, as well as of the corresponding sectors of rotation. To date, rigorous results in this direction have only been obtained by Wechselberger [36] for systems of general folded-node type, via a bifurcation analysis of resonances. To the best of our knowledge, no comparable analysis has been available so far for other realizations of the generalized canard mechanism. The three time-scale structure of our problem in combination with the resulting near-integrability, however, allows us to obtain rather specific results; in particular, it enables us to derive a more or less explicit asymptotic estimate for the sector size: given the definition of the critical canard value \bar{w}_0^c , as well as of the \bar{w} -value \bar{w}_k^c corresponding to the k th secondary canard Γ_ε^k , it follows with $w = \sqrt{\varepsilon}\bar{w}$ that $w^c = \mathcal{O}(\varepsilon)$ after “blow-down,” as well as that

$$\Delta w^k := \sqrt{\varepsilon}\Delta\bar{w}^k \sim 2\mu\varepsilon^{\frac{3}{2}}\sqrt{-2\ln\varepsilon}$$

is the width of $RS^k \subset \mathcal{C}_\varepsilon^-$, independent of k to leading order. This estimate confirms the well-known fact [33, 36] that the canard phenomenon is fairly “robust” in three dimensions, in the sense that the relevant parameter intervals are relatively large, whereas in two dimensions, they are only exponentially small [20]: in our case, the width of the relevant w -interval will roughly be $\mathcal{O}(\varepsilon)$.

Finally, given the above discussion, our partly rigorous and partly heuristic conclusions on the bifurcation (Farey) structure of the mixed-mode dynamics which will typically be observed in (1.5) can be summed up as follows:

- (i) Symbolic sequences of the form $\{1^k\}$ and $\{1^k 1^{k-1}\}$ dominate the stable dynamics; such sequences correspond to MMO trajectories that visit only one sector of rotation and two adjacent sectors, respectively; see Figure 17.
- (ii) Stable 1^k -type orbits are observed in a relatively small parameter range. Consequently, non- 1^k orbits (i.e., orbits that are not periodic with Farey sequence $\{1^k\}$) dominate a significant portion of the parameter space. Moreover, they occur more frequently with increasing k , since the 1^k -stability intervals decrease in size as k increases; cf. Figures 17 and 18.
- (iii) For $L_j \geq 2$, segments of the form $L_j^{k_j}$ are not generically observed when $k_j \geq 2$, except for the segment 2^2 . The segment L_j^1 , on the other hand, is possible for any $L_j \geq 1$; see Figure 19.
- (iv) As μ increases, the Farey sequences observed in the transition are roughly of the form $\dots \rightarrow 1^k \rightarrow 1^k 1^{k-1} \rightarrow 1^{k-1} \rightarrow \dots$; in particular, all sectors of rotation are “swept through” until $\mu > \mu^c$, when the dynamics finally enters the relaxation regime (cf. Figures 18 and 20).
- (v) The local dynamics depends quite sensitively on the curvature of $f(v)$, i.e., on the coefficient f_2 ; in particular, 1^k -type orbits become increasingly harder to observe with growing f_2 , see Figure 21(a).
- (vi) The number of sectors visited is also influenced by the strength of the global dynamics, i.e., by how far “back” w is reset after relaxation: the smaller the parameter g_1 is, the closer to the strong canard trajectories will return after relaxation, and the smaller the relevant μ -interval will be; cf. Figure 21(b).
- (vii) Since $w = \mathcal{O}(\varepsilon)$ throughout, see Figure 18(f), the global return point will be $\mathcal{O}(\varepsilon)$ -close (in w) to the strong canard. This implies that only the “lower” sectors will typically be

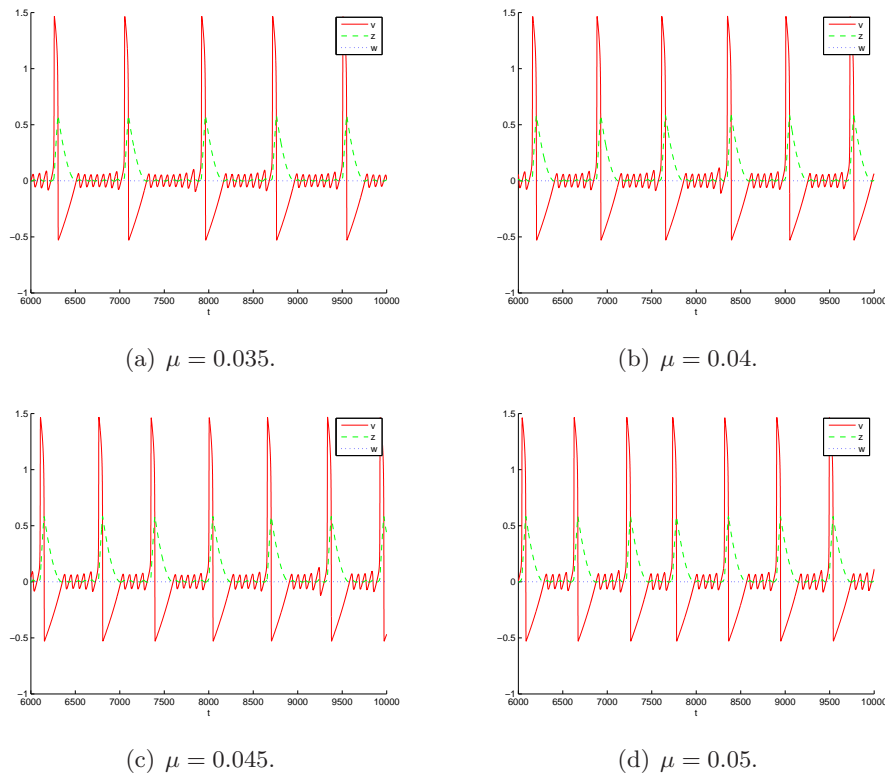


FIGURE 17. The time series of v , z , and w in (1.5) for $f_2 = 1.5$, $f_3 = -1$, $g_1 = 0.5$, and $\varepsilon = 0.01$. As μ increases from (a) 0.035 via (b) 0.04 and (c) 0.045 to (d) 0.05, one observes a transition from $1^7 1^6$ via $1^6 1^5$ and $1^5 1^4$ to $1^4 1^3$ in the resulting Farey sequences.

involved in the dynamics, resulting in MMO trajectories with a sub-maximum number of small oscillations.

- (viii) As k increases or, alternatively, as μ decreases, the sectors of rotation decrease in size. Overall, however, the dynamics seems to become less expanding with higher k , making it less likely for sequences containing segments of the form $1^k 1^{k-\ell}$, $\ell > 1$, to occur.

With the exception of the conjecture in (viii), these observations are reflected by our numerical findings, see Figures 17 to 21 as referred to in the individual items. Figure 17 shows a sample of regular $1^k 1^{k-1}$ -type orbits for $k = 4, \dots, 7$, while Figure 18 illustrates the transition from 1^2 to 1^1 via mixed transitory segments of the form $2^2 1^2 1^1$; Figure 19 indicates how Farey sequences with mixed segments containing 1^1 , 2^2 , and 2^1 , as well as L_j^1 -type sequences with $L_j \geq 1$, can arise; Figure 20 illustrates the transition from mixed-mode dynamics to the pure relaxation regime at $\mu = \mu^c$ in (1.5); finally, in Figure 21, (a) and (b) exemplify the effects of a change in f_2 and g_1 , respectively, on the dynamics of (1.5). In each case, the relevant parameter regimes are specified in detail in the corresponding captions. All numerical simulations were performed in MATLAB using the predefined routine `ode23tb` with absolute and relative accuracies 10^{-10} and 10^{-8} , respectively. For clarity, the results are illustrated starting at $t = 6000$, after initial transients have subsided.

Acknowledgment. The authors are grateful to Horacio Rotstein for his involvement during the early stages of this work, as well as to Alexey Kuznetsov, Georgi Medvedev, and Martin Wechselberger for valuable discussions and comments and to Heidi Lyons and Paola Malerba for their

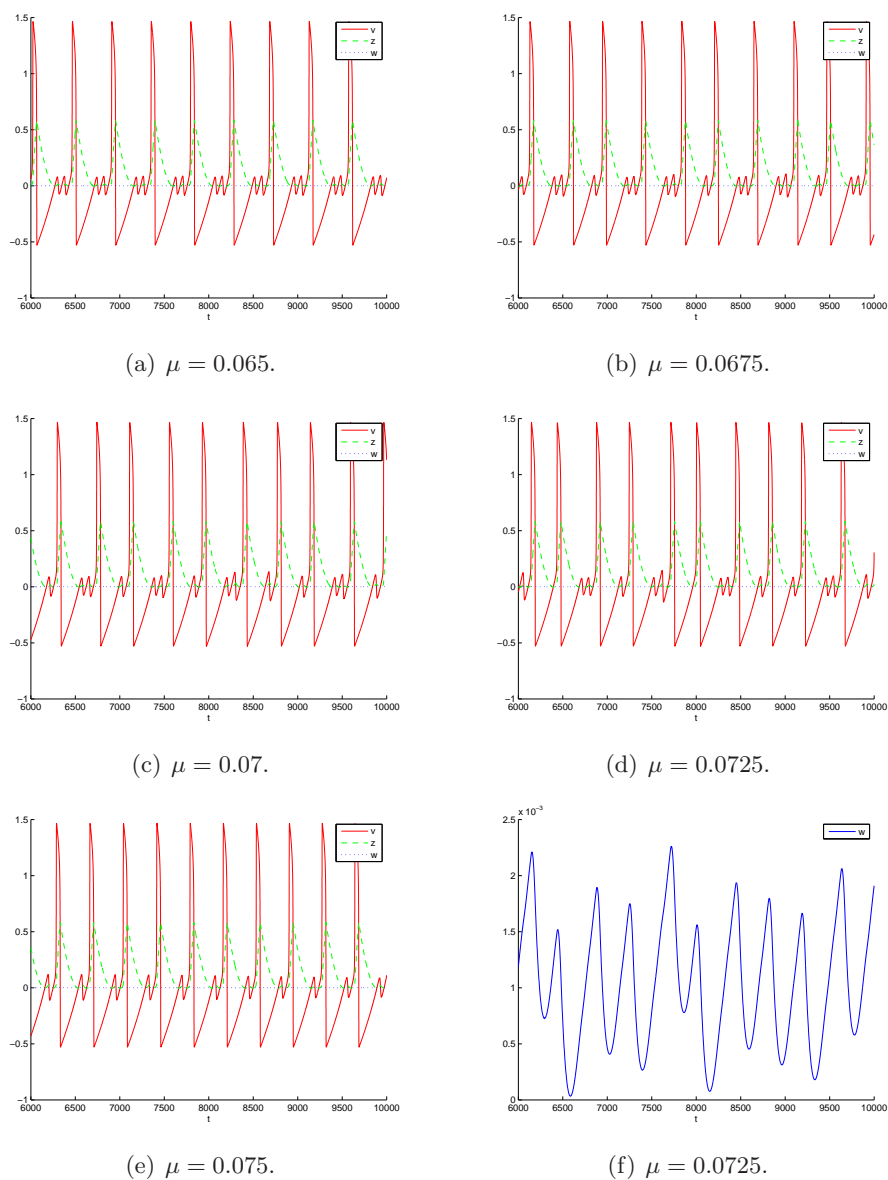
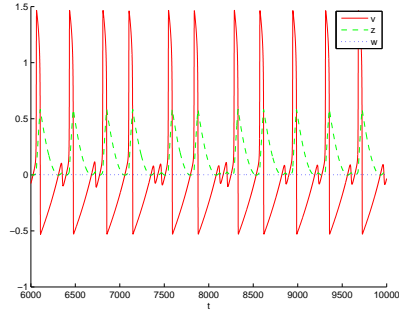
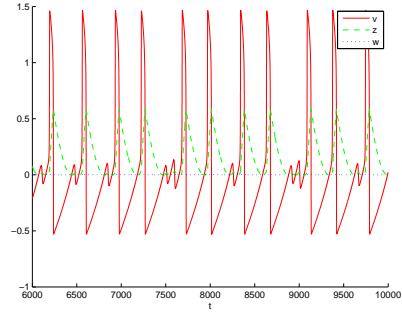


FIGURE 18. The time series of v , z , and w in (1.5) for $f_2 = 1.5$, $f_3 = -1$, $g_1 = 0.5$, and $\varepsilon = 0.01$. As μ increases from (a) 0.065 via (b) 0.0675, (c) 0.07, and (d) 0.0725 to (e) 0.075, one observes a transition from 1^2 to 1^1 in the resulting Farey sequences, with transitory sequences which contain mixed segments of the form $1^2 1^1$ as well as $2^2 1^2 1^1$. Panel (f) shows a zoom on the time series of w for $\mu = 0.0725$; clearly, $w = \mathcal{O}(\varepsilon)$, in accordance with Assumption 1 (cf. also Section 3.3).

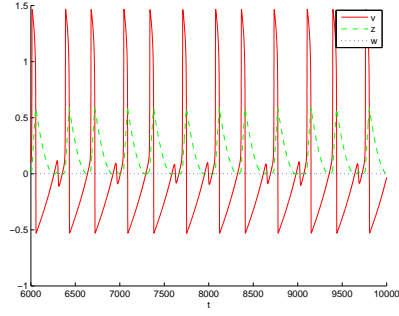
careful reading of (parts of) the original manuscript. The research of M.K. was supported in part by NSF grant DMS-0406608. The research of N.P. was supported by NSF grants DMS-0109427 (to N.K.), DMS-0211505 (to N.K.), and DMS-0406608 (to M.K.). The research of N.K. was supported in part by NSF grant DMS-0211505.



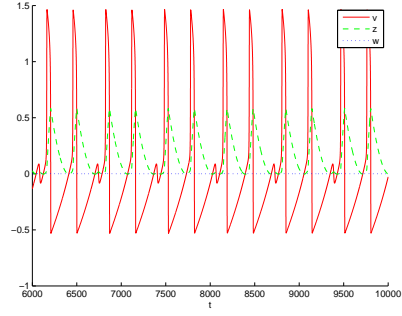
(a) $\mu = 0.0775$.



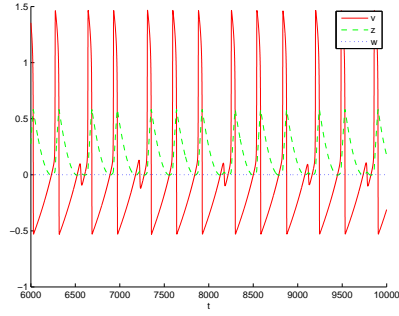
(b) $\mu = 0.08$.



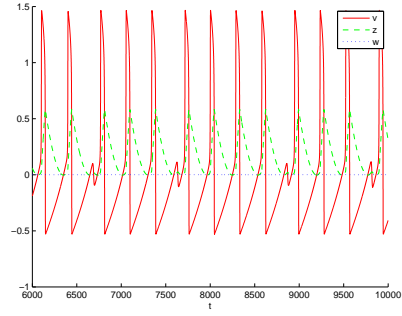
(c) $\mu = 0.0825$.



(d) $\mu = 0.085$.



(e) $\mu = 0.0875$.



(f) $\mu = 0.09$.

FIGURE 19. The time series of v , z , and w in (1.5) for $f_2 = 1.5$, $f_3 = -1$, $g_1 = 0.5$, and $\varepsilon = 0.01$. As μ increases from (a) 0.0775 via (b) 0.08 to (c) 0.0825, one observes a variety of complex Farey sequences, with segments containing 1^1 , 2^2 , and 2^1 as well as repetitions thereof. As μ is increased further to 0.09, one observes a transition from (c) $1^1 2^1$ via (d) 2^1 and (e) $2^1 3^1$ to (f) $3^1 4^1$, as predicted analytically in Section 3.5.

APPENDIX A. SOME ASYMPTOTIC RESULTS

In this appendix, we summarize a few results on the asymptotics of the rescaled system (2.3), as well as of its generalization in (2.8). Recall that the equations in (2.3) are given by

$$(A.1a) \quad \bar{v}' = -\bar{z} + f_2 \bar{v}^2 + \sqrt{\varepsilon} f_3 \bar{v}^3,$$

$$(A.1b) \quad \bar{z}' = \bar{v} - \bar{w},$$

$$(A.1c) \quad \bar{w}' = \varepsilon(\mu - g_1 \bar{v} \bar{z}),$$

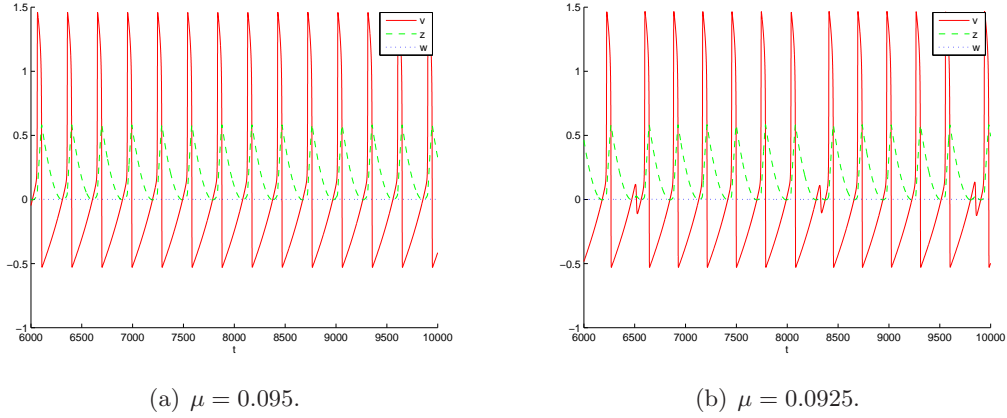


FIGURE 20. The time series of v , z , and w for $\mu = 0.095$ and $\mu = 0.0925$. Clearly, the system is in the pure relaxation regime in (a), whereas in (b), one observes already mixed-mode dynamics, in agreement with the theoretical prediction that the critical μ -value should be $\mu^c \approx 0.0938$, up to an $\mathcal{O}(\varepsilon)$ -error.

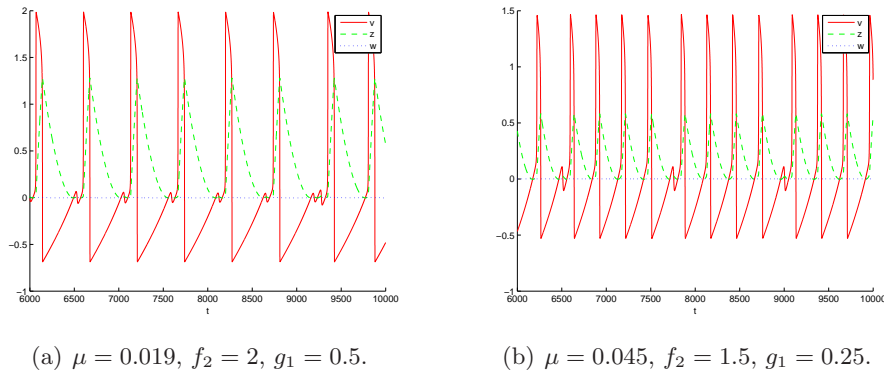


FIGURE 21. The effects of a change of (a) f_2 and (b) g_1 on the dynamics of (1.5). As f_2 is increased from 1.5 to 2, the stability interval of 1^1 -type orbits decreases, since $D_\mu = 2.25$ is replaced by $D_\mu = 4$ and since $\Delta\mu^1 \propto D_\mu^{-1}$, see Theorem 3.7; as g_1 is decreased from 0.5 to 0.25, the dynamics recurs to lower sectors of rotation, cf. Figure 17(c).

as well as that they reduce, for $\varepsilon = 0$, to

$$(A.2a) \quad \bar{v}' = -\bar{z} + f_2 \bar{v}^2,$$

$$(A.2b) \quad \bar{z}' = \bar{v} - \bar{w},$$

$$(A.2c) \quad \bar{w}' = 0,$$

cf. (2.4). For $\bar{w} = 0$, the system in (A.2) is integrable. Moreover, given the constant of motion

$$(A.3) \quad H(\bar{v}, \bar{z}) = \frac{1}{2} e^{-2f_2 \bar{z}} \left(-\bar{v}^2 + \frac{\bar{z}}{f_2} + \frac{1}{2f_2^2} \right)$$

as defined in (2.5), the orbits of (A.2) correspond in a unique fashion to the level curves of H with $H = h$ constant, cf. Section 2. More precisely, to any $h < h_0 = (4f_2^2)^{-1}$, we can assign a unique

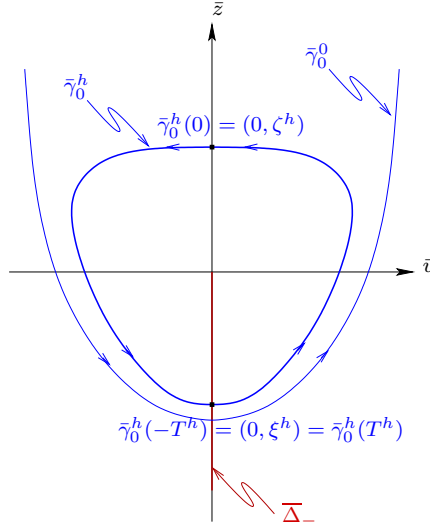


FIGURE 22. A typical solution of (A.2).

\bar{z} -value \bar{z}^h in $\bar{\Delta}_-$. For any such point $(0, \bar{z}^h, \bar{w}) \in \bar{\Delta}_-$, we denote the corresponding solution to (A.1) by $\bar{\gamma}_\varepsilon^h$. Here, we assume the parametrization to be such that $\bar{\gamma}_\varepsilon^h(-T^h(\bar{w})) = (0, \bar{z}^h, \bar{w})$ holds and that $\bar{\gamma}_\varepsilon^h(T^h(\bar{w}))$ is the point of first return to $\bar{\Delta}_-$, recall Figure 6.

In the particular case when $\bar{w} = 0$, we write $T^h = T^h(0)$. Let $h > 0$ be fixed, and let $\bar{\gamma}_0^h$ denote the corresponding (periodic) solution of (A.2). For convenience, we denote the \bar{z} -coordinates of the two points of intersection of $\bar{\gamma}_0^h$ with $\bar{\Delta}$ by ξ^h and ζ^h , respectively; see Figure 22.

Lemma A.1. *There holds $\zeta^h = \frac{1}{2f_2}(-\ln h) + \mathcal{O}(1)$ and $\xi^h = -\frac{1}{2f_2} + \mathcal{O}(h)$.*

Proof. The assertion follows from (A.3): note that $\bar{v} = 0$ in $\bar{\Delta}_-$, and expand $\frac{\bar{z}}{f_2} + \frac{1}{2f_2^2} = h\frac{1}{2}e^{2f_2\bar{z}}$ for \bar{z} large, respectively, for \bar{z} (asymptotically) constant to obtain the expansions for ζ^h and ξ^h , respectively. \blacksquare

Given Lemma A.1, we have the following result on the asymptotics of T^h :

Lemma A.2. *There holds $T^h = \sqrt{2}(-\ln h)^{\frac{1}{2}} + \mathcal{O}(1)$.*

Proof. Given (A.3), we first express \bar{v} via

$$(A.4) \quad \bar{v} = \sqrt{\frac{\bar{z}}{f_2} + \frac{1}{2f_2^2} - 2he^{2f_2\bar{z}}} = \sqrt{\frac{\bar{z}}{f_2}} \sqrt{1 + \frac{1}{2f_2\bar{z}} - 2f_2h\frac{e^{2f_2\bar{z}}}{\bar{z}}}$$

and then make use of $\bar{v} = \bar{z}' = \frac{d\bar{z}}{dt}$ for $\bar{w} = 0$, see (A.4), to obtain

$$\int_{\xi^h}^{\zeta^h} \frac{d\bar{z}}{\sqrt{\frac{\bar{z}}{f_2}} \sqrt{1 + \frac{1}{2f_2\bar{z}} - 2f_2h\frac{e^{2f_2\bar{z}}}{\bar{z}}}} = \int_{-T^h}^0 dt.$$

Integrating the left-hand side by parts, we find that

$$(A.5) \quad T^h = 2\sqrt{f_2\bar{z}} \left(1 + \frac{1}{2f_2\bar{z}} - 2f_2h \frac{e^{2f_2\bar{z}}}{\bar{z}}\right)^{-\frac{1}{2}} \Big|_{\xi^h}^{\zeta^h} \\ + \int_{\xi^h}^{\zeta^h} \sqrt{f_2\bar{z}} \left(1 + \frac{1}{2f_2\bar{z}} - 2f_2h \frac{e^{2f_2\bar{z}}}{\bar{z}}\right)^{-\frac{3}{2}} \left(-\frac{1}{2f_2\bar{z}^2} - 2f_2h \frac{e^{2f_2\bar{z}}}{\bar{z}^2} (2f_2\bar{z} - 1)\right) d\bar{z}.$$

From Lemma A.1, it follows that the leading-order contribution in the first term on the right-hand side of (A.5) comes from the evaluation at the upper limit ζ^h . Moreover, by expanding the integrand in the second term, one can check that the corresponding integral will contribute only terms of $\mathcal{O}(1)$. Hence, again by Lemma A.1, $T^h \sim 2\sqrt{f_2\zeta^h} \sim \sqrt{2}(-\ln h)^{\frac{1}{2}}$. This concludes the proof. \blacksquare

Recall the definitions of $d_{\sqrt{\varepsilon}}^h$ and $d_{\bar{w}}^h$ in (2.10) and (2.11), respectively:

$$(A.6a) \quad d_{\sqrt{\varepsilon}}^h = \int_{-T^h}^{T^h} \nabla H(\bar{\gamma}_0^h(t)) \cdot (f_3\bar{v}_0^h(t)^3, 0)^T dt,$$

$$(A.6b) \quad d_{\bar{w}}^h = \int_{-T^h}^{T^h} \nabla H(\bar{\gamma}_0^h(t)) \cdot (0, -1)^T dt.$$

For a numerical evaluation of the transition map $\bar{\Pi} : \bar{\Delta}_- \rightarrow \bar{\Delta}_-$ (as defined in Section 2.2), it is convenient to express $d_{\sqrt{\varepsilon}}^h$ and $d_{\bar{w}}^h$ as follows:

Lemma A.3. *Let the integrals \mathcal{I}_1 and \mathcal{I}_2 be defined by*

$$\mathcal{I}_1(h) := 2 \int_{\xi^h}^{\zeta^h} e^{-2f_2\bar{z}} \bar{v}_0^h(\bar{z}) d\bar{z} \quad \text{and} \quad \mathcal{I}_2(h) := 2 \int_{\xi^h}^{\zeta^h} e^{-2f_2\bar{z}} \bar{v}_0^h(\bar{z})^3 d\bar{z},$$

respectively, with ξ^h and ζ^h as above. Then, there holds

$$(A.7) \quad d_{\bar{w}}^h = -2f_2\mathcal{I}_1(h) \quad \text{and} \quad d_{\sqrt{\varepsilon}}^h = -f_3\mathcal{I}_2(h).$$

Proof. We will verify the assertion for $d_{\sqrt{\varepsilon}}^h$ first: since

$$\frac{\partial H}{\partial \bar{v}} = -\bar{v}e^{-2f_2\bar{z}} \quad \text{and} \quad \frac{\partial H}{\partial \bar{z}} = (f_2\bar{v}^2 - \bar{z})e^{-2f_2\bar{z}},$$

it follows that $\nabla H \cdot (f_3\bar{v}^3, 0)^T = -f_3\bar{v}^4e^{-2f_2\bar{z}}$. To replace the t -integration in (A.6a) by an integration with respect to \bar{z} , we make use of the fact that $\frac{d\bar{z}}{dt} = \bar{z}' = \bar{v}$ for $\bar{w} = 0$. Then,

$$d_{\sqrt{\varepsilon}}^h = -2f_3 \int_{\xi^h}^{\zeta^h} e^{-2f_2\bar{z}} \bar{v}_0^h(\bar{z})^3 d\bar{z},$$

since $(\bar{v}_0^h, \bar{z}_0^h)(-t) = (-\bar{v}_0^h, \bar{z}_0^h)(t)$ on $\bar{\gamma}_0^h$. To evaluate $d_{\bar{w}}^h$, note that the corresponding integrand in (A.6b) is given by $-f_2\bar{v}^2 + \bar{z}$. Also, it follows from (A.4) that \bar{v} and \bar{z} are related via $\bar{z} = -\bar{v}' + f_2\bar{v}^2$. The result then follows from an integration by parts, since $\bar{v}_0^h(\xi^h) = 0 = \bar{v}_0^h(\zeta^h)$ by definition. \blacksquare

In general, for $h \neq 0$, the integrals \mathcal{I}_1 and \mathcal{I}_2 cannot be computed analytically but have to be approximated numerically. However, for $h = 0$, one can evaluate \mathcal{I}_1 and \mathcal{I}_2 exactly by integrating by parts repeatedly. Recalling the definition of $\bar{\gamma}_0^0$ in (2.6), one finds, for instance,

$$\mathcal{I}_1(0) = \frac{e}{4f_2^2} \int_{-\infty}^{\infty} t^2 e^{-\frac{t^2}{2}} dt = \frac{e}{4f_2^2} \left(-te^{-\frac{t^2}{2}} \Big|_{-\infty}^{\infty} + \int_{-\infty}^{\infty} t^2 e^{-\frac{t^2}{2}} dt \right) = \frac{e\sqrt{2\pi}}{4f_2^2}.$$

Similarly, one can show $\mathcal{I}_2(0) = \frac{3e\sqrt{2\pi}}{16f_2^4}$, see also [19, 20]. In particular, this implies

$$d_w^0 = -\frac{1}{2f_2}\sqrt{2\pi}e < 0 \quad \text{and} \quad d_{\sqrt{\varepsilon}}^0 = -\frac{3f_3}{16f_2^4}\sqrt{2\pi}e > 0.$$

We require the following result on the asymptotics of $\mathcal{I}_2(h)$ for h small:

Lemma A.4. *There holds $\mathcal{I}_2(h) = \mathcal{I}_2(0) - \frac{\sqrt{2}}{f_2^2}h(-\ln h)^{\frac{3}{2}} + \mathcal{O}(h(-\ln h)^{\frac{1}{2}})$.*

Proof. We will prove the assertion by first determining the leading-order behavior of $\frac{d\mathcal{I}_2}{dh}$: given $\bar{v}^2 = \frac{\bar{z}}{f_2} + \frac{1}{2f_2^2} - he^{2f_2\bar{z}}$, we obtain by implicit differentiation that $\frac{\partial \bar{v}}{\partial h} = -\bar{v}^{-1}e^{2f_2\bar{z}}$ and, hence, that

$$\frac{d\mathcal{I}_2(h)}{dh} \sim -6 \int_{\xi^h}^{\zeta^h} \bar{v}_0^h(\bar{z}) d\bar{z}.$$

As in the proof of Lemma A.1, we now make use of (A.4) and then perform an integration by parts to find

$$(A.8) \quad \frac{d\mathcal{I}_2(h)}{dh} = -\frac{4}{\sqrt{f_2}}(\zeta^h)^{\frac{3}{2}} + \mathcal{O}((\zeta^h)^{\frac{1}{2}}) = -\frac{\sqrt{2}}{f_2^2}(-\ln h)^{\frac{3}{2}} + \mathcal{O}((-\ln h)^{\frac{1}{2}}).$$

The assertion follows by integrating (A.8) with respect to h , to leading order. ■

Given Lemma A.4, one can write

$$(A.9) \quad d_{\sqrt{\varepsilon}}^h = d_{\sqrt{\varepsilon}}^0 + \mathcal{R}(h) = d_{\sqrt{\varepsilon}}^0 + h\tilde{\mathcal{R}}(h),$$

where $\mathcal{R}(h)$ denotes the corresponding remainder term and $\tilde{\mathcal{R}}(h) = -f_3\frac{d\mathcal{I}_2}{dh}$ is the first-order coefficient in the Taylor expansion of $d_{\sqrt{\varepsilon}}^h$ about $h = 0$. Note that the leading-order asymptotics of d_w^h can be obtained in a similar manner.

Finally, recall the generalized system of equations from (2.8), as well as the definition of the corresponding return map in (3.16),

$$\bar{\Pi}(h, \bar{w}) = \begin{pmatrix} P_h \bar{\Pi}_0(h, \bar{w}) + \varepsilon \mu \mathcal{K}(h) + \mathcal{O}(\varepsilon^2) \\ \bar{w} + 2\varepsilon \mu T^h + \mathcal{O}(\varepsilon^2) \end{pmatrix},$$

where $\bar{\Pi}_0$ denotes the return map for (3.14) and \mathcal{K} is defined via

$$\mathcal{K}(h) = \int_{-T^h}^{T^h} \nabla H(\bar{\gamma}_0^h(t)) \cdot (G(0, 0), -1)^T (t + T^h) dt.$$

An estimate for \mathcal{K} is derived as follows:

Lemma A.5. *There holds*

$$(A.10) \quad \mathcal{K}(h) = 2d_w^0 T^h + \mathcal{O}(1).$$

Proof. Recall that, by definition, we have

$$\int_{-T^h}^{T^h} \nabla H(\bar{\gamma}_0^h(t)) \cdot (G(0, 0), -1)^T dt = \int_{-T^h}^{T^h} \nabla H(\bar{\gamma}_0^h(t)) \cdot (0, -1)^T dt = d_w^h,$$

see (A.6b) and the proof of Proposition 2.2. It follows that

$$\mathcal{K}(h) = d_w^h T^h + \int_{-T^h}^{T^h} \nabla H(\bar{\gamma}_0^h(t)) \cdot (G(0, 0), -1)^T t dt.$$

To estimate the above integral, note that

$$(A.11) \quad \int_{-T^h}^{T^h} \nabla H(\bar{\gamma}_0^h(t)) \cdot (G(0,0), -1)^T t dt = -G(0,0) \int_{-T^h}^{T^h} \bar{v}_0^h(t) e^{-2f_2 \bar{z}_0^h(t)} t dt \\ - \int_{-T^h}^{T^h} (f_2 \bar{v}_0^h(t)^2 - \bar{z}_0^h(t)) e^{-2f_2 \bar{z}_0^h(t)} t dt.$$

Since the integrand in the second integral on the right-hand side of (A.11) is odd in t , that integral vanishes. Hence, it remains to estimate the first integral: using integration by parts, we obtain

$$(A.12) \quad \int_{-T^h}^{T^h} \bar{v}_0^h(t) e^{-2f_2 \bar{z}_0^h(t)} t dt = T^h \int_{-T^h}^{T^h} \bar{v}_0^h(t) e^{-2f_2 \bar{z}_0^h(t)} dt - \int_{-T^h}^{T^h} \int_{-T^h}^t \bar{v}_0^h(s) e^{-2f_2 \bar{z}_0^h(s)} ds dt.$$

The first integral on the right-hand side of (A.12) is again zero, since the corresponding integrand is odd in t . Next, we recall that $(\bar{v}_0^h, \bar{z}_0^h)(t)$ is a solution of (A.2) for $\bar{w} = 0$ and, hence, that

$$\bar{v}_0^h(s) e^{-2f_2 \bar{z}_0^h(s)} = -\frac{1}{2f_2} \frac{d}{ds} (e^{-2f_2 \bar{z}_0^h(s)}).$$

Consequently,

$$\int_{-T^h}^t \bar{v}_0^h(s) e^{-2f_2 \bar{z}_0^h(s)} ds = -\frac{1}{2f_2} (e^{-2f_2 \bar{z}_0^h(t)} - e^{-2f_2 \xi^h}),$$

where $\xi^h = \bar{z}_0^h(\pm T^h)$, as before. Now, since

$$\int_{-T^h}^{T^h} e^{-2f_2 \bar{z}_0^h(t)} dt$$

is bounded, i.e., $\mathcal{O}(1)$, we conclude that

$$\int_{-T^h}^{T^h} \bar{v}_0^h(t) e^{-2f_2 \bar{z}_0^h(t)} t dt \sim \frac{1}{f_2} T^h e^{-2f_2 \xi^h},$$

and it remains only to estimate $G(0,0)$: indeed, by (2.36) and (2.37), there holds

$$G(0,0) = -\frac{d\bar{z}^{h^+}(\bar{w}, \varepsilon)}{d\bar{w}}(0,0).$$

Recalling that the relationship between \bar{z}^h and h is given implicitly by

$$\frac{1}{2f_2} e^{-2f_2 \bar{z}^h} \left(\bar{z}^h + \frac{1}{2} \right) = h,$$

cf. (A.3), we find from an implicit differentiation that

$$\frac{d\bar{z}^h}{dh} = 2f_2 e^{2f_2 \bar{z}^h} + \mathcal{O}(h).$$

Since $\xi^h = \bar{z}^h$, (2.35) shows that

$$\frac{dh^+(\bar{w}, \sqrt{\varepsilon})}{d\bar{w}}(0,0) = d_{\bar{w}}^+ = -\frac{1}{2} d_{\bar{w}}^0$$

and, hence, that $G(0,0) = d_{\bar{w}}^0 f_2 e^{2f_2 \xi^h}$. The result follows. ■

REFERENCES

- [1] E. Benoit, J.-L. Callot, F. Diener, and M. Diener. Chasse au canard. *Collect. Math.*, 32:37–119, 1981.
- [2] M. Brøns, M. Krupa, and M. Wechselberger. Mixed mode oscillations due to the generalized canard phenomenon. In *Bifurcation Theory and Spatio-Temporal Pattern Formation*, volume 49 of *Fields Inst. Commun.*, pages 39–63, Providence, RI, 2006. Amer. Math. Soc.
- [3] M. Brøns, M. Krupa, and M. Wechselberger. Dynamics near a folded saddle-node of type II. In preparation, 2007.
- [4] K.M. Brucks and C. Tresser. A Farey Tree Organization of Locking Regions for Simple Circle Maps. *Proc. Amer. Math. Soc.*, 124(2):637–647, 1996.
- [5] M. Diener. The canard unchained or how fast/slow dynamical systems bifurcate. *Math. Intelligencer*, 6(3):38–49, 1984.
- [6] J. Drover, J. Rubin, J. Su, and B. Ermentrout. Analysis of a canard mechanism by which excitatory synaptic coupling can synchronize neurons at low firing frequencies. *SIAM J. Appl. Math.*, 65(1):69–92, 2004.
- [7] F. Dumortier. Techniques in the Theory of Local Bifurcations: Blow-Up, Normal Forms, Nilpotent Bifurcations, Singular Perturbations. In D. Schlomiuk, editor, *Bifurcations and Periodic Orbits of Vector Fields*, number 408 in NATO ASI Series C, Mathematical and Physical Sciences, pages 19–73, Dordrecht, The Netherlands, 1993. Kluwer Academic Publishers.
- [8] F. Dumortier and R. Roussarie. Canard Cycles and Center Manifolds. *Mem. Amer. Math. Soc.*, 121(577), 1996.
- [9] W. Eckhaus. Relaxation oscillations including a standard chase on French ducks. In *Asymptotic Analysis, II*, volume 985 of *Lecture Notes in Math.*, pages 449–494, Berlin, 1983. Springer-Verlag.
- [10] I.R. Epstein and K. Showalter. Nonlinear chemical dynamics: Oscillations, patterns, and chaos. *J. Phys. Chem.*, 100(31):13132–13147, 1996.
- [11] N. Fenichel. Geometric singular perturbation theory for ordinary differential equations. *J. Differential Equations*, 31(1):53–98, 1979.
- [12] J. Guckenheimer, R. Harris-Warwick, J. Peck, and A. Wilms. Bifurcation, bursting and frequency spike adaptation. *J. Comp. Neurosci.*, 4(3):255–277, 1997.
- [13] J. Guckenheimer and A. Wilms. Asymptotic analysis of subcritical Hopf-homoclinic bifurcation. *Phys. D*, 139:196–216, 2000.
- [14] C.K.R.T. Jones. Geometric Singular Perturbation Theory. In *Dynamical Systems (Montecatini Terme, 1994)*, volume 1609 of *Springer Lecture Notes in Mathematics*, pages 44–118, Berlin, 1995. Springer-Verlag.
- [15] N. Kopell and L.N. Howard. Bifurcations and Trajectories Joining Critical Points. *Advances in Math.*, 18(3):306–358, 1975.
- [16] M.T.M. Koper. Bifurcations of mixed-mode oscillations in a three-variable autonomous Van der Pol-Duffing model with a cross-shaped phase diagram. *Phys. D*, 80(1-2):72–94, 1995.
- [17] M. Krupa. Mixed-mode oscillations in systems with more than two slow dimensions. In preparation, 2007.
- [18] M. Krupa, N. Popović, N. Kopell, and H.G. Rotstein. Mixed-Mode Oscillations in a Three Time-Scale Model for the Dopaminergic Neuron. To appear in *Chaos*, 2008.
- [19] M. Krupa and P. Szmolyan. Extending geometric singular perturbation theory to nonhyperbolic points—fold and canard points in two dimensions. *SIAM J. Math. Anal.*, 33(2):286–314, 2001.
- [20] M. Krupa and P. Szmolyan. Relaxation Oscillation and Canard Explosion. *J. Differential Equations*, 174(2):312–368, 2001.
- [21] R. Larter and C.G. Steinmetz. Chaos via mixed-mode oscillations. *Phil. Trans. R. Soc. Lond. A*, 337:291–298, 1991.
- [22] R. Larter, C.G. Steinmetz, and B.D. Aguda. Fast-slow variable analysis of the transition to mixed-mode oscillations and chaos in the peroxidase reaction. *J. Phys. Chem.*, 89(10):6506–6514, 1988.
- [23] G. S. Medvedev and J. E. Cisternas. Multimodal regimes in a compartmental model of the dopamine neuron. *Phys. D*, 194(3-4):333–356, 2004.
- [24] G.S. Medvedev, C.J. Wilson, J.C. Callaway, and N. Kopell. Dendritic Synchrony and Transient Dynamics in a Coupled Oscillator Model of the Dopaminergic Neuron. *J. Comp. Neurosci.*, 15(1):53–69, 2003.
- [25] W. De Melo and S. Van Strien. *One-dimensional dynamics*, volume 25 of *Ergebnisse der Mathematik und ihrer Grenzgebiete (3)*. Springer-Verlag, Berlin, 1993.
- [26] A. Milik and P. Szmolyan. Multiple time scales and canards in a chemical oscillator. In C.K.R.T. Jones and A.I. Khibnik, editors, *Multiple-time-scale dynamical systems*, volume 122 of *IMA Vol. Math. Appl.*, pages 117–140. Springer-Verlag, New York, 2001.
- [27] A. Milik, P. Szmolyan, H. Löffelmann, and E. Gröller. Geometry of mixed-mode oscillations in the 3-d autocatalator. *Internat. J. Bifur. Chaos Appl. Sci. Engrg.*, 8:505–519, 1998.
- [28] J. Moehlis. Canards in a surface oxidation reaction. *J. Nonlinear Sci.*, 12(4):319–345, 2002.

- [29] C.A. Del Negro, C.G. Wilson, R.J. Butera, H. Rigatto, and J.C. Smith. Periodicity, Mixed-Mode Oscillations, and Quasiperiodicity in a Rhythm-Generating Neural Network. *Biophys. J.*, 82(1):206–214, 2002.
- [30] H.G. Rotstein and R. Kuske. Localized and asynchronous patterns via canards in coupled calcium oscillators. *Phys. D*, 215(1):46–61, 2006.
- [31] H.G. Rotstein, T. Oppermann, J.A. White, and N. Kopell. The dynamic structure underlying subthreshold oscillatory activity and the onset of spikes in a model of medial entorhinal cortex stellate cells. *J. Comp. Neurosci.*, 21(3):271–292, 2006.
- [32] J. Rubin and M. Wechselberger. Giant Squid—Hidden Canard: the 3D Geometry of the Hodgkin-Huxley Model. *Biol. Cybernet.*, 97(1):5–32, 2007.
- [33] P. Szmolyan and M. Wechselberger. Singularly perturbed folds and canards in \mathbb{R}^3 . *J. Differential Equations*, 177:419–453, 2001.
- [34] P. Szmolyan and M. Wechselberger. Relaxation oscillations in \mathbb{R}^3 . *J. Differential Equations*, 200:69–104, 2004.
- [35] M. Wechselberger. Personal communication.
- [36] M. Wechselberger. Existence and Bifurcation of Canards in \mathbb{R}^3 in the Case of a Folded Node. *SIAM J. Appl. Dyn. Syst.*, 4(1):101–139, 2005.
- [37] C.J. Wilson and J.C. Callaway. Coupled oscillator model of the dopaminergic neuron of the substantia nigra. *J. Neurophysiol.*, 83(5):3084–3100, 2000.
- [38] A.M. Zhabotinsky. Periodic kinetics of oxidation of malonic acid in solution. *Biofizika*, 9:306–311, 1964.
E-mail address: mkrupa@nmsu.edu, nikola.popovic@ed.ac.uk, nk@math.bu.edu

NEW MEXICO STATE UNIVERSITY, DEPARTMENT OF MATHEMATICAL SCIENCES, P.O. BOX 30001 DEPARTMENT 3MB, LAS CRUCES, NM 88003, U.S.A.

UNIVERSITY OF EDINBURGH, SCHOOL OF MATHEMATICS, JAMES CLERK MAXWELL BUILDING, KING’S BUILDINGS, MAYFIELD ROAD, EDINBURGH, EH9 3JZ, UNITED KINGDOM

BOSTON UNIVERSITY, CENTER FOR BIODYNAMICS AND DEPARTMENT OF MATHEMATICS AND STATISTICS, 111 CUMMINGTON STREET, BOSTON, MA 02215, U.S.A.